Aerosolization and Atmospheric Transformation of Engineered Nanoparticles

Andrea J. Tiwari

Dissertation submitted to the faculty of the Virginia Polytechnic Institute and State University in partial fulfillment of the requirements for the degree of

Doctor of Philosophy
In
Civil Engineering

Linsey C. Marr, Chair
Peter J. Vikesland
Michael F. Hochella, Jr.
John R. Morris

March 13th, 2014
Blacksburg, VA

Keywords: aerosol, nanoparticle, atmosphere

Aerosolization and Atmospheric Transformation of Engineered Nanoparticles

Andrea Jean Tiwari

Abstract

While research on the environmental impacts of engineered nanoparticles (ENPs) is growing, the potential for them to be chemically transformed in the atmosphere has been largely ignored. The overall objective of this work was to assess the atmospheric transformation of carbonaceous nanoparticles (CNPs). The research focuses on C_{60} fullerene because it is an important member of the carbonaceous nanoparticle (CNP) family and is used in a wide variety of applications.

The first specific objective was to review the potential of atmospheric transformations to alter the environmental impacts of CNPs. We described atmospheric processes that were likely to physically or chemically alter aerosolized CNPs and demonstrated their relevance to CNP behavior and toxicity in the aqueous and terrestrial environment.

In order to investigate the transformations of CNP aerosols under controlled conditions, we developed an aerosolization technique that produces nano-scale aerosols without using solvents, which can alter the surface chemistry of the aerosols. We demonstrated the technique with carbonaceous (C_{60}) and metal oxide (TiO_2, CeO_2) nanoparticle powders. All resulting aerosols exhibited unimodal size distributions and mode particle diameters below 100 nm.

We used the new aerosolization technique to investigate the reaction between aerosolized C_{60} and atmospherically realistic levels of ozone (O_3) in terms of reaction products, reaction rate, and oxidative stress potential. We identified $C_{60}O$, $C_{60}O_2$, and $C_{60}O_3$ as products of the C_{60}-O_3 reaction. We demonstrated that the oxidative stress potential of C_{60} may be enhanced by exposure to O_3. We found the pseudo-first order reaction rate to be 9×10^{-6} to 2×10^{-5} s^{-1}, which is several orders of magnitude lower than the rate for several PAH species under comparable conditions.

This research has demonstrated that a thorough understanding of atmospheric chemistry of ENPs is critical for accurate prediction of their environmental impacts. It has also enabled future research in that vein by developing a novel technique to produce nanoscale aerosols from nanoparticle powders. Results of this research will help guide the formulation of appropriate environmental policy concerning the regulation of ENPs.

To HT for his love and encouragement.

Acknowledgements

This dissertation would not have been possible without the support and encouragement of a great number of people. First and foremost, I would like to thank my husband, Himanshu Tiwari, for his unending support, patience, and belief in my potential. I would also like to thank my mother, Stephanie Dunker, for her patience throughout my graduate studies, and for instilling a strong work ethic, a sense of persistence, and diverse interests in me from my youth.

I am grateful for the significant support I received from the faculty members on my committee: Drs. Peter Vikesland, Michael Hochella, John Morris, and (2009 – 2013) John Little. Their suggestions and perspectives have proven very valuable.

As is likely the case with nearly anyone completing a dissertation in the Environmental & Water Resources area, I am indebted to Jody Smiley, Julie Petruska, Beth Lucas, and Betty Wingate for their assistance and experience. Jody, thank you for enduring my HPLC struggles; your help was indispensable. My research has also benefitted greatly from analyses conducted at Virginia Tech's Nanoscale Characterization and Fabrication Laboratory (NCFL). There I have had the pleasure of working with, and having samples analyzed by, Andrew Giordani, Dr. Jerry Hunter, and Dr. Steve McCartney. I am also thankful to Dr. Mehdi Ashraf of the Chemistry department for being flexible and not insignificantly adventurous when it came to analyzing my complex samples.

I am very fortunate to have been supported throughout my Ph.D. work by funding from a variety of sources. I would like to acknowledge funding from Virginia Tech's EIGER (Exploring Interfaces through Graduate Education & Research) Fellowship; a US Environmental Protection Agency Science to Achieve Results (STAR) Graduate Fellowship; funding from the Center for the Environmental Implications of Nanomaterials (CEINT); and the Via Academic Prep program within the Civil & Environmental Engineering department, which provided me with the opportunity to expand my teaching experience to the undergraduate level. I would also like to thank Virginia Tech's Institute for Critical Technology & Applied Science (ICTAS) for providing me with the infrastructure that has greatly enabled this research.

One's graduate experience and success are closely tied to the quality of colleagues one has; in this respect I have been very fortunate as well. I am so very grateful to all the members of the Environmental Nanoscience & Technology Lab (ENT) and AirVT groups for their collegiality, knowledge, perspective, and ever-present willingness to help. I am particularly indebted to Drs. Nina Quadros, Amara Holder, Eric Vejerano, and Jennifer Benning for all manner of aerosol-related conversations.

Lastly, I would like to thank my advisor, Dr. Linsey Marr, for her experience, creative thinking, patience, hard work, encouragement, and high standards. All of these factors have contributed to my completion of this work, and have helped to open doors for me that I would not have dreamt of when I first enrolled at Virginia Tech.

Table of Contents

List of Figures

List of Tables

List of Abbreviations

aqu/nC_{60}	an aqueous suspension of C_{60} colloids prepared without the use of intermediate solvents
CNP	carbonaceous nanoparticle
CNT	carbon nanotube
DWNT	double-walled carbon nanotube
ENP	engineered nanoparticle
FTIR	Fourier transform infrared spectroscopy
MWNT	multi-walled carbon nanotube
NOM	natural organic matter
NP	nanoparticle
SWNT	single-walled carbon nanotube
THF/nC_{60}	an aqueous suspension of C_{60} colloids prepared via the intermediate solvent tetrahydrofuran

Chapter 1 – Introduction

C_{60} fullerenes (C_{60}) have generated intense interest among researchers in academia and industry due to their unique properties. C_{60} molecules act as electron acceptors and can be readily functionalized in a variety of ways. Since their discovery nearly 30 years ago,[1] significant innovations have resulted from research on the potential application of this molecule and its derivatives to challenging problems such as photovoltaics,[2, 3] non-linear optics,[4] computer memory,[5] drug delivery,[6, 7] and treatment of cancer[8] and inflammatory diseases.[7] C_{60} and other carbonaceous nanoparticles (CNPs) are depicted in Figure 1-1.

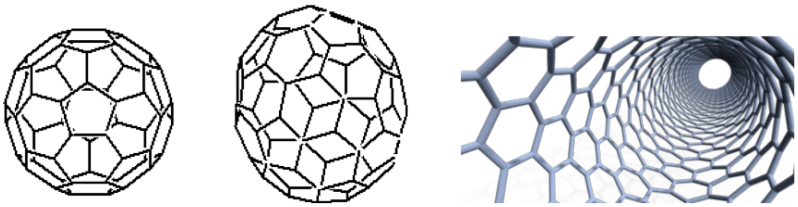

Figure 1-1: Carbonaceous nanoparticles. From left to right: C_{60}, C_{70}, and an interior view of a carbon nanotube. Nanotube image used with the permission of James Hedburg.[9]

Manufactured C_{60} may enter the environment through accidental releases,[10] via its use in environmental remediation activities,[11] or through degradation or disposal of commercial or industrial products containing C_{60}.[12] It is also possible that C_{60} may be emitted to the environment as an "incidental" particle, produced unintentionally during human activities such as propane[13] combustion, or industrial processes.[14] C_{60} fullerenes (and in some cases C_{70} also) have been detected in the atmosphere in the United States[15] and over the Mediterranean Sea,[14] as well as in river sediment,[16] wastewater effluent,[17] sand,[16] and rocks.[18, 19] While these fullerenes are considered to be natural or incidental in origin, the possibility that some of them may have

been intentionally manufactured, and released to the environment through one of the pathways described above, cannot be ruled out. Nanotechnology is a rapidly growing industry,[20] and future emissions of manufactured C_{60} to the environment are expected to rise.

Toxicological research on C_{60} has shown that it is suspected to inhibit the activity of human enzymes,[21] as well as exert various toxic effects on rodents[22-24] and fish.[25, 26] Conversely, C_{60} has shown no effect on the function of human serum albumin[27] and macrophages,[28] and slight, temporary, or no toxic effects on rats,[29] rabbits,[30] and fruit flies.[31] Exposure to C_{60} is associated with toxic effects in plants,[32, 33] worms,[34, 35] and several different bacterial species.[36-38] Numerous studies, however, have shown negligible or no effect of C_{60} exposure on a variety of organisms.[39-41] In addition to effects on particular species, C_{60} has shown the ability to enhance the transport of organic contaminants in the environment[42] and affect the ability of common crops to take up pesticides.[33] Taken together, the seemingly contradictory findings on C_{60} toxicity and ecotoxicity and C_{60}'s unique property of being able to both scavenge and generate reactive oxygen species[43-45] result in an incomplete understanding of the potential environmental impacts of this nanomaterial.

The scientific literature on the environmental impacts of nanotechnology is replete, especially in the early years of the research, with studies that examined the toxicity of pristine nanoparticles.[46] While the results of these studies may be illuminative in some respects, caution must be employed when relating their conclusions to real environmental matrices, in which nanoparticles are likely to undergo a variety of transformations.[12, 47, 48] As this field has become more sophisticated, researchers now frequently incorporate environmental transformations into their

study designs and use a wider variety of starting materials. Despite this increased awareness, however, the atmosphere is frequently overlooked as a setting for nanoparticle transformation.[49] Processes such as oxidation, coagulation, and coating may significantly alter the surface chemistry of nanoparticles, and thus alter their environmental impact they will have once deposited to the earth's surface,[49] as well as potentially enhance radiative forcing in the atmosphere.[50] These processes impact many facets of environmental research on nanoparticles, including transport and fate,[51] detection,[15] and toxicity.[52, 53] These transformations and their implications are detailed for C_{60} and other carbonaceous nanoparticles in Chapter 2.

For carbon-based compounds, oxidation by ozone (O_3) is an important atmospheric transformation.[54] Previous studies on the oxidation of C_{60} by O_3 have shown significant oxidation, but they have either occurred in liquid (by bubbling gas-phase O_3 through a solvent in which C_{60} is dissolved or suspended)[55-57] or have used mixing ratios of gas-phase O_3 that are five to six orders of magnitude more concentrated than found in the troposphere.[58] Investigating the interaction of C_{60} with environmentally relevant mixing ratios of O_3 is a necessary step towards assessing the environmental impacts of nanotechnology.

Studying the atmospheric transformations of nanoparticles necessitates their aerosolization. Standard 'wet' aerosol generation methods (which start with a solution or suspension of the desired material) may produce aerosols with modified surface chemistry relative to the original material.[59, 60] Alternatively, 'dry' aerosol generation methods produce particles that are frequently larger than one micron;[60, 61] such particles are too large to be considered nano-scale, and are likely inappropriate for studying reactions involving nanoparticles. Both of these

variables – surface chemistry and particle size – can impact the process under study, whether the focus is inhalation toxicology or aerosol chemistry. Since aerosolization of manufactured fullerenes and other carbonaceous nanoparticles has been observed in manufacturing facilities;[10, 62, 63] developing an aerosol generation method that preserves nanoparticle surface chemistry while producing truly nano-scale particles would be of significant relevance and utility for several research fields, including toxicology and aerosol chemistry.

Based on the motivations described above, we identified two primary concerns related to the environmental impacts of C_{60}: (1) the generation of nano-scale C_{60} aerosols from dry nanoparticle powders without the use of solvents, and (2) the potential oxidation of aerosolized C_{60} by atmospherically relevant O_3 levels. To address these concerns, we defined the following hypotheses and research objectives:

Hypothesis 1.1: Atmospheric processing is likely to transform carbonaceous nanoparticles, their interactions in the environment, and toxicity.

Objective 1: Review the potential for transformation of carbon-based nanoparticles in the atmosphere.

Hypothesis 2.1: Nano-scale aerosol particles can be generated from dry powders using a simple, cost-effective method.

Objective 2: Develop a method to generate nano-scale aerosols from dry powdered C_{60} nanoparticles.

Hypothesis 3.1: Exposure to ambient levels of ozone causes C_{60} to oxidize and form several reaction products, including $C_{60}O$.

Hypothesis 3.2: Elevated water vapor concentrations enhance the $C_{60} – O_3$ reaction.

Hypothesis 3.3: Exposure to ozone enhances the ability of C_{60} aerosols to exert oxidative stress, as measured by cell-free assays.

Objective 3: Identify and quantify the reaction rate, reaction products, and oxidative stress potential of aerosol-phase C_{60} nanoparticles due to exposure to atmospherically relevant levels of O_3.

This work represents a multifaceted approach to studying the environmental impacts of C_{60}. The manuscript resulting from Objective 1 is the only work to date emphasizing that the atmosphere should not be regarded merely as an inert transport pathway, but rather has important implications for studies on the environmental impacts of nanomaterials. The aerosolization method developed in Objective 2 is unique among those described in the literature in its ability to produce nano-scale aerosols inexpensively without the use of solvents. This method is a more accurate representation of some forms of nanoparticle exposure, and it avoids chemical and physical artifacts that are associated with 'wet' aerosol generation methods. Work relating to Objective 3 is unique in that the C_{60}-O_3 reaction has never previously been examined under atmospherically realistic O_3 levels.

Organization of the Dissertation

Chapter 2, *The Role of Atmospheric Transformations in Determining Environmental Impacts of Carbonaceous Nanoparticles,* is a literature review that addresses Objective 1. In this review we show that carbonaceous nanoparticles (CNPs) will be subject to several transformations upon emission into, or exposure to, the atmosphere, and we detail how these transformations have implications for CNPs' solubility, attachment to natural surfaces, and toxicity. We describe future research directions that have the potential to improve our understanding of the atmospheric transformation of CNPs and the implications of those processes for the environment.

Chapter 3, *A Cost-Effective Method of Aerosolizing Dry Powdered Nanoparticles,* describes the development of an aerosolization method pursuant to Objective 2. We describe the design and operation of a device capable of producing sub-100 nm aerosol particles from dry powdered nanomaterials without the use of solvents and characterize the resulting aerosols in terms of size and morphology. The aerosolization method produces aerosols from C_{60}, TiO_2, and CeO_2 powders with mode diameters of 91, 65, and 40 nm, respectively. Aerosol mass concentrations produced by the method vary linearly with the mass of nanomaterial powder loaded into the device. Due to its repeatable production of sub-100 nm aerosols without the use of solvents, this aerosolization method may be applicable to research in the fields of inhalation toxicology and aerosol chemistry.

Chapter 4, *Oxidation of C_{60} Aerosols by Atmospherically Relevant Levels of O_3,* addresses Objective 3 and describes the products of the reaction between C_{60} aerosols and O_3 and the resulting oxidative stress potential of the aerosols. We determine that this reaction results in a variety of oxygen-containing products: $C_{60}O$, $C_{60}O_2$, $C_{60}O_3$, and potentially also cross-linked C_{60} oligomers. Exposure to O_3 results in the C_{60} aerosol exerting elevated oxidative stress in the dichlorofluorescein assay, but not in assays based on the consumption of dithiothreitol, glutathione, uric acid, and ascorbic acid. Our results suggest that C_{60} will be oxidized by realistic levels of ozone, and consequently, that C_{60} stored for use in laboratories and industrial environments is subject to becoming functionalized in a manner that may alter its behavior in the user's intended application.

Chapter 5 concludes this dissertation by describing the main outcomes of the work and making recommendations for future work.

Attributions

Dr. Linsey C. Marr, of the Virginia Tech Civil & Environmental Engineering department, is the primary advisor for this work. She has provided guidance and suggestions regarding project design, execution, and writing for the work in Chapters 2, 3, and 4. She has also offered editing advice for other portions of this dissertation. Dr. Marr also provided financial support for this work (NSF Cooperative Agreement EF-0830093, Center for the Environmental Implications of NanoTechnology (CEINT)).

Dr. Peter Vikesland, of the Virginia Tech Civil & Environmental Engineering department, has

provided guidance and suggestions regarding the experimental design of work included in Chapter 4, as well as suggestions on other ongoing work not included in this dissertation.

Dr. John Morris, of the Virginia Tech Chemistry department, has provided guidance and suggestions regarding data interpretation for the work presented in Chapter 4, as well as editing suggestions for the manuscript resulting from that work.

Dr. Michael Hochella, of the Virginia Tech Geosciences department, has provided guidance and suggestions regarding data interpretation for the work presented in Chapter 4, editing suggestions for the manuscript resulting from that work, and suggestions on other work not included in this dissertation.

Dr. Erin Davis, formerly of the Virginia Tech Chemistry department, has provided guidance and assistance with sample analysis for work described in Chapter 4.

Alec Wagner and **Yafen Zhang**, of the Virginia Tech Chemistry department, have provided assistance with sample analysis for work described in Chapter 4.

Caleb Fields, of the University of Vermont, has provided assistance with experiments and data analysis included in Chapter 3.

Dr. Eric Vejerano, of the Virginia Tech Civil & Environmental Engineering department, provided assistance in the analysis of the oxidative stress potential of O_3-exposed C_{60} aerosols

shown in Chapter 4.

Dr. Steve McCartney, of the Virginia Tech Nanoscale Characterization and Fabrication Laboratory (NCFL), assisted in the collection of the scanning electron microscope (SEM) images shown in Chapter 4.

Dr. Chris Winkler and Dr. Nina Quadros, of the Virginia Tech NCFL and Institute for Critical Technology and Applied Science, respectively, assisted in the collection of the transmission electron microscope (TEM) images shown in Chapters 3 and 4, respectively.

Complementary work

During the course of the work presented in this dissertation, we presented interim results in nine conference presentations:

- Tiwari, A.J., **Marr, L.C.,** Oxidation of Aerosolized C_{60} by Ozone (oral). In *32nd Annual Conference of the American Association for Aerosol Research (AAAR),* Portland, OR, 2013.

- **Tiwari, A.J.**, Marr, L.C., Oxidation of C_{60} aerosol by ozone (poster). In *Center for the Environmental Implications of Nanotechnology (CEINT), Internal Scientific Meeting,* Durham, NC, 2013.

- **Tiwari, A.J.,** Marr, L.C., Oxidation of C_{60} aerosols by ozone (poster). In *Sustainable*

Nanotechnology Organization (SNO) conference, Arlington, VA, 2012.

- **Tiwari, A.J.,** Marr, L.C., Oxidation of C_{60} aerosols by ozone (poster). In *31st Annual Conference of the American Association for Aerosol Research (AAAR),* Minneapolis, MN, 2012.

- **Tiwari, A.J.,** Fields, C.G., Marr, L.C., A cost-effective method of aerosolizing dry powdered nanomaterials (poster). In *31st Annual Conference of the American Association for Aerosol Research (AAAR),* Minneapolis, MN, 2012.

- **Marr, L.C.**, Tiwari, A.J., Lu, J.W., Morris, J.R., Atmospheric transformations of carbonaceous nanomaterials (oral). At *American Chemical Society Spring 2012 National Meeting,* San Diego, CA, 2012.

- **Tiwari, A.J.,** Lu, J.W., Morris, J. R., Marr, L.C., Oxidation of C_{60} Aerosol by Ozone (poster). In *2011 European Aerosol Conference,* Manchester, U.K., 2011.

- **Tiwari, A.J**., Marr, L.C., Atmospheric Oxidation of C_{60} Fullerenes by Ozone (poster). In *Center for the Environmental Implications of Nanotechnology (CEINT), Internal Scientific Meeting,* Durham, NC, 2010.

- **Tiwari, A.J.,** Marr, L.C., Oxidation of Carbonaceous Nanoparticles in the Atmosphere: Effects of Ozonation on C_{60} Aqueous Solubility (oral). In *International Conference on*

the Environmental Implications of NanoTechnology (ICEIN 2009), Washington, D.C., 2009.

As a result of developing the aerosolization system discussed in Chapter 3, we collaborated with researchers at Aerodyne Research, Inc. and Boston College regarding the development of an aerosol measurement instrument, the soot particle aerosol mass spectrometer. Work stemming from that collaboration has been included in a publication:

- Onasch, T.G., Fortner, E.C., Trimborn, A.M., Lambe, A. T., Tiwari, A. J., Marr, L.C., Vander Wal, R. L., Williams, L. R., Worsnop, D. R., Davidovits, P. Aerosol mass spectrometry of refractory black carbon particles. *Atmospheric Measurement Techniques*, submitted.

References

1. Kroto, H. W.; Heath, J. R.; Obrien, S. C.; Curl, R. F.; Smalley, R. E. C-60 - Buckminsterfullerene. *Nature.* **1985,** *318*, (6042), 162-163.

2. Sariciftci, N. S.; Braun, D.; Zhang, C.; Srdanov, V. I.; Heeger, A. J.; Stucky, G.; Wudl, F. Semiconducting polymer-buckminsterfullerene heterojunctions - diodes, photodiodes, and photovoltaic cells *Appl. Phys. Lett.* **1993,** *62*, (6), 585-587.

3. Yu, G.; Gao, J.; Hummelen, J. C.; Wudl, F.; Heeger, A. J. Polymer photovoltaic cells - enhanced efficiences via a network of internal donor-acceptor heterojunctions *Science.* **1995,** *270*, (5243), 1789-1791.

4. Lopez, A. M.; Mateo-Alonso, A.; Prato, M. Materials chemistry of fullerene C-60 derivatives. *J. Mater. Chem.* **2011,** *21*, (5), 1305-1318.

5. Beckmeier, D.; Baumgartner, H. Metal-oxide-semiconductor diodes containing C-60 fullerenes for non-volatile memory applications. *J. Appl. Phys.* **2013,** *113*, (4), 6.

6. Bakry, R.; Vallant, R. M.; Najam-Ul-Haq, M.; Rainer, M.; Szabo, Z.; Huck, C. W.; Bonn, G. K. Medicinal applications of fullerenes. *Int. J. Nanomedicine.* **2007,** *2*, (4), 639-649.

7. Dellinger, A.; Zhou, Z. G.; Connor, J.; Madhankumar, A. B.; Pamujula, S.; Sayes, C. M.; Kepley, C. L. Application of fullerenes in nanomedicine: an update. *Nanomedicine.* **2013,** *8*, (7), 1191-1208.

8. Markovic, Z.; Trajkovic, V. Biomedical potential of the reactive oxygen species generation and quenching by fullerenes (C-60). *Biomaterials.* **2008,** *29*, (26), 3561-3573.

9. Hedburg, J. Free Science Images. http://www.jameshedberg.com/scienceGraphics.php?sort=all&id=carbon-nanotube-3D-model-axial (6 February 2014). <div xmlns:cc="http://creativecommons.org/ns" about="http://www.jameshedberg.com/scienceGraphics.php?sort=all&id=carbon-nanotube-3D-model-axial rel="cc:attributionURL" property="cc:attributionName" href="http://www.jameshedberg.com Hedberg / <a rel="license" href="http://creativecommons.org/licenses/by-nc-sa/3.0/ BY-NC-SA 3.0

10. Yeganeh, B.; Kull, C. M.; Hull, M. S.; Marr, L. C. Characterization of airborne particles during production of carbonaceous manomaterials. *Environ. Sci. Technol.* **2008,** *42*, (12), 4600-4606.

11. Mauter, M. S.; Elimelech, M. Environmental applications of carbon-based nanomaterials. *Environmental Science & Technology.* **2008,** *42*, (16), 5843-5859.

12. Nowack, B.; Bucheli, T. D. Occurrence, behavior and effects of nanoparticles in the environment. *Environ. Pollut.* **2007,** *150*, (1), 5-22.

13. Murr, L. E.; Bang, J. J.; Esquivel, E. V.; Guerrero, P. A.; Lopez, A. Carbon nanotubes, nanocrystal forms, and complex nanoparticle aggregates in common fuel-gas combustion sources and the ambient air. *J. Nanopart. Res.* **2004,** *6*, (2-3), 241-251.

14. Sanchís, J.; Berrojalbiz, N.; Caballero, G.; Dachs, J.; Farré, M.; Barceló, D. Occurrence of Aerosol-Bound Fullerenes in the Mediterranean Sea Atmosphere. *Environmental Science & Technology.* **2011**.

15. Benn, T.; Herckes, P.; Westerhoff, P. Fullerenes in Environmental Samples: C-60 in Atmospheric Particulate Matter. In *Analysis and Risk of Nanomaterials in Environmental and Food Samples*, Elsevier Science Bv: Amsterdam, 2012; Vol. 59, pp 291-303.

16. Sanchis, J.; Bozovic, D.; Al-Harbi, N. A.; Silva, L. F.; Farre, M.; Barcelo, D. Quantitative trace analysis of fullerenes in river sediment from Spain and soils from Saudi Arabia. *Anal. Bioanal. Chem.* **2013,** *405*, (18), 5915-5923.

17. Farre, M.; Perez, S.; Gajda-Schrantz, K.; Osorio, V.; Kantiani, L.; Ginebreda, A.; Barcelo, D. First determination of C(60) andC(70) fullerenes and N-methylfulleropyrrolidine C(60) on the suspended material of wastewater effluents by liquid chromatography hybrid quadrupole linear ion trap tandem mass spectrometry. *J. Hydrol.* **2010,** *383*, (1-2), 44-51.

18. Buseck, P. R.; Tsipursky, S. J.; Hettich, R. Fullerenes from the geological environment. *Science.* **1992,** *257*, (5067), 215-217.

19. Jehlicka, J.; Svatos, A.; Frank, O.; Uhlik, F. Evidence for fullerenes in solid bitumen from pillow lavas of proterozoic age from Mitov (Bohemian Massif, Czech Republic). *Geochim. Cosmochim. Acta.* **2003,** *67*, (8), 1495-1506.

20. RNCOS, I. R. S. Nanotechnology Market Forecast to 2014. **2012**, 175.

21. Kankanala, R.; Ganugapati, J.; Vutukuru, S. S.; Sai, K. Molecular Docking Analysis of Fullerene (C-60) with Human Antioxidant Enzymes: Implications in Inhibition of Enzymes. *J. Comput. Theor. Nanosci.* **2013,** *10*, (6), 1403-1407.

22. Trpkovic, A.; Todorovic-Markovic, B.; Trajkovic, V. Toxicity of pristine versus functionalized fullerenes: mechanisms of cell damage and the role of oxidative stress. *Arch. Toxicol.* **2012,** *86*, (12), 1809-1827.

23. Ema, M.; Kobayashi, N.; Naya, M.; Hanai, S.; Nakanishi, J. Reproductive and developmental toxicity studies of manufactured nanomaterials. *Reprod. Toxicol.* **2010,** *30*, (3), 343-352.

24. Ding, N.; Kunugita, N.; Ichinose, T.; Song, Y.; Yokoyama, M.; Arashidani, K.; Yoshida, Y. Intratracheal administration of fullerene nanoparticles activates splenic CD11b(+) cells. *J. Hazard. Mater.* **2011,** *194*, 324-330.

25. Zhu, S. Q.; Oberdorster, E.; Haasch, M. L. Toxicity of an engineered nanoparticle (fullerene, C-60) in two aquatic species, Daphnia and fathead minnow. *Mar. Environ. Res.* **2006,** *62*, S5-S9.

26. Oberdorster, E. Manufactured nanomaterials (Fullerenes, C-60) induce oxidative stress in the brain of juvenile largemouth bass. *Environ. Health Perspect.* **2004,** *112*, (10), 1058-1062.

27. Li, S.; Zhao, X. C.; Mo, Y. M.; Cummings, P. T.; Heller, W. T. Human serum albumin interactions with C-60 fullerene studied by spectroscopy, small-angle neutron scattering, and molecular dynamics simulations. *J. Nanopart. Res.* **2013,** *15*, (7), 11.

28. Fiorito, S.; Serafino, A.; Andreola, F.; Bernier, P. Effects of fullerenes and single-wall carbon nanotubes on murine and human macrophages. *Carbon.* **2006,** *44*, (6), 1100-1105.

29. Ogami, A.; Yamamoto, K.; Morimoto, Y.; Fujita, K.; Hirohashi, M.; Oyabu, T.; Myojo, T.; Nishi, K.; Kadoya, C.; Todoroki, M.; Yamamoto, M.; Murakami, M.; Shimada, M.; Wang, W. N.; Shinohara, N.; Endoh, S.; Uchida, K.; Nakanishi, J.; Tanaka, I. Pathological features of rat lung following inhalation and intratracheal instillation of C-60 fullerene. *Inhal. Toxicol.* **2011,** *23*, (7), 407-416.

30. Ema, M.; Matsuda, A.; Kobayashi, N.; Naya, M.; Nakanishi, J. Dermal and ocular irritation and skin sensitization studies of fullerene C-60 nanoparticles. *Cutan. Ocul. Toxicol.* **2013,** *32*, (2), 128-134.

31. Liu, X. Y.; Vinson, D.; Abt, D.; Hurt, R. H.; Rand, D. M. Differential Toxicity of Carbon Nanomaterials in Drosophila: Larval Dietary Uptake Is Benign, but Adult Exposure Causes Locomotor Impairment and Mortality. *Environ. Sci. Technol.* **2009,** *43*, (16), 6357-6363.

32. Santos, S. M. A.; Dinis, A. M.; Rodrigues, D. M. F.; Peixoto, F.; Videira, R. A.; Jurado, A. S. Studies on the toxicity of an aqueous suspension of C-60 nanoparticles using a bacterium (gen. Bacillus) and an aquatic plant (Lemna gibba) as in vitro model systems. *Aquat. Toxicol.* **2013,** *142*, 347-354.

33. De La Torre-Roche, R.; Hawthorne, J.; Deng, Y. Q.; Xing, B. S.; Cai, W. J.; Newman, L. A.; Wang, Q.; Ma, X. M.; Hamdi, H.; White, J. C. Multiwalled Carbon Nanotubes and C-60 Fullerenes Differentially Impact the Accumulation of Weathered Pesticides in Four Agricultural Plants. *Environmental Science & Technology.* **2013,** *47*, (21), 12539-12547.

34. Marques, B. F.; Cordeiro, L. F.; Kist, L. W.; Bogo, M. R.; Lopez, G.; Pagano, G.; Muratt, D. T.; de Carvalho, L. M.; Kulkamp-Guerreiro, I. C.; Monserrat, J. M. Toxicological effects

induced by the nanomaterials fullerene and nanosilver in the polychaeta Laeonereis acuta (Nereididae) and in the bacteria communities living at their surface. *Mar. Environ. Res.* **2013,** *89*, 53-62.

35. Van der Ploeg, M. J. C.; Handy, R. D.; Heckmann, L. H.; Van der Hout, A.; Van den Brink, N. W. C-60 exposure induced tissue damage and gene expression alterations in the earthworm Lumbricus rubellus. *Nanotoxicology.* **2013,** *7*, (4), 432-440.

36. Hancock, D. E.; Indest, K. J.; Gust, K. A.; Kennedy, A. J. Effects of C60 on the Salmonella typhimurium TA100 transcriptome expression: Insights into C60-mediated growth inhibition and mutagenicity. *Environ. Toxicol. Chem.* **2012,** *31*, (7), 1438-1444.

37. Fang, J. S.; Lyon, D. Y.; Wiesner, M. R.; Dong, J. P.; Alvarez, P. J. J. Effect of a fullerene water suspension on bacterial phospholipids and membrane phase behavior. *Environ. Sci. Technol.* **2007,** *41*, (7), 2636-2642.

38. Lyon, D. Y.; Adams, L. K.; Falkner, J. C.; Alvarez, P. J. J. Antibacterial activity of fullerene water suspensions: Effects of preparation method and particle size. *Environ. Sci. Technol.* **2006,** *40*, (14), 4360-4366.

39. Li, D.; Lyon, D. Y.; Li, Q.; Alvarez, P. J. J. Effect of soil sorption and aquatic natural organic matter on the antibacterial activity of a fullerene water suspension. *Environ. Toxicol. Chem.* **2008,** *27*, (9), 1888-1894.

40. Nyberg, L.; Turco, R. F.; Nies, L. Assessing the impact of nanomaterials on anaerobic microbial communities. *Environ. Sci. Technol.* **2008,** *42*, (6), 1938-1943.

41. Tong, Z. H.; Bischoff, M.; Nies, L.; Applegate, B.; Turco, R. F. Impact of fullerene (C-60) on a soil microbial community. *Environ. Sci. Technol.* **2007,** *41*, (8), 2985-2991.

42. Wang, L. L.; Fortner, J. D.; Hou, L.; Zhang, C. D.; Kan, A. T.; Tomson, M. B.; Chen, W. Contaminant-mobilizing capability of fullerene nanoparticles (nC60): Effect of solvent-exchange process in nC60 formation. *Environ. Toxicol. Chem.* **2013,** *32*, (2), 329-336.

43. Kong, L. J.; Zepp, R. G. Production and consumption of reactive oxygen species by fullerenes. *Environ. Toxicol. Chem.* **2012,** *31*, (1), 136-143.

44. Hotze, E. M.; Labille, J.; Alvarez, P.; Wiesner, M. R. Mechanisms of photochemistry and reactive oxygen production by fullerene suspensions in water. *Environ. Sci. Technol.* **2008,** *42*, (11), 4175-4180.

45. Pickering, K. D.; Wiesner, M. R. Fullerol-sensitized production of reactive oxygen species in aqueous solution. *Environmental Science & Technology.* **2005,** *39*, (5), 1359-1365.

46. Nowack, B.; Ranville, J. F.; Diamond, S.; Gallego-Urrea, J. A.; Metcalfe, C.; Rose, J.; Horne, N.; Koelmans, A. A.; Klaine, S. J. Potential scenarios for nanomaterial release and subsequent alteration in the environment. *Environ. Toxicol. Chem.* **2012,** *31*, (1), 50-59.

47. Wang, Z. Y.; von dem Bussche, A.; Kabadi, P. K.; Kane, A. B.; Hurt, R. H. Biological and Environmental Transformations of Copper-Based Nanomaterials. *ACS Nano.* **2013,** *7*, (10), 8715-8727.

48. Levard, C.; Hotze, E. M.; Lowry, G. V.; Brown, G. E. Environmental Transformations of Silver Nanoparticles: Impact on Stability and Toxicity. *Environmental Science & Technology.* **2012,** *46*, (13), 6900-6914.

49. Tiwari, A. J.; Marr, L. C. The Role of Atmospheric Transformations in Determining Environmental Impacts of Carbonaceous Nanoparticles. *Journal of Environmental Quality.* **2010,** *39*, (6), 1883-1895.

50. Lambe, A. T.; Cappa, C. D.; Massoli, P.; Onasch, T. B.; Forestieri, S. D.; Martin, A. T.; Cummings, M. J.; Croasdale, D. R.; Brune, W. H.; Worsnop, D. R.; Davidovits, P. Relationship between Oxidation Level and Optical Properties of Secondary Organic Aerosol. *Environmental Science & Technology.* **2013,** *47*, (12), 6349-6357.

51. Burns, J. M.; Pennington, P. L.; Sisco, P. N.; Frey, R.; Kashiwada, S.; Fulton, M. H.; Scott, G. I.; Decho, A. W.; Murphy, C. J.; Shaw, T. J.; Ferry, J. L. Surface Charge Controls the Fate of Au Nanorods in Saline Estuaries. *Environmental Science & Technology.* **2013,** *47*, (22), 12844-12851.

52. Jackson, P.; Jacobsen, N. R.; Baun, A.; Birkedal, R.; Kuhnel, D.; Jensen, K. A.; Vogel, U.; Wallin, H. Bioaccumulation and ecotoxicity of carbon nanotubes. *Chem. Cent. J.* **2013,** *7*, 21.

53. Kopova, I.; Bacakova, L.; Lavrentiev, V.; Vacik, J. Growth and Potential Damage of Human Bone-Derived Cells on Fresh and Aged Fullerene C-60 Films. *Int. J. Mol. Sci.* **2013,** *14*, (5), 9182-9204.

54. Finlayson-Pitts, B.; Pitts, J., *Chemistry of the Upper and Lower Atmosphere*. Academic Press: 2000.

55. Fortner, J. D.; Kim, D. I.; Boyd, A. M.; Falkner, J. C.; Moran, S.; Colvin, V. L.; Hughes, J. B.; Kim, J. H. Reaction of water-stable C-60 aggregates with ozone. *Environ. Sci. Technol.* **2007,** *41*, (21), 7497-7502.

56. Bulgakov, R. G.; Nevyadovskii, E. Y.; Belyaeva, A. S.; Golikova, M. T.; Ushakova, Z. I.; Ponomareva, Y. G.; Dzhemilev, U. M.; Razumovskii, S. D.; Valyamova, F. G. Water-soluble polyketones and esters as the main stable products of ozonolysis of fullerene C-60 solutions. *Russ. Chem. Bull.* **2004,** *53*, (1), 148-159.

57. Heymann, D.; Bachilo, S. M.; Aronson, S. Thermolysis and photolysis of C-60 diozonides. *Fuller. Nanotub. Carbon Nanostruct.* **2005,** *13*, (1), 73-88.

58. Cataldo, F. Ozone reaction with carbon nanostructures 1: Reaction between solid C-60 and C-70 fullerenes and ozone. *J. Nanosci. Nanotechnol.* **2007,** *7*, (4-5), 1439-1445.

59. Biskos, G.; Vons, V.; Yurteri, C. U.; Schmidt-Ott, A. Generation and sizing of particles for aerosol-based nanotechnology. *KONA Powder Part. J.* **2008,** *26*, 13-35.

60. Masuda, H. Dry dispersion of fine particles in gaseous phase. *Adv. Powder Technol.* **2009,** *20*, (2), 113-122.

61. Calvert, G.; Ghadiri, M.; Tweedie, R. Aerodynamic dispersion of cohesive powders: A review of understanding and technology. *Adv. Powder Technol.* **2009,** *20*, (1), 4-16.

62. Fujitani, Y.; Kobayashi, T.; Arashidani, K.; Kunugita, N.; Suemura, K. Measurement of the physical properties of aerosols in a fullerene factory for inhalation exposure assessment. *J. Occup. Environ. Hyg.* **2008,** *5*, (6), 380-389.

63. Maynard, A. D.; Baron, P. A.; Foley, M.; Shvedova, A. A.; Kisin, E. R.; Castranova, V. Exposure to carbon nanotube material: Aerosol release during the handling of unrefined single-walled carbon nanotube material. *J. Toxicol. Env. Health Pt A.* **2004,** *67*, (1), 87-107.

Chapter 2 – The Role of Atmospheric Transformations in Determining the Environmental Impacts of Carbonaceous Nanoparticles

Andrea J. Tiwari and Linsey C. Marr*

Submitted: February 2010
To: Journal of Environmental Quality
Status: Published November-December 2010

Abstract

In studies that have explored the potential environmental impacts of manufactured nanomaterials, the atmosphere has largely been viewed as an inert setting that acts merely as a route for inhalation exposure. Manufactured nanomaterials will enter the atmosphere during production, use, and disposal, and rather than simply being transported, airborne nanoparticles are in fact subject to physical and chemical transformations that could modify their fate, transport, bioavailability, and toxicity once they deposit to aqueous and terrestrial ecosystems.

The objective of this paper is to review the factors affecting carbonaceous nanomaterials' behavior in the environment and to show that atmospheric transformations, often overlooked, have the potential to alter nanoparticles' physical and chemical properties and thus influence their environmental fate and impact. Atmospheric processing of naturally occurring and incidental nanoparticles takes place through coagulation, condensation, and oxidation; these phenomena are expected to affect manufactured nanoparticles as well. It is likely that

carbonaceous nanomaterials in the atmosphere will be oxidized, effectively functionalizing them. By influencing size, shape, and surface chemistry, atmospheric transformations have the potential to affect a variety of nanoparticle-environment interactions, including solubility, interaction with natural surfactants, deposition to porous media, and ecotoxicity. Potential directions for future research are suggested to address the current lack of information surrounding atmospheric transformations of engineered nanomaterials.

Introduction

In recent years, many scientists and policymakers have raised concerns about the potential health and environmental risks of manufactured nanoparticles (NPs).[1-12] The great diversity of NPs being produced today supports a wide variety of industrial and consumer applications, such as appliances, surface coatings, automobile parts, electronics, sunscreen, and cosmetics, but also presents unknown health and environmental effects.[3-6, 13]

Due to the unique physical and chemical properties of manufactured NPs, they may behave very differently in the environment from their bulk forms, as well as from natural and incidental NPs. Natural NPs are those produced in the environment by wildfires, volcanic eruptions, sea spray, erosion, and biological and geological processes. Incidental NPs are unintentional byproducts of human activities. For example, combustion of fossil fuels and industrial processes produce incidental NPs. The magnitude and nature of manufactured NPs' potentially novel environmental impacts remain open questions. Concentrations of manufactured NPs in the environment have not yet been reported,[3] but just as other industrial chemicals such as polychlorinated biphenyls have spread to all corners of the earth, from ocean sediment to Arctic air,[14] manufactured nanoparticles are also likely to find their way into every ecosystem.

Inevitably, the production, use, and disposal of NPs will introduce them into groundwater, surface water, soil, and the atmosphere. Their movements within and between these media, and their effects on biota, remain largely unknown.[3, 15, 16] They may flow directly into natural waters from domestic and industrial wastewater if they are not eliminated by wastewater treatment processes.[17, 18] They may be emitted into the atmosphere by manufacturing facilities, consumer products during use, or accidental releases.[3, 5, 19-22] The dominant cross-media transport of NPs in the environment is likely to be deposition from the atmosphere the surface, although it is also possible for NPs to be suspended from aqueous and terrestrial systems by waves, bubbles, and wind.

The presence of manufactured NPs in the atmosphere is of concern to both human and environmental health. Inhalation of nanoscale particles has been linked to adverse effects on the pulmonary and cardiovascular systems.[23, 24] In sufficient quantities, such particles could also affect visibility and climate. In studies that have explored the potential environmental impacts of manufactured nanomaterials, the atmosphere has largely been viewed as an inert setting that acts merely as a route for inhalation exposure. However, particles in the atmosphere can undergo physical and chemical changes, which could alter their health and environmental effects. Cross-media effects (i.e., transformations in the atmosphere that may affect fate in the aquatic or terrestrial environments or vice versa) have been largely overlooked in discussions of the environmental impacts of NPs.

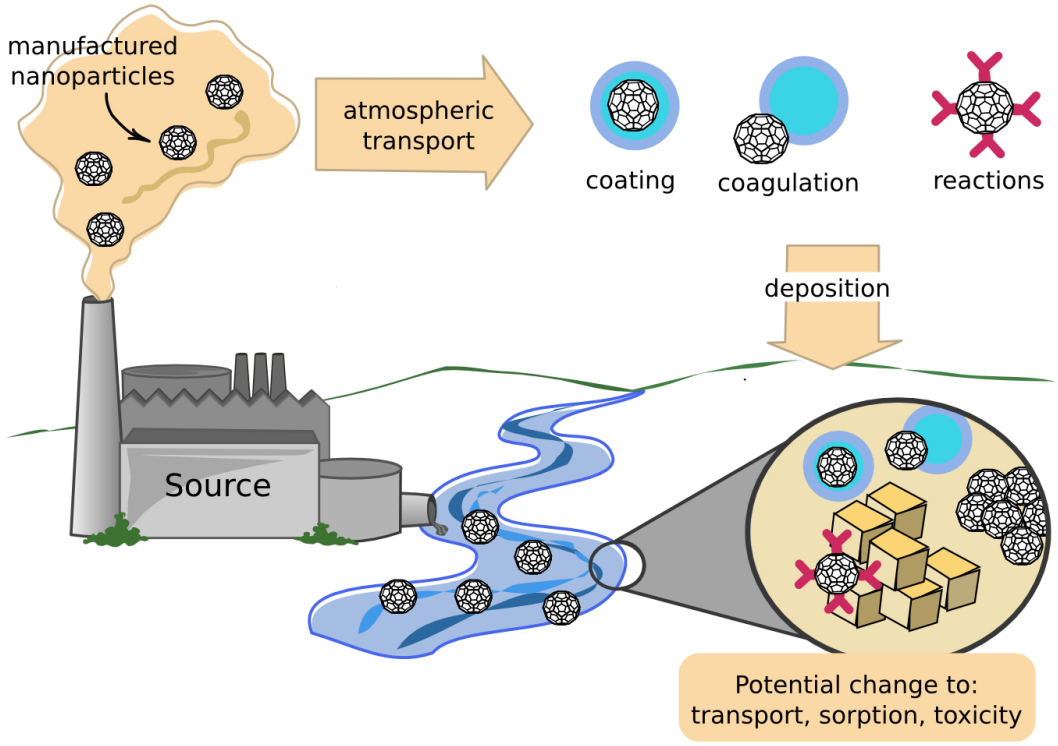

Figure 2-1: Potential routes of carbonaceous nanoparticles (CNPs), depicted here by a C_{60} fullerene, to the natural aqueous environment. CNPs may be discharged directly to a natural waterway, or may deposit there after having been emitted to the atmosphere. Between emission and deposition, a variety of atmospheric transformations may occur. These transformations could alter CNP behavior in the aqueous environment. Used with permission of Dr. Nina Eller Quadros.

A complete assessment of the environmental impacts of nanotechnology must consider the possibility that NPs could undergo physical and chemical transformations in the atmosphere that could alter their fate and transport when they deposit to aqueous or terrestrial settings, as depicted in Figure 2-1. Particles in the atmosphere are subject to coagulation, surface coating through condensation of semivolatile compounds, and heterogeneous reactions with gaseous pollutants. The atmosphere contains strong oxidants, such as the hydroxyl and nitrate radicals, and ozone. The oxidation of NPs could alter their surface chemistry enough to affect their solubility and/or their propensity to aggregate once they enter an aqueous or terrestrial

environment. These changes could then affect bioavailability, toxicity, and deposition in porous media.

The goal of this review is to illuminate the importance of atmospheric transformations in determining the fate and transport of NPs in the environment, and to identify gaps in knowledge that should be targeted for future research. We focus on carbonaceous nanoparticles (CNPs), specifically C_{60} fullerenes and carbon nanotubes (CNTs), because of their large production volumes, probable toxicity, and relatively richer history in the literature. In an inventory of consumer products, those containing CNPs account for the second highest number of applications; only silver nanoparticles are used more extensively.[25] Additionally, the wealth of studies involving soot, which consists mostly of amorphous carbon and possibly some fullerenes and carbon nanotubes, may inform the findings for fullerenes. The specific objectives of this review are to: (i) synthesize information on the physical and chemical transformations that CNPs may undergo in the atmosphere, (ii) propose how such transformations may affect fate and transport of CNPs in aquatic and terrestrial systems, and (iii) identify future research directions aimed at filling the gaps in knowledge regarding cross-media effects on CNPs' fate and transport in the environment.

Physical transformations in the atmosphere

Atmospheric scientists describe NPs as ultrafine particles, a category consisting of particles smaller than ~10 nm (referred to as nucleation mode) and those from ~10-100 nm (referred to as Aitken mode). Particles in this size range originate mainly from combustion and photochemical reactions involving sulfuric acid or organic compounds with low volatility. Natural and incidental NPs dominate the number distribution of particles in the atmosphere. In polluted

urban, rural, remote continental, and marine atmospheres, typical concentration ranges are 10^5 – 4×10^6 cm^{-3}, 2000 – 10,000 cm^{-3}, 50-10,000 cm^{-3}, and 100-400 cm^{-3}, respectively.[26] The physical transformations that naturally occurring and incidental NPs undergo in the atmosphere are well understood and will apply to engineered NPs also. These transformations will change the particles' size and morphology. NPs tend to grow larger and fewer by coagulation with other particles. They may also increase in size due to condensation of low-volatility compounds in the atmosphere onto the particles' surfaces.

For submicron particles, coagulation is dominated by Brownian (i.e., thermal) motion that leads particles to collide with each other, grow in size, and shrink in number. Coagulation could lead to a new class of particles that consists of an engineered NP combined with a naturally occurring one. Coagulation rates are low when particles are of the same size but increase by orders of magnitude as the difference in size grows. This occurs because of the synergism between a high Brownian diffusivity of the smaller particle and large surface area available for contact with the bigger particle. The timescale for coagulation is heavily dependent on the particle size of interest and background particle size distribution. In a monodisperse population of 20-nm particles, the timescales for coagulation in urban and rural settings are ~10 min and ~10 h, respectively. The timescale in polydisperse particle size distributions measured in urban to rural locations in Denmark has been estimated to be 16 to 25 h,[27] and corresponding physical modeling predicts a decrease in number concentration of 13-23%.[28] Coagulation of engineered NPs will be maximal when the size distribution is polydisperse and number concentrations are high. For incidental and natural NPs, such situations are most commonly encountered near roadways and during "bursts" of nucleation-mode particles[29] involving sulfuric acid or ions.[30] For engineered NPs, conditions

ideal for coagulation are most likely to be found in accidental industrial releases or in exhaust that contains a mixture of incidental and engineered NPs.

Nanoparticles in the atmosphere may grow via condensation of semi-volatile compounds and water, where the NP forms the core of the particle and the condensed material the shell. Both inorganic compounds, often sulfate, nitrate, and ammonium, and organic compounds may coat pre-existing particles. Typical growth rates are 1-20 nm h^{-1} and are highest during the summer in urban and some marine areas.[30] Over the course of a day, a 30-nm engineered NP could grow large enough to no longer be considered nanoscale, but the engineered NP would remain at the "fattened" particle's core. In polluted atmospheres, fresh soot particles can become coated by ammonium sulfate in as little as 1 h.[31] Common types of naturally occurring particles in the atmosphere consist of a black carbon, or soot, core covered by aqueous-phase components and organic compounds condensed on dust.[32] Analogously, carbonaceous and metallic engineered NPs could become internally mixed by condensation of organic and inorganic compounds on the particle surface. Condensational growth not only makes particles larger but also makes particles more spherical,[32, 33] so the high aspect ratio of CNTs could be reduced by this process. While we have treated coagulation and condensation separately in this discussion, both can occur simultaneously.

Coagulation and condensation can obviously modify the morphology of the outline, or skin, of particles, but the skeletons of core particles may also undergo rearrangement. In laboratory experiments, fractal soot particles have been found to collapse to more compact structures on coating with an organic compound[33] or wetting.[34] Based on these results, it is possible that fractal

and non-spherical engineered NPs, such as aggregated fullerenes and tangles of CNTs, could become more spherical through atmospheric processing.

Particles are removed from the atmosphere mainly by Brownian diffusion, gravitational settling, and wet deposition in precipitation to the Earth's surface. The time scale for wet deposition is highly dependent on the frequency of precipitation events in any given location. During a precipitation event, atmospheric nanoparticles may be removed via wet deposition mechanisms in a matter of minutes to hours[26, 35, 36] depending upon precipitation type and particle size. The timescale for removal by dry deposition (primarily diffusion and settling) in an urban area is ~20 h for particle size distributions considered in Denmark with median diameters of 40 to 50 nm.[27] The efficiency of removal reaches a minimum for a particle size range of 100 to 1000 nm. So if engineered NPs grow into this size range by coagulation and/or condensation, their lifetimes in the atmosphere may be extended from hours to days. In this case, not only has their size changed, but because of their longer lifetimes, they have also become more susceptible to heterogeneous chemical transformations, which are described in the following section. Further processing can occur in cloud droplets, where aqueous-phase reactions take place.

Observing and understanding physical transformations of engineered NPs in the atmosphere will require the ability to distinguish them from background (naturally occurring and incidental) NPs, which under most conditions will be dominant in number by orders of magnitude. Distinguishing between the two will be easier for exotic metals that are not present in ambient particles but especially challenging for carbonaceous particles because soot, a combustion byproduct, contains fullerenic compounds and carbon nanostructures.[37] Recently, researchers developed a near-

infrared fluorescence spectroscopic method capable of detecting single-walled carbon nanotubes in complex environmental matrices (Ferguson, L. P., 2009, personal communication), and future research in this vein is needed. A second topic for future research is to determine how the properties of engineered NPs change if atmospheric processing creates "internally mixed" particles, which may consist of combinations of material from different sources. Do engineered NPs retain any of their catalytic, therapeutic, or toxicological properties? A third topic for future research is the treatment of engineered NPs in atmospheric chemical-transport models. Those currently used for regulatory purposes lump NPs together with all "fine" particles smaller than ~2.5 μm and treat them on the basis of mass, an approach that favors larger particles. Can existing aerosol modules be extended to account for engineered NPs simply as another chemical species? Or, are new or more detailed representations needed? It may be necessary to incorporate more highly resolved particle size distributions within models in order to address size-specific behavior of manufactured NPs.

Oxidation

It is well established that organic aerosols in the atmosphere are oxidized by reactions with hydroxyl radicals, ozone, and other oxidants, leading to the formation of oxide, carbonyl, hydroxyl, carboxylic acid, and other functionalities that make the particles more hydrophilic.[38] Evidence suggests that CNPs may undergo similar reactions. This section considers the oxidation of CNPs in both liquid and gaseous systems because results from one phase are expected to inform the other. Oxidation is important because it should increase CNPs' solubility, which is critical for determining environmental effects.

The majority of studies on fullerene oxidation in liquids have involved an organic solvent, most commonly toluene. One of the earliest studies of solution-based fullerene oxidation showed that bubbling ozone (O_3) gas through solutions of C_{60} and/or C_{70} in toluene produces fullerene dimers: C_{119}, C_{129}, and C_{139}.[39] In similar types of experiments, epoxides $C_{60}O_n$ (n = 1 – 5) are also produced.[40-42] Dimerization is very unlikely to take place in atmospheric systems because dispersion would dilute fullerenes to levels that are unfavorable to the reaction. However, ozone in the atmosphere could be responsible for the formation of oxides. Oxides are likely to have lower octanol-water partitioning coefficients and thus to be more mobile in aqueous systems. Additionally, even short (5 min) ozone exposures in toluene result in the precipitation of highly oxidized derivatives of C_{60}, exhibiting ester, ketone, and epoxide functionalities.[43] These functionalities may have environmental implications, as discussed below.

The kinetics and products of fullerene oxidation reactions in organic solvents are influenced by oxidizing species, temperature, and fullerene type. These three variables could all be relevant to atmospheric processing of fullerenes. Firstly, ozone is a much more effective oxidant of C_{60} than molecular oxygen, producing a reaction rate five orders of magnitude higher in a toluene solution.[44] C_{60} and C_{70} oxidize readily in toluene solution at temperatures ranging from -78 ºC to 100 ºC, and C_{70} seems to be more resistant to oxidation. Rupture of the fullerene cages may occur at $C_{60}O_5$ and $C_{70}O_3$. Cage rupture may be important for engineered NPs because it could result in the release of metals contained inside endohedral metallofullerenes, which show promising applications in medicine and energy. Although toluene itself had been thought to play a negligible role in the fullerene oxidation process, it is not completely inert to O_3. An intermediate product of toluene ozonolysis could also serve as an oxidizing agent, complicating

the kinetics of the reaction. Toluene and other organic compounds are present in polluted atmospheres. So they too, in addition to traditional oxidants, might participate in chemical transformations of CNPs.

Carbonaceous nanoparticles in the natural environment, however, will not be present in an organic solvent but rather in an aqueous solution. Aqueous C_{60} colloids prepared using tetrahydrofuran as an intermediate solvent (THF/nC_{60}) oxidize readily upon exposure to an O_2/O_3 gas stream. The reaction rate increases slightly at higher pH values.[45] As many as 27 moles of O_3 are consumed per mole of C_{60}, a ratio much higher than in organic solvents and in agreement with an earlier study.[46] The resulting molecules are soluble in an aqueous system, exhibiting hydroxyl and hemiketal (R-O-C-OH) functionalities, and maintaining their carbon cage structure.[45] These results could be relevant to fullerenes in the atmosphere that become coated by a film of water.

Carbon nanotubes can also be oxidized in aqueous solutions when exposed to ozone. Bubbling 5% ozone through a suspension of single-walled carbon nanotubes (SWNTs) results in increased particle stability in solution, decreased particle diameter, decreased zeta potential, and the formation of hydroxyl, carbonyl, and carboxyl groups.[47] Interestingly, a separate study found that while electrophoretic mobility is poorly correlated with the stability of oxidized CNTs in solution, surface charge is a much more accurate indicator.[48] As studies begin to investigate the aqueous behavior of atmospherically processed CNTs, surface charge will be an important parameter to monitor.

Of course, studies examining the reactions between O_3 and fullerenes in the gas phase are the most informative for atmospheric processing. Summarized in Table 2-1, these studies, while fewer in number than those in the liquid phase, demonstrate that reaction pathways are influenced by temperature, oxidant identity, and fullerene type. Upon exposure to 2.6% O_3 at room temperature, crystalline C_{60} disappears slowly, losing 80% of fullerenes after 7 d and producing no detectable oxides.[44] Heating the crystalline C_{60} in ambient air to 250 ºC produces no definitive evidence of C_{60} oxidation. Compared to pure C_{60}, a mixture of 90% C_{60} and 10% C_{70} is much more susceptible to oxidation from O_2 in air at 300 ºC.[49] As a result, fullerenic materials exhausted from various combustion sources[50] at high temperatures may undergo oxidation if C_{70} molecules are present. It is evident that investigations into the reaction kinetics of fullerenes will have to carefully consider exact nanomaterial speciation.

At high ozone levels, both C_{60} and C_{70} oxidize readily. Exposing C_{60} and C_{70} separately to O_2 with a 6.4% v/v concentration of O_3 at room temperature results in the formation of gaseous CO_2 and the development of carboxyl, ketone, and aldehyde groups on the C_{60} sample; similar results are seen for C_{70}.[51] These functional groups could influence the reactivity, toxicity, fate, and transport of oxidized fullerenes on introduction to the aquatic or terrestrial environment, as discussed below. Here again, the atmospheric relevance of these results is unknown because the ozone concentration used in the experiments is six orders of magnitude higher than typically observed in the lower layer of the atmosphere. Plus, the atmosphere is composed of 78% molecular nitrogen and 21% O_2 rather than pure O_2.

Table 2-1: Results of gas-phase oxidation experiments with carbonaceous nanoparticles (CNPs).

CNP species*	Initial conditions	Pressure	T	Oxidant and concentration (volumetric)	Duration	Functional groups/ results	Reference
C_{60}	> 0.01 mol% other fullerenes	N/A**	298 K	2.6% O_3	7 d	80% C_{60} lost	44
90% C_{60}, 10% C_{70}	C:O ratio = 31.9	N/A**	573 K	Air	24 h	C:O ratio = 2.3	49
C_{60}	99+% pure	N/A§	N/A§	6.4% O_3	~16 min	Carboxyl, aldehyde, ketone	51
C_{70}	98+% pure	N/A§	N/A§	6.4% O_3	~16 min	Carboxyl, aldehyde, ketone	51
SWNT	No data; pretreated at 1073 K	No data; low pressure	298 K	~70% O_3	~100 Torr·min	Ester, quinone; CO, CO_2 produced	52
SWNT	No data; pretreated at 373 K	$7 \cdot 10^{-4}$ to $1 \cdot 10^{-2}$ atm	300 K	~70% O_3	Up to 6 h	Ester, quinone; CO, CO_2 produced	53
SWNT	No data	~ 1 atm	298 K	[O_3] not monitored; ~10 μW cm^{-2} and 1 mW cm^{-2} UV lamps, ambient air	Up to 400 min	Carbonyl, ether, or epoxide (1 mW cm^{-2})	54
DWNT	No data; pretreated at ~1000 °C	$3 \cdot 10^{-11}$ to $2 \cdot 10^{-10}$ atm	298 K	Atomic oxygen	Up to 260 min	Ether, epoxy (initially); carbonyls (ultimately)	55
MWNT	90% pure, 10% residual catalyst	N/A§	N/A§	≤ 6.3%	Up to ~2 h	Ketones	56

* SWNT, single-walled carbon nanotube; MWNT, multiwalled carbon nanotube; DWNT, double-walled carbon nanotube.
** Not specified, but the experiment is believed to have been conducted near standard pressure.
§ Not specified, but the chamber is believed to be near standard temperature and pressure.

While O_3 is a more efficient oxidant than O_2, C_{60} will react with O_2 under certain conditions. Subjecting crystalline C_{60} to mechanical stress in a vibrational ball mill in a pure oxygen atmosphere for several hours results in an average fullerene composition of $C_{60}O_{8.6}$.[57] The reaction seems to require singlet molecular oxygen ($^1O_2$), which is generated by the process. Theoretical investigations of C_{60} oxides indicate that $C_{60}O$ should have two isomers, differentiated by the position of the oxygen bridge (over the 5-6 or 6-6 C-C bond on the fullerene cage), and that the most common isomer of $C_{60}O$ exhibits the 6-6 bridging.[58, 59] The interconversion pathway between the two isomers presents a large energy barrier, so isolating the two isomers from one another should be possible.[60] The addition of oxygen over 6-6 bonds only disturbs the local carbon network, leaving the majority of the fullerene cage unchanged electronically.[61] The importance of this difference for environmental impacts is unknown.

One of the earliest studies of CNT oxidation was conducted in the absence of a solvent and used Fourier Transform Infrared Spectroscopy to track the reaction of SWNTs with ozone. Upon exposure to 70% O_3 and 30% O_2 under low-pressure conditions, ester and quinone groups form, as do carbon monoxide and dioxide gases, indicating the removal of carbon from the SWNT sample.[52] The authors suggest that the reaction slows with higher O_3 exposures because SWNT endcaps are consumed, reducing the number of preferential reaction sites. Further work indicates the formation of hydroxyl and carboxyl groups on the surface, as well as the evolution of a broad carbonyl band.[53] Other studies have found that O_3 exposure leads to the formation of a variety of ketonic groups on multi-walled carbon nanotubes (MWNTs)[56] and carbonyl and epoxide groups on SWNT sidewalls.[54] Under low-pressure conditions, ether and epoxide groups may form on double-walled nanotubes (DWNTs) within a matter of minutes.[55] If atmospheric processing of

CNTs results in the formation of oxygen-containing functional groups, as these studies suggest, this outcome may affect CNTs' interactions with natural organic matter (NOM), deposition to porous media, and ecotoxicity.

The extent to which oxidation of CNPs in the atmosphere will take place remains unknown. Most airborne CNPs would not come into contact with extremely high O_3 levels or temperatures, and CNPs undergoing erosion would likely not be subject to the strain present in a ball mill. While the lowest O_3 mixing ratio tested in the previously mentioned experiments was 2.6%, typical ambient concentrations are five to six orders of magnitude smaller. Other compounds, such as the hydroxyl and nitrate radicals, intermediates of photochemical ozone production, and acid gases, may also participate in CNP chemistry in the atmosphere. However, such reactions have not yet been investigated in laboratory studies.

Future work is needed to determine the rates at which airborne CNPs will be oxidized, and to identify the reaction products. First, lower, atmospherically relevant oxidant concentrations should be investigated in carrier gases that have more similar composition to the actual atmosphere, including photochemically generated species. Second, the oxidation of CNPs in an atmospherically relevant state, such as aerosolized nanoscale particles, must be investigated, since some CNPs will be emitted in this form. Aerosolized CNPs will have a far greater specific surface area exposed for potential oxidation than the powders used in the studies described above. Thus, actual reaction rates could be higher than the apparent ones that have been reported. Studies of gas-phase kinetics of CNP oxidation will need to characterize carefully the species contained within an NP sample. Since a 90:10 C_{60}:C_{70} mixture is much more prone to oxidation

than C_{60} alone, measures must be taken to understand not only the content of a sample, but the impact different CNP species may have on one another during an oxidative process. If aerosolized CNPs become oxidized to a greater extent than the oxidized CNPs used in the studies pertaining to solubility, natural surfactants, deposition, and ecotoxicology described below, then conclusions drawn from these studies may not be indicative of outcomes in natural settings.

Photolysis

It is well established that numerous natural and manmade compounds can undergo direct or indirect photolysis in both water and air.[26, 62] Fullerenes appear to be susceptible to photolysis in laboratory studies and possibly in the natural aqueous environment. Exposure of C_{60} to UV light can produce reactive oxygen species (ROS) ($OH\bullet$, $^1O_2$ and $O_2^{\bullet-}$), in the presence of surfactants and clusters of hydroxylated C_{60}, but not in pure aqueous solutions.[63-65] Consequently, atmospheric processing (and thus functionalization) of C_{60} may influence fullerenes' potential for undergoing photolysis in the natural environment. Exposing aqueous C_{60} clusters to sunlight and 300 to 400 nm lamplight results in a decrease in colloid size, loss of solution color, and the production of water-soluble products that either mineralize or volatilize.[66] Oxygen is believed to play a role in the transformation. Aggregation of fullerenes in the aqueous phase reduces the photolysis rate significantly,[67] so this transformation may not be significant in natural waters. However, in the atmosphere, aggregation is less likely under typical conditions, so photolysis may be important for C_{60} aerosols.

Carbon nanotubes may also undergo photolysis. Single-walled carbon nanotubes dispersed in an aqueous solution with the aid of certain surfactants become hydroxylated on irradiation at 254 nm.[68] While the mechanism of this reaction is unknown, introduction of molecular oxygen as a

radical scavenger suppresses the hydroxylation, suggesting that ROS are being formed. Multi-walled nanotubes exposed to UV radiation under a molecular nitrogen/oxygen atmosphere exhibit surface oxygen concentrations of 7.5% after 4 h and exhibit ether, epoxy, and carbonate moieties.[69]

The extent to which photolysis of CNPs in the atmosphere may occur is unknown. The study of photochemistry at interfaces, specifically the air-particle one, is still in its infancy.[70] The oxidation studies recommended in the previous section should be expanded to account for photodegradation. Future research on the potential for CNP photolysis in the presence of molecular oxygen could clarify the relative importance of ozone and molecular oxygen for atmospheric processing of CNPs. A second area of research would be to investigate the photolysis of aerosolized CNPs.

Solubility

One of the most obvious mechanisms by which atmospheric transformations may influence the environmental fate of engineered CNPs is through enhancement of their aqueous solubility. The solubility of unfunctionalized CNPs in water is extremely low, due to their highly hydrophobic nature.[71, 72] While using organic intermediate solvents and surfactants may facilitate the preparation of aqueous CNP suspensions, these processes may not be relevant to the natural environment. Atmospheric transformations, in particular, may impact CNP fate and transport in aqueous systems due to the addition of various hydrophilic functional groups. Gas-phase oxidation of carbonaceous particles is known to cause an increase in hygroscopicity.[73]

Unmodified fullerenes introduced directly to water are estimated to have a solubility less than 10^{-12} mg mL^{-1}.[74] Calculations based on various C_{60} solubility experiments predict aqueous solubilities ranging from 1.3×10^{-11} mg mL^{-1} [75] to nearly 8×10^{-9} mg mL^{-1}.[76] Fullerene solubility in certain organic and inorganic solvents, however, is orders of magnitude higher,[77-80] up to 51 mg mL^{-1} in 1-chloronaphthalene.[81]

Unfunctionalized CNTs have widely been considered insoluble in all organic solvents, as well as in aqueous solutions.[72, 82] Their insolubility has been a major hurdle facing the industrial application of CNTs and has spurred a great number of studies on functionalization.[72, 83, 84] More recent publications, however, provide solubility data for as-produced nanotubes in a variety of organic solvents,[85, 86] including 3.5 mg mL^{-1} in cyclohexyl-pyrrolidinone.[87]

Despite the hydrophobic nature of CNPs, aqueous suspensions may be attained through a variety of laboratory methods. Aqueous colloidal solutions of fullerenes have been successfully prepared via solvent evaporation,[88-91] leading to an apparent solubility more than eight orders of magnitude higher than that of C_{60} in its hydrophobic, crystalline form.[92] Some colloids exhibit a fractal structure, which could contain some water molecules or traces of the original organic solvent.[89, 93, 94]

Aqueous solutions of C_{60} colloids can also be prepared via extended mechanical stirring of C_{60} in water,[95, 96] a method thought to be more environmentally relevant. While a theoretical study argues that the fullerene colloid most stable in water should be a spherical cluster consisting of 33 fullerenes at 3.56 nm in diameter,[97] solutions prepared via mechanical stirring consist of

highly polydisperse colloids of diameters 20 to 500 nm, with both angular and rounded colloid morphologies.[96] C_{60} colloids formed in natural aqueous systems would likely also be highly diverse in both size and morphology. These colloids can also have a net negative charge and a face-centered cubic crystal structure.[95] Surface hydrolysis and charge transfer have been suggested as probable sources of this negative charge, which affords the colloids electrophoretic mobility.[93]

C_{60} colloids generated in natural aqueous systems are likely to be polydisperse in size with varying morphologies. The increased hydrophilicity of these colloids (*aqu/*nC_{60}) may be attributed to hydroxylation at the colloid surface. The formation of hydroxyl groups is likely to occur under conditions found in the natural aqueous environment[98] and could also occur in the atmosphere. Certain functionalized C_{60} fullerenes also form colloids during extended stirring, although the functional groups can inhibit colloid formation up to a certain concentration. These colloids may be more persistent in the natural environment due to their hydrophilic functional groups.[99]

Aqueous preparations of CNTs are most often accomplished through the use of surfactants or through functionalization.[100-103] A variety of acids may be used to functionalize CNTs with hydrophilic groups.[48] The concentration of oxygen-containing functional groups, particularly carboxyl, on the surface of MWNTs is correlated with colloidal surface charge and aqueous stability under environmentally relevant pH conditions.[48] Thus, atmospheric processing (and thus potential functionalization) of CNTs may have significant impacts on CNT fate and transport within an aqueous system.

The aqueous solubility and resulting size distribution of CNPs is affected by their surface functionalization. Atmospheric processes, such as condensation of organic molecules, coagulation of CNPs, incorporation of CNPs into internally mixed aerosols, and oxidation, are likely to affect CNPs' properties in the aqueous phase through the addition of a variety of hydrophilic functional groups on the CNP surface. The most efficient way to model this cross-media effect would be to develop quantitative structure-activity relationships for CNP functional groups. Then, the solubilities of CNPs that have undergone atmospheric processing could more easily be predicted.

Adsorption of organic matter

Adsorption of natural organic matter (NOM) to CNPs is a key determinant of their fate and longevity in natural systems. Because it is dominated by surface characteristics, it can readily be affected by atmospheric processing. Furthermore, CNPs depositing from the atmosphere to aqueous and terrestrial systems are likely to carry their own coating of humic-like substances that are the end result of aerosol processing.[38] The presence of NOM in an aqueous system can affect C_{60} colloid stability, size, and morphology.[95, 104] Presumably interactions between NOM and atmospherically processed C_{60} would lead to different physical characteristics of the colloids. Sorption of NOM to colloids could potentially allow very small colloids to exist in natural waters and affect their toxicity.[104] Humic acid's effect on C_{60} colloids can differ depending upon the electrolytic composition of the solution.[105]

Natural humic substances also help to stabilize CNTs in aqueous solution, resulting in a smaller average particle diameter and a less polydisperse particle population.[106] The ability of a humic or

fulvic substance to stabilize CNTs is influenced by chemical structure. Highly hydrophilic substances will exert a reduced stabilizing effect, whereas those containing some hydrophobic groups interact more readily with CNTs, stabilizing them more readily.[106-108] The ability of some field-collected natural substances to stabilize MWNTs in aqueous solution may even surpass that of common industrial surfactants.[109] Other natural molecules, such as tannic acid, peptone, and phenylalanine, also sorb readily to MWNT.[110, 111]

Hydrophilic functional groups, such as hydroxyl and carboxyl groups, aid in MWNT stability in aqueous solution; this effect is significantly enhanced in the presence of NOM.[112] These interactions are expected to be modified by atmospheric processing of the CNTs. Furthermore, CNTs that have passed through the atmosphere may become associated with airborne humic-like substances,[113] which may affect the CNT's stability once they deposit back to the earth's surface.

As CNP interaction with NOM is nearly inevitable upon the introduction of CNPs to an aqueous system, the effect of atmospheric processing on CNP – NOM interactions, as well as subsequent consequences for CNP fate, transport, and ecotoxicity, merits further study.

Attachment to environmental surfaces

Interactions with porous media and removal efficiency by filtration in water and wastewater are important to determining the fate and transport of CNPs in the environment. These interactions depend on aqueous chemistry, as well as the CNPs' chemical and physical properties.

By increasing the hydrophilicity of CNPs, atmospheric processing will probably enhance their mobility in the aqueous phase. C_{60} aggregates deposit more readily to sand at higher ionic

strengths and lower flow velocities.[114] Surface functionalization is critical. A study with glass beads demonstrated that while approximately 45% of C_{60} colloids (prepared using organic solvents) remained trapped in the column, nearly all of the hydroxylated fullerenes [$C_{60}(OH)_{22-26}$] flushed out.[115] Hydroxylated fullerenes may have localized regions of hydrophobicity or hydrophilicity, which may reduce their attachment efficiency.[115, 116] Sorption of humic acid to colloids, which is thought to occur in the presence of certain ions[105] and is affected by functionalization of the fullerenes, could reduce the attachment efficiency of colloids to media such as soil and sand. Atmospheric processing may then have an impact on C_{60} deposition by affecting C_{60}-NOM interactions.

Carbon nanotube aggregates may deposit more readily than C_{60} aggregates in sand and soil due to their high aspect ratio. Their aspect ratio could be reduced in the atmosphere by condensation of semi-volatile compounds, or sorption and evaporation of solvents. While C_{60} aggregate deposition shows a strong sensitivity to ionic strength, physical straining likely influences carboxyl-functionalized SWNT deposition at lower ionic strengths and physicochemical filtering dominates at higher ionic strengths.[117] Carbon nanotube deposition is also influenced by ionic composition and strength,[118] flow rate,[119] media composition,[120] and functionalization. The presence of carboxyl groups on SWNTs is associated with the greatest change in the particles' point of zero charge.[121] These results illustrate that the fate of CNPs in water and soil is strongly influenced by environmental factors and the physical and chemical state of the CNPs themselves, which could be affected by atmospheric processing.

The results reviewed above provide an informative but incomplete picture of the influence of various environmental factors on CNP fate and transport in aqueous and terrestrial environments. Studies of CNP deposition to porous media must be continued and expanded to include a full suite of aquatic chemistry parameters and atmospherically processed CNPs. The ability of conventional water and wastewater treatment processes to remove NPs is of concern. A recent study demonstrates that C_{60} colloids, stabilized by NOM, are removed via conventional water treatment processes. Removal efficiency is greatly influenced by water quality parameters and coagulant used.[122] While these findings may apply to C_{60} discharged directly to a waterway, atmospheric transformations of CNPs may influence how effectively they can be removed using standard water treatment methods. This question serves as another area of future research.

Environmental toxicology

The CNPs have a variety of effects on a broad range of organisms, from protozoa to fish. The route of exposure strongly influences toxicity, as may transformations in the environment – most notably functionalization. Given our focus on the atmosphere, we initially review toxicity associated with inhalation exposure and then compile evidence showing how atmospheric transformations may affect toxicity in aqueous environments.

In vivo inhalation studies of C_{60} are few in number to date. The first study was published in early 2008 and found no significant toxicological effects across a wide range of endpoints.[123] Carbon black, an amorphous product of incomplete combustion, has been shown to be more toxic than either C_{60} or single-walled carbon nanotubes (SWNTs) to a mouse lung endothelial cell line *in vitro*.[124] To our knowledge, no papers have yet been published on the inhalation toxicity of functionalized C_{60}. However, tracheal instillation (deposition in a liquid solution) of $C_{60}(OH)_x$ (x

= 22 or 24) is associated with dose-dependent oxidative stress and inflammation.[125] These results suggest that atmospheric transformations of C_{60} may result in increased inhalation toxicity relative to untransformed C_{60}.

While at least two classic studies on the pulmonary effects of CNTs used instillation as an exposure method,[126, 127] true inhalation studies began to appear in literature in 2007.[128] Inhalation of SWNTs and MWNTs has been associated with oxidative stress, inflammation, fibrosis, multifocal granulomatous inflammation and pneumonia, free radical production, reduced cell viability, induction of apoptosis, and subpleural fibrosis, some of which exhibit dose-dependent behavior.[129-132] To our knowledge, no inhalation studies with functionalized CNTs have yet been published. However, carboxylated SWNTs administered to rats via aspiration resulted in increased pulmonary toxicity and myocardial degeneration compared to unfunctionalized SWNTs.[133] As with C_{60}, it appears that atmospheric processing of CNTs could enhance their inhalation toxicity.

Ecotoxicity studies of CNPs are great in number and do not yet present a cohesive picture of CNP toxicity in the aqueous phase. Factors affecting CNPs' aqueous ecotoxicity include sample preparation method, coating with surfactants such as NOM, and functionalization. As atmospheric processing may influence these factors, CNPs' toxicity may be modified if they pass through the atmosphere, but studies to date do not account for this cross-media effect. Each of the three factors is discussed here for both C_{60} and CNTs.

Exposure to an aqueous C_{60} suspension affects a variety of toxicity endpoints in many organisms,[134-140] but a few studies show no change in health indicators.[141, 142] The outcomes of toxicity studies can be impacted by the method of aqueous C_{60} colloid preparation,[94, 139, 143-145] so atmospheric and aqueous processing of C_{60} have the potential to alter toxicity.

The interaction of C_{60} aggregates and natural substances, which can be affected by atmospheric transformations, can also influence C_{60} toxicity. Attachment of C_{60} to soil may reduce toxicity, depending on soil type.[146] The presence of dissolved NOM in the cultures also significantly reduces C_{60} toxicity. Functionalization of CNPs can either enhance or reduce their toxicity in aqueous suspensions. In a dermal culture, $C_{60}(OH)_{24}$ exhibits no cytotoxicity up to saturation concentrations, whereas unfunctionalized C_{60} reduces cell viability.[147] However, $C_{60}(O)_x(OH)_y$ produced by ozonation of C_{60} colloids are more toxic to *E. coli* than unozonated C_{60} aggregates.[148] These results illustrate that C_{60} functionalization, one potential outcome of atmospheric processing, may have important implications for C_{60} toxicity and that the direction of the effect cannot presently be predicted.

Carbon nanotubes have been shown to be toxic to a variety of organisms, not all of which are affected by C_{60} suspensions.[140, 149-152] Evidence suggests that functionalization substantially impacts MWNT toxicity, and as with C_{60}, the nature of the functionalization may change the toxic effect. Hydroxylated and carboxylated MWNTs affect *C. dubia* minimally,[112] while MWNTs with alkyl and amine groups exert a stronger impact than do unfunctionalized MWNTs.[153] Both functionalized and unfunctionalized CNTs may bioaccumulate in a variety of

organisms.[112, 154-156] As atmospheric transformations of CNPs would likely result in their functionalization, atmospheric processing has important implications for toxicological outcomes.

The current understanding of CNP ecotoxicity is far from complete. A number of reviews of the toxicology of NPs summarize additional studies and highlight the many unknowns surrounding this topic,[157-161] although none address atmospheric processing of CNPs and the potential effects of this processing on human and ecological toxicity. Addressing the issue of atmospheric (and aqueous and biological) transformations would move research efforts toward a greater degree of environmental relevance.

To develop a more comprehensive, reliable knowledge base of the ecotoxicological effects of CNPs, standardization must be introduced at several points. First, CNPs used in toxicity studies must be fully characterized to account for the potential presence of functional groups and metal contaminants. Second, CNP doses must be prepared via consistent, well-defined, environmentally relevant methods. A third need is to accurately characterize the ratio of CNP colloids vs. individual CNPs in toxicity testing.

It is feasible that a non-negligible percentage of CNPs in an ecosystem could have undergone a variety of atmospheric processes, including coagulation, condensation, inclusion into internally mixed aerosols, oxidation, and photolysis. The impacts of atmospheric processing on ecotoxicology outcomes must be investigated in order to develop a comprehensive perspective on the environmental impacts of CNPs. Atmospheric transformations are also involved in all three preceding research needs: these processes will alter the surface functionality of CNPs,

which must be characterized prior to testing. Environmentally relevant preparation methods for atmospherically processed CNPs must be developed and adopted. And, atmospheric processing may alter CNP dispersion behavior in aqueous media – potentially affecting the outcome of toxicity tests.

Future directions

While some argue that CNPs' levels in and impacts on the environment are far outweighed by those of black carbon,[162, 163] investigations into the potential environmental impacts of CNPs must continue out of an abundance of caution. Examples of manufactured compounds that originally were thought to be inert or whose health and environmental impacts were not investigated fully but that were later found to be seriously harmful are plentiful. Examples include asbestos, chlorofluorocarbons (CFCs), polychlorinated biphenyls, and synthetic hormones. To justify the concern over atmospheric transformations, we invoke especially the history with CFCs, which are transformed through reactions in the atmosphere into catalytic destroyers of stratospheric ozone.

A comprehensive risk assessment requires a cross-media approach to understanding the fate and transport of nanomaterials. Research needs specific to cross-media effects encompass investigating the possibility of physical and chemical transformations of CNPs in the atmosphere and propagating the effects of those transformations as the CNPs move throughout the ecosystem. Recommended future research can be categorized as CNP detection and characterization, atmospheric chemistry, modeling, aqueous-phase properties, and ecotoxicity. Many of the research directions can be extended to other types of nanomaterials as well.

CNP detection and characterization

The ability to distinguish engineered NPs from naturally occurring and incidental NPs in the atmosphere is critical. CNPs pose a particular challenge here, since black carbon and other chemically similar soot products are widely found in the natural environment. The near-infrared fluorescence spectroscopic method capable of detecting single-walled carbon nanotubes in complex environmental matrices is a promising step in this direction. In all nanomaterial-related research, especially toxicological studies, the CNP sample should be fully characterized, preferably in terms of functional groups and metal contaminants. Carbonaceous nanoparticle functionalization impacts solubility, colloidal stability, deposition, and toxicity. So, having direct information on CNP functionalization before a particular study would help enhance the understanding of the relationships between functionalization and specific outcomes. Additionally, CNPs must be characterized in terms of species, since not all CNPs are equally susceptible to oxidation. One challenge will be studying the changes in properties after CNPs are incorporated into internally mixed aerosols (i.e., aerosols composed of both engineered NPs and aerosols or molecules already present in the atmosphere).

Atmospheric chemistry

Since CNPs will be released into the atmosphere, studies of their chemical transformations must be conducted on CNPs in aerosolized form. These types of experiments are classically conducted in a smog chamber or flow tube. Atmospherically relevant oxidant concentrations must be used, as most gas-phase CNP oxidation studies to date have used unrealistically high ozone levels. Reaction rates and oxidation products must be measured, and the potential for cage rupture of CNPs must be determined. The potential for CNPs to act as catalysts for reactions in the

atmosphere that could create or destroy compounds with health or climate impacts should also be investigated. At the intersection of oxidation and photolysis, the relative importance of molecular oxygen and ozone to CNP oxidation must be established in the presence of light.

Modeling

Synthesizing the variety of results from studies on the environmental impacts of CNPs and predicting future effects would benefit from the development of theoretical models. First, emissions, transport, transformation, and deposition of CNPs—in fact of all types of NPs—should be incorporated into existing atmospheric chemical-transport models. Such updated models would provide guidance to experimentalists as well as policymakers. Additionally, the development of structure-activity relationships for the impact of atmospheric processing on CNP solubility would be of great value. Taken together, these two modeling efforts could greatly improve the current understanding of the aqueous fate and transport of atmospherically released CNPs.

Aqueous-phase properties

Measurements of solubility and colloidal size distributions should consider CNPs containing functional groups resulting from atmospheric oxidation; for example, oxides, hydroxyls, carbonyls, and carboxyls. Sorption isotherms are also likely to change with oxidation. Fate in water treatment plants is of interest because CNPs will be present in raw water. While conventional water treatment processes show promise at removing C_{60}, the removal of functionalized C_{60} and CNTs has not yet been addressed. The ability of drinking water and

wastewater treatment systems to remove NPs is of great concern, so further research in this area is critical.

Ecotoxicity

Finally, the impact of atmospheric processing on ecotoxicity must be probed. Ecotoxicology of NPs, particularly CNPs, has been plagued with apparent self-contradictions, most notably the conflict over C_{60} toxicity and the potential interference of intermediate solvents. It is sensible to expect that atmospheric processing, which could result in CNP functionalization, could alter toxicity, perhaps substantially. Accounting for atmospheric processing in toxicity studies can only enhance their environmental relevance.

Although this work has emphasized the role of atmospheric processing, we observed that environmental processing, in general, whether in the aqueous phase or involving organisms, should be taken into greater account in studies of the solubility, sorption, transport, transformation, and toxicity of manufactured nanomaterials. Inclusion of environmental processing in such studies is an important prerequisite to developing a realistic assessment of the environmental risks posed by nanotechnology.

Acknowledgements

Support for this research was provided by the National Science Foundation (NSF), CBET-0537117, as well as NSF Cooperative Agreement #EF-0830093. Additional support was provided by the Center for the Environmental Implications of Nanotechnology, headquartered at Duke University, as well as Virginia Tech's Institute for Critical Technology and Applied Sciences. A. Tiwari is supported by an NSF Integrative Graduate Education and Research

Traineeship fellowship. We thank Marina Eller Quadros for preparing the figure and Peter Vikesland for helpful discussions.

References

1. Maynard, A. D.; Aitken, R. J.; Butz, T.; Colvin, V.; Donaldson, K.; Oberdorster, G.; Philbert, M. A.; Ryan, J.; Seaton, A.; Stone, V.; Tinkle, S. S.; Tran, L.; Walker, N. J.; Warheit, D. B. Safe handling of nanotechnology. *Nature.* **2006,** *444*, (7117), 267-269.

2. Christian, P.; Von der Kammer, F.; Baalousha, M.; Hofmann, T. Nanoparticles: structure, properties, preparation and behaviour in environmental media. *Ecotoxicol.* **2008,** *17*, (5), 326-343.

3. Klaine, S. J.; Alvarez, P. J. J.; Batley, G. E.; Fernandes, T. F.; Handy, R. D.; Lyon, D. Y.; Mahendra, S.; McLaughlin, M. J.; Lead, J. R. Nanomaterials in the environment: Behavior, fate, bioavailability, and effects. *Environ. Toxicol. Chem.* **2008,** *27*, (9), 1825-1851.

4. Guzman, K. A. D.; Taylor, M. R.; Banfield, J. F. Environmental risks of nanotechnology: National nanotechnology initiative funding, 2000-2004. *Environ. Sci. Technol.* **2006,** *40*, (5), 1401-1407.

5. Nowack, B.; Bucheli, T. D. Occurrence, behavior and effects of nanoparticles in the environment. *Environ. Pollut.* **2007,** *150*, (1), 5-22.

6. Stern, S. T.; McNeil, S. E. Nanotechnology safety concerns revisited. *Toxicol. Sci.* **2008,** *101*, (1), 4-21.

7. Wiesner, M. R.; Lowry, G. V.; Alvarez, P.; Dionysiou, D.; Biswas, P. Assessing the risks of manufactured nanomaterials. *Environ. Sci. Technol.* **2006,** *40*, (14), 4336-4345.

8. Wiesner, M. R.; Hotze, E. M.; Brant, J. A.; Espinasse, B. Nanomaterials as possible contaminants: the fullerene example. *Water Sci. Technol.* **2008,** *57*, (3), 305-310.

9. Handy, R. D.; Owen, R.; Valsami-Jones, E. The ecotoxicology of nanoparticles and nanomaterials: current status, knowledge gaps, challenges, and future needs. *Ecotoxicol.* **2008,** *17*, (5), 315-325.

10. Hassellov, M.; Readman, J. W.; Ranville, J. F.; Tiede, K. Nanoparticle analysis and characterization methodologies in environmental risk assessment of engineered nanoparticles. *Ecotoxicol.* **2008,** *17*, (5), 344-361.

11. Farre, M.; Gajda-Schrantz, K.; Kantiani, L.; Barcelo, D. Ecotoxicity and analysis of nanomaterials in the aquatic environment. *Anal. Bioanal. Chem.* **2009,** *393*, (1), 81-95.

12. Sweet, L.; Strohm, B. Nanotechnology - Life-cycle risk management. *Human & Ecol. Risk Assess.* **2006,** *12*, (3), 528-551.

13. Handy, R. D.; von der Kammer, F.; Lead, J. R.; Hassellov, M.; Owen, R.; Crane, M. The ecotoxicology and chemistry of manufactured nanoparticles. *Ecotoxicol.* **2008,** *17*, (4), 287-314.

14. Eckhardt, S.; Breivik, K.; Mano, S.; Stohl, A. Record high peaks in PCB concentrations in the Arctic atmosphere due to long-range transport of biomass burning emissions. *Atmos. Chem. Phys.* **2007,** *7*, (17), 4527-4536.

15. Anastasio, C.; Martin, S. T. Atmospheric nanoparticles. In *Nanoparticles and the Environment*, Mineralogical Society of America: Washington, 2001; Vol. 44, pp 293-349.

16. Moore, M. N. Do nanoparticles present ecotoxicological risks for the health of the aquatic environment? *Environ. Int.* **2006,** *32*, (8), 967-976.

17. Da Ros, T.; Prato, M. Medicinal chemistry with fullerenes and fullerene derivatives. *Chem. Commun.* **1999**, (8), 663-669.

18. Bakry, R.; Vallant, R. M.; Najam-Ul-Haq, M.; Rainer, M.; Szabo, Z.; Huck, C. W.; Bonn, G. K. Medicinal applications of fullerenes. *Int. J. Nanomedicine.* **2007,** *2*, (4), 639-649.

19. Maynard, A. D.; Kuempel, E. D. Airborne nanostructured particles and occupational health. *J. Nanopart. Res.* **2005,** *7*, (6), 587-614.

20. Navarro, E.; Baun, A.; Behra, R.; Hartmann, N. B.; Filser, J.; Miao, A. J.; Quigg, A.; Santschi, P. H.; Sigg, L. Environmental behavior and ecotoxicity of engineered nanoparticles to algae, plants, and fungi. *Ecotoxicol.* **2008,** *17*, (5), 372-386.

21. Wiesner, M. R. In *Responsible development of nanotechnologies for water and wastewater treatment*, 3rd IWA Leading-Edge Conference Water and Wastewater Treatment

Technologies, Sapporo, JAPAN, Jun 06-08, 2005; I W a Publishing: Sapporo, JAPAN, 2005; pp 45-51.

22. Yeganeh, B.; Kull, C. M.; Hull, M. S.; Marr, L. C. Characterization of airborne particles during production of carbonaceous manomaterials. *Environ. Sci. Technol.* **2008,** *42*, (12), 4600-4606.

23. Oberdorster, G. Pulmonary effects of inhaled ultrafine particles. *Int. Arch. Occup. Environ. Health.* **2001,** *74*, (1), 1-8.

24. Polichetti, G.; Cocco, S.; Spinali, A.; Trimarco, V.; Nunziata, A. Effects of particulate matter (PM10, PM2.5 and PM1) on the cardiovascular system. *Toxicology.* **2009,** *261*, (1-2), 1-8.

25. Project on Emerging Nanotechnologies Analysis, Consumer Products, Nanotechnology Project. http://www.nanotechproject.org/inventories/consumer/analysis_draft/ (14 February 2014).

26. Seinfeld, J. H.; Pandis, S. N., *Atmospheric Chemistry and Physics: From Air Pollution to Climate Change*. 2nd ed.; Wiley-Interscience: 2006.

27. Ketzel, M.; Berkowicz, R. Modelling the fate of ultrafine particles from exhaust pipe to rural background: an analysis of time scales for dilution, coagulation and deposition. *Atmos. Environ.* **2004,** *38*, (17), 2639-2652.

28. Ketzel, M.; Berkowicz, R. Multi-plume aerosol dynamics and transport model for urban scale particle pollution. *Atmos. Environ.* **2005,** *39*, (19), 3407-3420.

29. Kerminen, V. M.; Lehtinen, K. E. J.; Anttila, T.; Kulmala, M. Dynamics of atmospheric nucleation mode particles: a timescale analysis. *Tellus Ser. B.* **2004,** *56*, (2), 135-146.

30. Kulmala, M.; Vehkamaki, H.; Petaja, T.; Dal Maso, M.; Lauri, A.; Kerminen, V. M.; Birmili, W.; McMurry, P. H. Formation and growth rates of ultrafine atmospheric particles: a review of observations. *J. Aerosol Sci.* **2004,** *35*, (2), 143-176.

31. Johnson, K. S.; Zuberi, B.; Molina, L. T.; Molina, M. J.; Iedema, M. J.; Cowin, J. P.; Gaspar, D. J.; Wang, C.; Laskin, A. Processing of soot in an urban environment: case study from the Mexico City Metropolitan Area. *Atmos. Chem. Phys.* **2005,** *5*, 3033-3043.

32. Takahama, S.; Liu, S.; Russell, L. M. Coatings and clusters of carboxylic acids in carbon-containing atmospheric particles from spectromicroscopy and their implications for cloud-nucleating and optical properties. *J. Geophys. Res.-Atmos.* **2010,** *115*.

33. Slowik, J. G.; Cross, E. S.; Han, J. H.; Kolucki, J.; Davidovits, P.; Williams, L. R.; Onasch, T. B.; Jayne, J. T.; Kolb, C. E.; Worsnop, D. R. Measurements of morphology changes of fractal soot particles using coating and denuding experiments: Implications for optical absorption and atmospheric lifetime. *Aerosol Sci. Technol.* **2007,** *41*, (8), 734-750.

34. Weingartner, E.; Burtscher, H.; Baltensperger, U. Hygroscopic properties of carbon and diesel soot particles. *Atmos. Environ.* **1997,** *31*, (15), 2311-2327.

35. Laakso, L.; Gronholm, T.; Rannik, U.; Kosmale, M.; Fiedler, V.; Vehkamaki, H.; Kulmala, M. Ultrafine particle scavenging coefficients calculated from 6 years field measurements. *Atmos. Environ.* **2003,** *37*, (25), 3605-3613.

36. Zhao, H. B.; Zheng, C. G. Stochastic algorithm and numerical simulation for drop scavenging of aerosols. *Appl. Math. Mech.-Engl. Ed.* **2006,** *27*, (10), 1321-1332.

37. Grieco, W. J.; Howard, J. B.; Rainey, L. C.; Vander Sande, J. B. Fullerenic carbon in combustion-generated soot. *Carbon.* **2000,** *38*, (4), 597-614.

38. Jimenez, J. L.; Canagaratna, M. R.; Donahue, N. M.; Prevot, A. S. H.; Zhang, Q.; Kroll, J. H.; DeCarlo, P. F.; Allan, J. D.; Coe, H.; Ng, N. L.; Aiken, A. C.; Docherty, K. S.; Ulbrich, I. M.; Grieshop, A. P.; Robinson, A. L.; Duplissy, J.; Smith, J. D.; Wilson, K. R.; Lanz, V. A.; Hueglin, C.; Sun, Y. L.; Tian, J.; Laaksonen, A.; Raatikainen, T.; Rautiainen, J.; Vaattovaara, P.; Ehn, M.; Kulmala, M.; Tomlinson, J. M.; Collins, D. R.; Cubison, M. J.; Dunlea, E. J.; Huffman, J. A.; Onasch, T. B.; Alfarra, M. R.; Williams, P. I.; Bower, K.; Kondo, Y.; Schneider, J.; Drewnick, F.; Borrmann, S.; Weimer, S.; Demerjian, K.; Salcedo, D.; Cottrell, L.; Griffin, R.; Takami, A.; Miyoshi, T.; Hatakeyama, S.; Shimono, A.; Sun, J. Y.; Zhang, Y. M.; Dzepina, K.; Kimmel, J. R.; Sueper, D.; Jayne, J. T.; Herndon, S. C.; Trimborn, A. M.; Williams, L. R.; Wood, E. C.; Middlebrook, A. M.; Kolb, C. E.; Baltensperger, U.; Worsnop, D. R. Evolution of Organic Aerosols in the Atmosphere. *Science.* **2009,** *326*, (5959), 1525-1529.

39. McElvany, S. W.; Callahan, J. H.; Ross, M. M.; Lamb, L. D.; Huffman, D. R. Large odd-numbered carbon clusters from fullerene-ozone reactions. *Science.* **1993,** *260*, (5114), 1632-1634.

40. Deng, J. P.; Ju, D. D.; Her, G. R.; Mou, C. Y.; Chen, C. J.; Lin, Y. Y.; Han, C. C. Odd-numbered fullerene fragment ions from C-60 oxides *J. Phys. Chem.* **1993,** *97*, (45), 11575-11577.

41. Deng, J. P.; Mou, C. Y.; Han, C. C. Electrospray and laser-desorption ionization studies of C60O and isomers of C60O2 *J. Phys. Chem.* **1995,** *99*, (41), 14907-14910.

42. Deng, J. P.; Mou, C. Y.; Han, C. C. Oxidation of fullerenes by ozone. *Fullerene Sci. Technol.* **1997,** *5*, (5), 1033-1044.

43. Malhotra, R.; Kumar, S.; Satyam, A. Ozonolysis of [60]fullerene *J. Chem. Soc., Chem. Commun.* **1994**, (11), 1339-1340.

44. Chibante, L. P. F.; Heymann, D. On the geochemistry of fullerenes - stability of C60 in ambient air and the role of ozone *Geochim. Cosmochim. Acta.* **1993,** *57*, (8), 1879-1881.

45. Fortner, J. D.; Kim, D. I.; Boyd, A. M.; Falkner, J. C.; Moran, S.; Colvin, V. L.; Hughes, J. B.; Kim, J. H. Reaction of water-stable C-60 aggregates with ozone. *Environ. Sci. Technol.* **2007,** *41*, (21), 7497-7502.

46. Anachkov, M. P.; Cataldo, F.; Rakovsky, S. K. Reaction kinetics of C-60 fullerene ozonation. *Fuller. Nanotub. Carbon Nanostruct.* **2003,** *11*, (2), 95-103.

47. Li, M. H.; Boggs, M.; Beebe, T. P.; Huang, C. P. Oxidation of single-walled carbon nanotubes in dilute aqueous solutions by ozone as affected by ultrasound. *Carbon.* **2008,** *46*, (3), 466-475.

48. Smith, B.; Wepasnick, K.; Schrote, K. E.; Cho, H. H.; Ball, W. P.; Fairbrother, D. H. Influence of Surface Oxides on the Colloidal Stability of Multi-Walled Carbon Nanotubes: A Structure-Property Relationship. *Langmuir.* **2009,** *25*, (17), 9767-9776.

49. Scanlon, J. C.; Brown, J. M.; Ebert, L. B. Oxidative Stability of Fullerenes. *J. Phys. Chem.* **1994,** *98*, (15), 3921-3923.

50. Murr, L. E.; Soto, K. F. A TEM study of soot, carbon nanotubes, and related fullerene nanopolyhedra in common fuel-gas combustion sources. *Mater. Charact.* **2005,** *55*, (1), 50-65.

51. Cataldo, F. Ozone reaction with carbon nanostructures 1: Reaction between solid C-60 and C-70 fullerenes and ozone. *J. Nanosci. Nanotechnol.* **2007,** *7*, (4-5), 1439-1445.

52. Mawhinney, D. B.; Naumenko, V.; Kuznetsova, A.; Yates, J. T.; Liu, J.; Smalley, R. E. Infrared spectral evidence for the etching of carbon nanotubes: Ozone oxidation at 298 K. *J. Am. Chem. Soc.* **2000,** *122*, (10), 2383-2384.

53. Mawhinney, D. B.; Yates, J. T. FTIR study of the oxidation of amorphous carbon by ozone at 300 K - Direct COOH formation. *Carbon.* **2001,** *39*, (8), 1167-1173.

54. Simmons, J. M.; Nichols, B. M.; Baker, S. E.; Marcus, M. S.; Castellini, O. M.; Lee, C. S.; Hamers, R. J.; Eriksson, M. A. Effect of ozone oxidation on single-walled carbon nanotubes. *J. Phys. Chem. B.* **2006,** *110*, (14), 7113-7118.

55. Larciprete, R.; Gardonio, S.; Petaccia, L.; Lizzit, S. Atomic oxygen functionalization of double walled C nanotubes. *Carbon.* **2009,** *47*, (11), 2579-2589.

56. Cataldo, F. A study on the action of ozone on multiwall carbon nanotubes. *Fuller. Nanotub. Carbon Nanostruct.* **2008,** *16*, (1), 1-17.

57. Watanabe, H.; Matsui, E.; Ishiyama, Y.; Senna, M. Solvent free mechanochemical oxygenation of fullerene under oxygen atmosphere. *Tetrahedron Lett.* **2007,** *48*, (46), 8132-8137.

58. Wang, B. C.; Chen, L. K.; Chou, Y. M. Theoretical studies of C-60/C-7O fullerene derivatives: C60O and C70O. *Theochem.* **1998,** *422*, 153-158.

59. Wang, B. C.; Chen, L.; Lee, K. J.; Cheng, C. Y. Semiempirical molecular dynamics studies of C-60/C-70 fullerene oxides: C60O, C60O2 and C70O. *Theochem.* **1999,** *469*, 127-134.

60. Raghavachari, K.; Sosa, C. Fullerene derivatives - comparative theoretical-study of C60O and C60CH2 *Chem. Phys. Lett.* **1993,** *209*, (3), 223-228.

61. Wang, X. B.; Woo, H. K.; Kiran, B.; Wang, L. S. Photoelectron spectroscopy and electronic structures of fullerene oxides: C60Ox- (x=1-3). *J. Phys. Chem. A.* **2005,** *109*, (49), 11089-11092.

62. Schwartzenbach, R. P., Gschwend, P.M., and Dieter M. Imboden, Environmental Organic Chemistry. In 2nd ed.; Wiley Interscience: 2003.

63. Lee, J.; Fortner, J. D.; Hughes, J. B.; Kim, J. H. Photochemical production of reactive oxygen species by C-60 in the aqueous phase during UV irradiation. *Environ. Sci. Technol.* **2007,** *41*, (7), 2529-2535.

64. Lee, J.; Kim, J. H. Effect of encapsulating agents on dispersion status and photochemical reactivity of C-60 in the aqueous phase. *Environ. Sci. Technol.* **2008,** *42*, (5), 1552-1557.

65. Hotze, E. M.; Labille, J.; Alvarez, P.; Wiesner, M. R. Mechanisms of photochemistry and reactive oxygen production by fullerene suspensions in water. *Environ. Sci. Technol.* **2008,** *42*, (11), 4175-4180.

66. Hou, W. C.; Jafvert, C. T. Photochemical transformation of aqueous C-60 clusters in sunlight. *Environ. Sci. Technol.* **2009,** *43*, (2), 362-367.

67. Lee, J.; Yamakoshi, Y.; Hughes, J. B.; Kim, J. H. Mechanism of C-60 photoreactivity in water: Fate of triplet state and radical anion and production of reactive oxygen species. *Environ. Sci. Technol.* **2008,** *42*, (9), 3459-3464.

68. Alvarez, N. T.; Kittrell, C.; Schmidt, H. K.; Hauge, R. H.; Engel, P. S.; Tour, J. M. Selective Photochemical Functionalization of Surfactant-Dispersed Single Wall Carbon Nanotubes in Water. *J. Am. Chem. Soc.* **2008,** *130*, (43), 14227-14233.

69. Parekh, B.; Debies, T.; Knight, P.; Santhanam, K. S. V.; Takacs, G. A. Surface functionalization of multiwalled carbon nanotubes with UV and vacuum UV photo-oxidation. *J. Adhes. Sci. Technol.* **2006,** *20*, (16), 1833-1846.

70. Nissenson, P.; Knox, C. J. H.; Finlayson-Pitts, B. J.; Phillips, L. F.; Dabdub, D. Enhanced photolysis in aerosols: evidence for important surface effects. *PCCP.* **2006,** *8*, (40), 4700-4710.

71. Kadish, K., and Ruoff, R. , *Fullerenes: Chemistry, Physics, and Technology*. Wiley-Interscience: 2000.

72. Tasis, D.; Tagmatarchis, N.; Bianco, A.; Prato, M. Chemistry of carbon nanotubes. *Chem. Rev.* **2006,** *106*, (3), 1105-1136.

73. Zuberi, B.; Johnson, K. S.; Aleks, G. K.; Molina, L. T.; Laskin, A. Hydrophilic properties of aged soot. *Geophys. Res. Lett.* **2005,** *32*, (1).

74. Khokhryakov, A. A.; Kyzyma, O. A.; Bulavin, L. A.; Len, A.; Avdeev, M. V.; Aksenov, V. L. Colloidal structure and stabilization mechanism of aqueous solutions of unmodified fullerene C-60. *Crystallogr. Rep.* **2007,** *52*, (3), 487-491.

75. Heymann, D. Solubility of fullerenes C-60 and C-70 in seven normal alcohols and their deduced solubility in water. *Fullerene Sci. Technol.* **1996,** *4*, (3), 509-515.

76. Jafvert, C. T.; Kulkarni, P. P. Buckminsterfullerene's (C-60) octanol-water partition coefficient (K-ow) and aqueous solubility. *Environ. Sci. Technol.* **2008,** *42*, (16), 5945-5950.

77. Sivaraman, N.; Dhamodaran, R.; Kaliappan, I.; Srinivasan, T. G.; Rao, P. R. V.; Mathews, C. K. Solubility of C-60 in organic-solvents *J. Org. Chem.* **1992,** *57*, (22), 6077-6079.

78. Scrivens, W. A.; Tour, J. M. Potent solvents for C-60 and their utility for the rapid acquisition of C-13 NMR data for fullerenes *J. Chem. Soc., Chem. Commun.* **1993**, (15), 1207-1209.

79. Ruoff, R. S.; Malhotra, R.; Huestis, D. L.; Tse, D. S.; Lorents, D. C. Anomalous solubility behavior of C60 *Nature.* **1993,** *362*, (6416), 140-141.

80. Heymann, D. Solubility of C-60 in alcohols and alkanes. *Carbon.* **1996,** *34*, (5), 627-631.

81. Beck, M. T.; Mandi, G. Solubility of C-60. *Fullerene Sci. Technol.* **1997,** *5*, (2), 291-310.

82. Saito, R.; Kataura, H. Optical Properties and Raman Spectroscopy of Carbon Nanotubes. In *Carbon Nanotubes: Synthesis, Structure, Properties, and Applications*, Dreselhaus, M. S.; Dresselhaus, G.; Avouris, P., Eds. Springer-Verlag: Heidelberg, 2001.

83. Hirsch, A. Functionalization of single-walled carbon nanotubes. *Angew. Chem. Int. Ed.* **2002,** *41*, (11), 1853-1859.

84. Hirsch, A.; Vostrowsky, O. Functionalization of carbon nanotubes. In *Functional Molecular Nanostructures*, Springer-Verlag Berlin: Berlin, 2005; Vol. 245, pp 193-237.

85. Bahr, J. L.; Mickelson, E. T.; Bronikowski, M. J.; Smalley, R. E.; Tour, J. M. Dissolution of small diameter single-wall carbon nanotubes in organic solvents? *Chem. Commun.* **2001**, (2), 193-194.

86. Bergin, S. D.; Sun, Z. Y.; Streich, P.; Hamilton, J.; Coleman, J. N. New Solvents for Nanotubes: Approaching the Dispersibility of Surfactants. *J. Phys. Chem. C.* **2010,** *114*, (1), 231-237.

87. Bergin, S. D.; Sun, Z. Y.; Rickard, D.; Streich, P. V.; Hamilton, J. P.; Coleman, J. N. Multicomponent Solubility Parameters for Single-Walled Carbon Nanotube-Solvent Mixtures. *ACS Nano.* **2009,** *3*, (8), 2340-2350.

88. Andrievsky, G. V.; Kosevich, M. V.; Vovk, O. M.; Shelkovsky, V. S.; Vashchenko, L. A. On the production of an aqueous colloidal solution of fullerenes *J. Chem. Soc., Chem. Commun.* **1995**, (12), 1281-1282.

89. Andrievsky, G. V.; Klochkov, V. K.; Karyakina, E. L.; McHedlov-Petrossyan, N. O. Studies of aqueous colloidal solutions of fullerene C-60 by electron microscopy. *Chem. Phys. Lett.* **1999,** *300*, (3-4), 392-396.

90. Deguchi, S.; Alargova, R. G.; Tsujii, K. Stable dispersions of fullerenes, C-60 and C-70, in water. Preparation and characterization. *Langmuir.* **2001,** *17*, (19), 6013-6017.

91. Scharff, P.; Risch, K.; Carta-Abelmann, L.; Dmytruk, I. M.; Bilyi, M. M.; Golub, O. A.; Khavryuchenko, A. V.; Buzaneva, E. V.; Aksenov, V. L.; Avdeev, M. V.; Prylutskyy, Y. I.; Durov, S. S. Structure of C-60 fullerene in water: spectroscopic data. *Carbon.* **2004,** *42*, (5-6), 1203-1206.

92. Isaacson, C. W. K., Markus; Field, J.A. . Quantitative Analysis of Fullerene Nanomaterials in Environmental Systems: A Critical Review. *Environ. Sci. Technol.* **2009,** *43*, (17), 6463-6474.

93. Brant, J.; Lecoanet, H.; Hotze, M.; Wiesner, M. Comparison of electrokinetic properties of colloidal fullerenes (n-C-60) formed using two procedures. *Environ. Sci. Technol.* **2005,** *39*, (17), 6343-6351.

94. Brant, J.; Labille, J.; Bottero, J. Y.; Wiesner, M. R. Characterizing the impact of preparation method on fullerene cluster structure and chemistry. *Langmuir.* **2006,** *22*, (8), 3878-3885.

95. Duncan, L. K.; Jinschek, J. R.; Vikesland, P. J. C-60 colloid formation in aqueous systems: Effects of preparation method on size, structure, and surface, charge. *Environ. Sci. Technol.* **2008,** *42*, (1), 173-178.

96. Labille, J.; Brant, J.; Villieras, F.; Pelletier, M.; Thill, A.; Masion, A.; Wiesner, M.; Rose, J.; Bottero, J. Y. Affinity of C-60 fullerenes with water. *Fuller. Nanotub. Carbon Nanostruct.* **2006,** *14*, (2-3), 307-314.

97. Prilutski, Y. I.; Durov, S. S.; Yashchuk, V. N.; Ogul'chansky, T. Y.; Pogorelov, V. E.; Astashkin, Y. A.; Buzaneva, E. V.; Kirghisov, Y. D.; Andrievsky, G. V.; Scharff, P. Theoretical predictions and experimental studies of self-organized C-60 nanoparticles in water solution and on the support. *Eur. Phys. J. D.* **1999,** *9*, (1-4), 341-343.

98. Labille, J.; Masion, A.; Ziarelli, F.; Rose, J.; Brant, J.; Villieras, F.; Pelletier, M.; Borschneck, D.; Wiesner, M. R.; Bottero, J. Y. Hydration and Dispersion of C-60 in Aqueous Systems: The Nature of Water-Fullerene Interactions. *Langmuir.* **2009,** *25*, (19), 11232-11235.

99. Bouchard, D.; Ma, X.; Issacson, C. Colloidal Properties of Aqueous Fullerenes: Isoelectric Points and Aggregation Kinetics of C-60 and C-60 Derivatives. *Environ. Sci. Technol.* **2009,** *43*, (17), 6597-6603.

100. Fernando, K. A. S.; Lin, Y.; Sun, Y. P. High aqueous solubility of functionalized single-walled carbon nanotubes. *Langmuir.* **2004,** *20*, (11), 4777-4778.

101. Tasis, D.; Tagmatarchis, N.; Georgakilas, V.; Prato, M. Soluble carbon nanotubes. *Chem. Eur. J.* **2003,** *9*, (17), 4001-4008.

102. Zeng, L. L.; Zhang, L.; Barron, A. R. Tailoring aqueous solubility of functionalized single-wall carbon nanotubes over a wide pH range through substituent chain length. *Nano Lett.* **2005,** *5*, (10), 2001-2004.

103. Tagmatarchis, N.; Prato, M. Carbon-based materials: From fullerene nanostructures to functionalized carbon nanotubes. *Pure Appl. Chem.* **2005,** *77*, (10), 1675-1684.

104. Xie, B.; Xu, Z. H.; Guo, W. H.; Li, Q. L. Impact of natural organic matter on the physicochemical properties of aqueous C-60 nanoparticles. *Environ. Sci. Technol.* **2008,** *42*, (8), 2853-2859.

105. Chen, K. L.; Elimelech, M. Influence of humic acid on the aggregation kinetics of fullerene (C-60) nanoparticles in monovalent and divalent electrolyte solutions. *J. Colloid Interface Sci.* **2007,** *309*, (1), 126-134.

106. Chappell, M. A.; George, A. J.; Dontsova, K. M.; Porter, B. E.; Price, C. L.; Zhou, P. H.; Morikawa, E.; Kennedy, A. J.; Steevens, J. A. Surfactive stabilization of multi-walled carbon nanotube dispersions with dissolved humic substances. *Environ. Pollut.* **2009,** *157*, (4), 1081-1087.

107. Yang, K.; Xing, B. S. Adsorption of fulvic acid by carbon nanotubes from water. *Environ. Pollut.* **2009,** *157*, (4), 1095-1100.

108. Hyung, H.; Kim, J. H. Natural organic matter (NOM) adsorption to multi-walled carbon nanotubes: Effect of NOM characteristics and water quality parameters. *Environ. Sci. Technol.* **2008,** *42*, (12), 4416-4421.

109. Hyung, H.; Fortner, J. D.; Hughes, J. B.; Kim, J. H. Natural organic matter stabilizes carbon nanotubes in the aqueous phase. *Environ. Sci. Technol.* **2007,** *41*, (1), 179-184.

110. Wang, X. L.; Lu, J. L.; Xing, B. S. Sorption of organic contaminants by carbon nanotubes: Influence of adsorbed organic matter. *Environ. Sci. Technol.* **2008,** *42*, (9), 3207-3212.

111. Lin, D. H.; Xing, B. S. Tannic acid adsorption and its role for stabilizing carbon nanotube suspensions. *Environ. Sci. Technol.* **2008,** *42*, (16), 5917-5923.

112. Kennedy, A. J.; Hull, M. S.; Steevens, J. A.; Dontsova, K. M.; Chappell, M. A.; Gunter, J. C.; Weiss, C. A. Factors influencing the partitioning and toxicity of nanotubes in the aquatic environment. *Environ. Toxicol. Chem.* **2008,** *27*, (9), 1932-1941.

113. Fuzzi, S.; Decesari, S.; Facchini, M. C.; Matta, E.; Mircea, M.; Tagliavini, E. A simplified model of the water soluble organic component of atmospheric aerosols. *Geophys. Res. Lett.* **2001,** *28*, (21), 4079-4082.

114. Espinasse, B.; Hotze, E. M.; Wiesner, M. R. Transport and retention of colloidal aggregates of C-60 in porous media: Effects of organic macromolecules, ionic composition, and preparation method. *Environ. Sci. Technol.* **2007,** *41*, (21), 7396-7402.

115. Lecoanet, H. F.; Wiesner, M. R. Velocity effects on fullerene and oxide nanoparticle deposition in porous media. *Environ. Sci. Technol.* **2004,** *38*, (16), 4377-4382.

116. Lecoanet, H. F.; Bottero, J. Y.; Wiesner, M. R. Laboratory assessment of the mobility of nanomaterials in porous media. *Environ. Sci. Technol.* **2004,** *38*, (19), 5164-5169.

117. Jaisi, D. P.; Elimelech, M. Single-Walled Carbon Nanotubes Exhibit Limited Transport in Soil Columns. *Environ. Sci. Technol.* **2009,** *43*, (24), 9161-9166.

118. Jaisi, D. P.; Saleh, N. B.; Blake, R. E.; Elimelech, M. Transport of Single-Walled Carbon Nanotubes in Porous Media: Filtration Mechanisms and Reversibility. *Environ. Sci. Technol.* **2008,** *42*, (22), 8317-8323.

119. Liu, X. Y.; O'Carroll, D. M.; Petersen, E. J.; Huang, Q. G.; Anderson, C. L. Mobility of Multiwalled Carbon Nanotubes in Porous Media. *Environ. Sci. Technol.* **2009,** *43*, (21), 8153-8158.

120. Han, Z. T.; Zhang, F. W.; Lin, D. H.; Xing, B. S. Clay minerals affect the stability of surfactant-facilitated carbon nanotube suspensions. *Environ. Sci. Technol.* **2008,** *42*, (18), 6869-6875.

121. McPhail, M. R.; Sells, J. A.; He, Z.; Chusuei, C. C. Charging Nanowalls: Adjusting the Carbon Nanotube Isoelectric Point via Surface Functionalization. *J. Phys. Chem. C.* **2009,** *113*, (32), 14102-14109.

122. Hyung, H.; Kim, J. H. Dispersion of C-60 in natural water and removal by conventional drinking water treatment processes. *Water Res.* **2009,** *43*, (9), 2463-2470.

123. Baker, G. L.; Gupta, A.; Clark, M. L.; Valenzuela, B. R.; Staska, L. M.; Harbo, S. J.; Pierce, J. T.; Dill, J. A. Inhalation toxicity and lung toxicokinetics of C-60 fullerene nanoparticles and microparticles. *Toxicol. Sci.* **2008,** *101*, (1), 122-131.

124. Jacobsen, N. R.; Pojana, G.; White, P.; Moller, P.; Cohn, C. A.; Korsholm, K. S.; Vogel, U.; Marcomini, A.; Loft, S.; Wallin, H. Genotoxicity, cytotoxicity, and reactive oxygen species induced by single-walled carbon nanotubes and C-60 fullerenes in the FE1-Muta (TM) mouse lung epithelial cells. *Environ. Mol. Mut.* **2008,** *49*, (6), 476-487.

125. Xu, J. Y.; Han, K. Y.; Li, S. X.; Cheng, J. S.; Xu, G. T.; Li, W. X.; Li, Q. N. Pulmonary responses to polyhydroxylated fullerenols, C-60(OH)(x). *J. Appl. Toxicol.* **2009,** *29*, (7), 578-584.

126. Lam, C. W.; James, J. T.; McCluskey, R.; Hunter, R. L. Pulmonary toxicity of single-wall carbon nanotubes in mice 7 and 90 days after intratracheal instillation. *Toxicol. Sci.* **2004,** *77*, (1), 126-134.

127. Warheit, D. B.; Laurence, B. R.; Reed, K. L.; Roach, D. H.; Reynolds, G. A. M.; Webb, T. R. Comparative pulmonary toxicity assessment of single-wall carbon nanotubes in rats. *Toxicol. Sci.* **2004,** *77*, (1), 117-125.

128. Mitchell, L. A.; Gao, J.; Wal, R. V.; Gigliotti, A.; Burchiel, S. W.; McDonald, J. D. Pulmonary and systemic immune response to inhaled multiwalled carbon nanotubes. *Toxicol. Sci.* **2007,** *100*, (1), 203-214.

129. Ma-Hock, L.; Treumann, S.; Strauss, V.; Brill, S.; Luizi, F.; Mertler, M.; Wiench, K.; Gamer, A. O.; van Ravenzwaay, B.; Landsiedel, R. Inhalation toxicity of multiwall carbon nanotubes in rats exposed for 3 months. *Toxicol. Sci.* **2009,** *112*, (2), 468-481.

130. Shvedova, A. A.; Kisin, E.; Murray, A. R.; Johnson, V. J.; Gorelik, O.; Arepalli, S.; Hubbs, A. F.; Mercer, R. R.; Keohavong, P.; Sussman, N.; Jin, J.; Yin, J.; Stone, S.; Chen, B. T.; Deye, G.; Maynard, A.; Castranova, V.; Baron, P. A.; Kagan, V. E. Inhalation vs. aspiration of single-walled carbon nanotubes in C57BL/6 mice: inflammation, fibrosis, oxidative stress, and mutagenesis. *Am. J. Physiol. - Lung C.* **2008,** *295*, (4), L552-L565.

131. Ravichandran, P.; Periyakaruppan, A.; Sadanandan, B.; Ramesh, V.; Hall, J. C.; Jejelowo, O.; Ramesh, G. T. Induction of Apoptosis in Rat Lung Epithelial Cells by Multiwalled Carbon Nanotubes. *J. Biochem. Mol. Toxicol.* **2009,** *23*, (5), 333-344.

132. Ryman-Rasmussen, J. P.; Cesta, M. F.; Brody, A. R.; Shipley-Phillips, J. K.; Everitt, J. I.; Tewksbury, E. W.; Moss, O. R.; Wong, B. A.; Dodd, D. E.; Andersen, M. E.; Bonner, J. C. Inhaled carbon nanotubes reach the subpleural tissue in mice. *Nature Nanotech.* **2009,** *4*, (11), 747-751.

133. Tong, H. Y.; McGee, J. K.; Saxena, R. K.; Kodavanti, U. P.; Devlin, R. B.; Gilmour, M. I. Influence of acid functionalization on the cardiopulmonary toxicity of carbon nanotubes and carbon black particles in mice. *Toxicol. Appl. Pharmacol.* **2009,** *239*, (3), 224-232.

134. Lyon, D. Y.; Fortner, J. D.; Sayes, C. M.; Colvin, V. L.; Hughes, J. B. Bacterial cell association and antimicrobial activity of a C-60 water suspension. *Environ. Toxicol. Chem.* **2005,** *24*, (11), 2757-2762.

135. Fortner, J. D.; Lyon, D. Y.; Sayes, C. M.; Boyd, A. M.; Falkner, J. C.; Hotze, E. M.; Alemany, L. B.; Tao, Y. J.; Guo, W.; Ausman, K. D.; Colvin, V. L.; Hughes, J. B. C-60 in water: Nanocrystal formation and microbial response. *Environ. Sci. Technol.* **2005,** *39*, (11), 4307-4316.

136. Fang, J. S.; Lyon, D. Y.; Wiesner, M. R.; Dong, J. P.; Alvarez, P. J. J. Effect of a fullerene water suspension on bacterial phospholipids and membrane phase behavior. *Environ. Sci. Technol.* **2007,** *41*, (7), 2636-2642.

137. Oberdorster, E. Manufactured nanomaterials (Fullerenes, C-60) induce oxidative stress in the brain of juvenile largemouth bass. *Environ. Health Perspect.* **2004,** *112*, (10), 1058-1062.

138. Zhu, S. Q.; Oberdorster, E.; Haasch, M. L. Toxicity of an engineered nanoparticle (fullerene, C-60) in two aquatic species, Daphnia and fathead minnow. *Mar. Environ. Res.* **2006,** *62*, S5-S9.

139. Johansen, A.; Pedersen, A. L.; Jensen, K. A.; Karlson, U.; Hansen, B. M.; Scott-Fordsmand, J. J.; Winding, A. Effects of C-60 fullerene nanoparticles on soil bacteria and protozoans. *Environ. Toxicol. Chem.* **2008,** *27*, (9), 1895-1903.

140. Kang, S.; Mauter, M. S.; Elimelech, M. Microbial Cytotoxicity of Carbon-Based Nanomaterials: Implications for River Water and Wastewater Effluent. *Environ. Sci. Technol.* **2009,** *43*, (7), 2648-2653.

141. Nyberg, L.; Turco, R. F.; Nies, L. Assessing the impact of nanomaterials on anaerobic microbial communities. *Environ. Sci. Technol.* **2008,** *42*, (6), 1938-1943.

142. Tong, Z. H.; Bischoff, M.; Nies, L.; Applegate, B.; Turco, R. F. Impact of fullerene (C-60) on a soil microbial community. *Environ. Sci. Technol.* **2007,** *41*, (8), 2985-2991.

143. Andrievsky, G.; Klochkov, V.; Derevyanchenko, L. Is the C-60 fullerene molecule toxic?! *Fuller. Nanotub. Carbon Nanostruct.* **2005,** *13*, (4), 363-376.

144. Gao, J.; Youn, S.; Hovsepyan, A.; Llaneza, V. L.; Wang, Y.; Bitton, G.; Bonzongo, J. C. J. Dispersion and Toxicity of Selected Manufactured Nanomaterials in Natural River Water Samples: Effects of Water Chemical Composition. *Environ. Sci. Technol.* **2009,** *43*, (9), 3322-3328.

145. Henry, T. B.; Menn, F. M.; Fleming, J. T.; Wilgus, J.; Compton, R. N.; Sayler, G. S. Attributing effects of aqueous C-60 nano-aggregates to tetrahydrofuran decomposition products in larval zebrafish by assessment of gene expression. *Environ. Health Perspect.* **2007,** *115*, (7), 1059-1065.

146. Li, D.; Lyon, D. Y.; Li, Q.; Alvarez, P. J. J. Effect of soil sorption and aquatic natural organic matter on the antibacterial activity of a fullerene water suspension. *Environ. Toxicol. Chem.* **2008,** *27*, (9), 1888-1894.

147. Sayes, C. M.; Fortner, J. D.; Guo, W.; Lyon, D.; Boyd, A. M.; Ausman, K. D.; Tao, Y. J.; Sitharaman, B.; Wilson, L. J.; Hughes, J. B.; West, J. L.; Colvin, V. L. The differential cytotoxicity of water-soluble fullerenes. *Nano Lett.* **2004,** *4*, (10), 1881-1887.

148. Cho, M.; Fortner, J. D.; Hughes, J. B.; Kim, J.-H. *Escherichia coli* Inactivation by Water-Soluble, Ozonated C60 Derivative: Kinetics and Mechanisms. *Environ. Sci. Technol.* **2009**.

149. Scott-Fordsmand, J. J.; Krogh, P. H.; Schaefer, M.; Johansen, A. The toxicity testing of double-walled nanotubes-contaminated food to Eisenia veneta earthworms. *Ecotoxicol. Environ. Saf.* **2008,** *71*, (3), 616-619.

150. Smith, C. J.; Shaw, B. J.; Handy, R. D. Toxicity of single walled carbon nanotubes to rainbow trout, (Oncorhynchus mykiss): Respiratory toxicity, organ pathologies, and other physiological effects. *Aquat. Toxicol.* **2007,** *82*, (2), 94-109.

151. Stampoulis, D.; Sinha, S. K.; White, J. C. Assay-Dependent Phytotoxicity of Nanoparticles to Plants. *Environ. Sci. Technol.* **2009,** *43*, (24), 9473-9479.

152. Simon-Deckers, A.; Loo, S.; Mayne-L'Hermite, M.; Herlin-Boime, N.; Menguy, N.; Reynaud, C.; Gouget, B.; Carriere, M. Size-, Composition- and Shape-Dependent Toxicological Impact of Metal Oxide Nanoparticles and Carbon Nanotubes toward Bacteria. *Environ. Sci. Technol.* **2009,** *43*, (21), 8423-8429.

153. Kennedy, A. J.; Gunter, J. C.; Chappell, M. A.; Goss, J. D.; Hull, M. S.; Kirgan, R. A.; Steevens, J. A. Influence of nanotube preparation in aquatic bioassays. *Environ. Toxicol. Chem.* **2009,** *28*, (9), 1930-1938.

154. Ghafari, P.; St-Denis, C. H.; Power, M. E.; Jin, X.; Tsou, V.; Mandal, H. S.; Bols, N. C.; Tang, X. W. Impact of carbon nanotubes on the ingestion and digestion of bacteria by ciliated protozoa. *Nature Nanotech.* **2008,** *3*, (6), 347-351.

155. Mouchet, F.; Landois, P.; Flahaut, E.; Pinelli, E.; Gauthier, L. Assessment of the potential in vivo ecotoxicity of Double-Walled Carbon Nanotubes (DWNTs) in water, using the amphibian Ambystoma mexicanum. *Nanotoxicology.* **2007,** *1*, (2), 149-156.

156. Petersen, E. J.; Akkanen, J.; Kukkonen, J. V. K.; Weber, W. J. Biological Uptake and Depuration of Carbon Nano-tubes by Daphnia magna. *Environ. Sci. Technol.* **2009,** *43*, (8), 2969-2975.

157. Tejral, G.; Panyala, N. R.; Havel, J. Carbon nanotubes: toxicological impact on human health and environment. *J. Appl. Biomed.* **2009,** *7*, (1), 1-13.

158. Perez, S.; Farre, M.; Barcelo, D. Analysis, behavior and ecotoxicity of carbon-based nanomaterials in the aquatic environment. *TrAC, Trends Anal. Chem.* **2009,** *28*, (6), 820-832.

159. Lam, C. W.; James, J. T.; McCluskey, R.; Arepalli, S.; Hunter, R. L. A review of carbon nanotube toxicity and assessment of potential occupational and environmental health risks. *Crit. Rev. Toxicol.* **2006,** *36*, (3), 189-217.

160. Helland, A.; Wick, P.; Koehler, A.; Schmid, K.; Som, C. Reviewing the environmental and human health knowledge base of carbon nanotubes. *Environ. Health Perspect.* **2007,** *115*, (8), 1125-1131.

161. Donaldson, K.; Aitken, R.; Tran, L.; Stone, V.; Duffin, R.; Forrest, G.; Alexander, A. Carbon nanotubes: A review of their properties in relation to pulmonary toxicology and workplace safety. *Toxicol. Sci.* **2006,** *92*, (1), 5-22.

162. Koelmans, A. A.; Nowack, B.; Wiesner, M. R. Comparison of manufactured and black carbon nanoparticle concentrations in aquatic sediments. *Environ. Pollut.* **2009,** *157*, (4), 1110-1116.

163. Gottschalk, F.; Sonderer, T.; Scholz, R. W.; Nowack, B. Modeled Environmental Concentrations of Engineered Nanomaterials (TiO2, ZnO, Ag, CNT, Fullerenes) for Different Regions. *Environ. Sci. Technol.* **2009,** *43*, (24), 9216-9222.

Chapter 3 – A Cost-Effective Method of Aerosolizing Dry Powdered Nanoparticles

Submitted: March 2013
To: Aerosol Science and Technology
Status: Published November 2013 (Vol. 47, Issue 11, p1267-1275.)

Abstract

The ability to produce nano-scale aerosols from dry powdered material is needed for studies of the toxicity and environmental transformation and fate of manufactured nanoparticles. Wet aerosol generation methods can alter particle chemistry, while dry methods often cannot produce truly nano-scale aerosols. We have developed a cost-effective dry dispersion technique for manufactured nanoparticles and have demonstrated its use with C_{60} fullerene, TiO_2, and CeO_2. The system disperses dry powders to create aerosols with mode diameters below 100 nm. Average mode and median diameters for each of the tested manufactured nanoparticles are 91 and 107 nm for C_{60}, 65 and 77 nm for TiO_2, and 40 and 43 nm for CeO_2. All aerosols exhibit right-skewed unimodal distributions and irregular morphology. Aerosol mass concentrations produced by the dispersion system vary linearly with the mass of nanomaterial loaded into it and are of a magnitude appropriate for inhalation nanotoxicology studies. This work demonstrates the ability of a simple device to produce nanoscale aerosols from powdered engineered nanoparticles.

Introduction

As part of the rapid growth in nanotechnology, potential inhalation exposure to manufactured nanoparticles (ENPs) has become a concern. ENPs have at least one, often three, dimensions that

measure 100 nm or less. ENPs are produced in industrial or research facilities, while "incidental" nanoparticles may be similar to ENPs in composition but are the unintentional byproducts of human activities. In addition to engineered and incidental nanoparticles, "natural" nanoparticles are produced in the environment independent of human activities. There are likely to be substantial chemical and morphological differences between incidental and natural nanoparticles and ENPs.[1]

Animal studies indicate that inhalation of ENPs leads to a variety of effects. Inhalation of gold nanoparticles by rats is associated with accumulation of gold nanoparticles in the lungs and kidneys,[2] while inhalation of multiwalled carbon nanotubes (MWNT) results in damage to DNA in rat lung cells.[3] Iron oxide nanoparticle inhalation by rats is associated with enhanced levels of inflammation markers in blood[4] as well as elevated levels of reactive oxygen species (ROS) in the lungs.[4, 5] The complex biological effects of inhaled manufactured nanoparticles are just beginning to be understood, however. Furthermore, nanotechnology as an economic sector is growing and is projected to exhibit an annual growth rate of 19% during 2011-2014.[6] Together, these facts underscore the need for more toxicology research focused on inhaled ENPs. Such research is important from several perspectives, including consumer safety and worker safety.

ENPs are typically found as agglomerates in the environment. Agglomerates may exert different toxicological effects than their primary particle constituents. For example, rats exposed to sub-100 nm and super-100 nm agglomerates of 5 nm TiO_2 ENPs via inhalation exhibited different markers of pulmonary toxicity, suggesting the agglomerate size, not the primary particle size, influenced the biological response.[7] Because both the physical and chemical characteristics of

inhaled particles can affect their toxicity, inhalation toxicology studies must take care to generate aerosols that represent fairly the substance of interest in a relevant exposure scenario. The choice of aerosol generation method, which can affect both of these characteristics, is an important one.

Aerosols may be generated through a variety of methods, both with and without the use of liquids. "Wet" aerosolization methods include pneumatic (nebulizing), electrospray, and ultrasonic techniques,[8] all of which create a spray from a liquid solution or suspension. Three types of aerosols can be produced: droplets from low-volatility liquids, or upon drying, salts of a dissolved compound, or solids from a suspension. If the drying is only partial, then some solvent may remain on the aerosols. The concentration of the solution/suspension and other process parameters can be adjusted to control characteristics of the resulting aerosol, such as size, morphology, and density.[9-11] Because of this degree of control, high number concentrations and particle sizes well below 100 nm are achievable. These methods are well established and numerous commercial devices employing them are available.

While wet methods can produce nano-scale particles with relative ease, there are drawbacks. Through interaction with impurities in the solvent or with the solvent itself, the particle surface may be chemically altered.[8, 12] Sullivan *et al.*[13] found that the hygroscopicity of wet-generated $CaCO_3$ aerosols exceeded that of dry-generated $CaCO_3$ aerosols by a factor of 100, and that the hygroscopicity increased with both increasing time spent in water and with decreasing particle size. The authors noted that any changes to $CaCO_3$ aerosols generated through wet methods had previously been assumed to be minimal, owing to the low solubility of $CaCO_3$ in water. In addition to chemical effects, the choice of aerosolization method can also have physical and

biological consequences. The viability of bacteria and fungi contained within grain dust aerosols (such as from wheat) is influenced by the aerosol generation method (wet or dry).[14] Additionally, this difference in aerosol generation method also resulted in a 10-fold difference in size. Consequently, we should be hesitant to assume that aerosols produced via wet generation methods are chemically and physically equivalent substitutes for those produced via dry methods.

There are several techniques for generating aerosol that do not involve the use of liquids. A variety of techniques, including eductors, nozzles, impaction plates, and fluidized beds has been used to disperse a dry powder into a gas flow.[15] With any of these methods, though, creating aerosols smaller than 20 μm has been difficult,[15] and achieving an aerosol size below 1 μm has been especially challenging.[12] As particle size decreases interparticle interactions, such as van der Waals and electrostatic forces, increase in relative importance.[16] Depending upon disperser design, forces supplied by the gas flow may not be able to overcome interparticle attraction, and the resulting agglomerates are mostly larger than 1 μm.

Although improved designs of commercial dry powder dispersers are enabling the production of significantly smaller particles, the generation of truly nano-scale aerosol remains elusive. A recent intercomparison of three commercial dispersers supplied with metal oxide NP powders demonstrated that while all produced sub-micron aerosols, most size distributions had mode diameters ranging from 200 nm to 400 nm, and none were below 100 nm.[17]

Several research groups have developed custom aerosolization devices, but in most cases the aerosols produced were not nano-scale. Tang *et al.*[18] used an inexpensive vacuum generator to disperse crystalline mannitol and amorphous bovine serum albumin, and produced aerosols with volume-weighted median diameters of 2.4 μm (mannitol) and 9.0 μm (BSA). These aerosols were only slightly larger than aerosols of the same materials generated by the Small Scale Powder Disperser (SSPD, TSI, Shoreview, MN) and Scirocco dry powder disperser (Malvern, Worcs, UK), suggesting that at least in the cases of mannitol and BSA, such a system may prove an adequate substitute for costly commercial dispersers. To produce TiO_2 agglomerates for a rat inhalation study, Noel *et al.*[7] coupled commercially available dispersion equipment with a custom-built venturi flow ejector; the median size of their aerosols was 185-194 nm. A custom-built system designed to aerosolize carbonaceous ENPs for inhalation toxicology studies produced single-walled carbon nanotube (SWNT) aerosols over 1 μm in size,[19] while a rodent inhalation study used a proprietary brush technique to generate multi-walled carbon nanotube (MWNT) aerosols 0.7 – 2.0 μm in size as measured by cascade impaction.[20]

To our knowledge, only two custom systems have produced nano-scale ENP aerosols. Schmoll *et al.*[21] used a speaker and a function generator to produce sub-100 nm aerosol from SiO_2 and SWNT. Size distributions for both particle types were bimodal, however, and the larger peak exceeded 100 nm. The system was not successful in aerosolizing TiO_2. To *et al*.[22] described a rapid expansion of high pressure or supercritical suspensions (REHPS) system, which used high pressure and temperature to produce aerosols from titania and alumina ENPs with primary particle sizes of 21 and 13 nm, respectively. Aerosols generated by this system exhibited mode diameters of 40 – 80 nm (titania) and 70 – 90 nm (alumina). One possible disadvantage of the

system is that the standard deviations of the size distributions were nearly as large as the mode diameter (70 – 80 for titania, 85 – 95 for alumina), indicating that the size distributions were quite wide.[22] The REHPS system required high pressure (1.7 – 7.9 MPa) and temperature (45 °C), which may be considered a drawback in some situations.

Producing sub-100 nm aerosol from ENPs via a dry dispersion process remains challenging. Most custom-designed systems are complex or labor-intensive while often generating aerosols that are larger than can be considered nano-scale. Commercially available dispersers have not been demonstrated to generate nano-scale aerosol and can be expensive (~$10,000). The objective of this work is to develop a cost-effective method to disperse bulk ENP powders into nano-scale aerosols. Based upon the work of Tang *et al.,*[18] we use a venturi vacuum generator to disperse powdered manufactured nanoparticles by dispensing them into a high-velocity jet of air. We test the dispersion system using both carbonaceous (C_{60}) and metal oxide (TiO_2, CeO_2) ENPs. The method shows promise for use in laboratory studies of both toxicity and environmental transformation and fate of ENPs.

Experimental

Disperser

The powder dispersion system is based on that of Tang et al.[18] and consists of a commercially available vacuum generating device (VCH10-018C, Pisco, Elmhurst, IL), which costs less than $100, and standard tubing and fittings. Joining the T-junction of the vacuum generator to tubing with a standard threading system requires an adaptor to fit the vacuum generator's "R" threading.

Other components are 0.635 cm o.d. tubing and compatible ball valves. A schematic and photograph of the setup are shown in Figure 1.

The vacuum generator is positioned so that the vacuum arm points upward; this is used as the entry point for the ENP powder. The filter and metal cap provided with the vacuum generator are removed to reveal a nozzle, which acts as the aerosol outlet. Compressed air or other gas is provided to the opposite end of the disperser via 8-mm o.d. tubing.

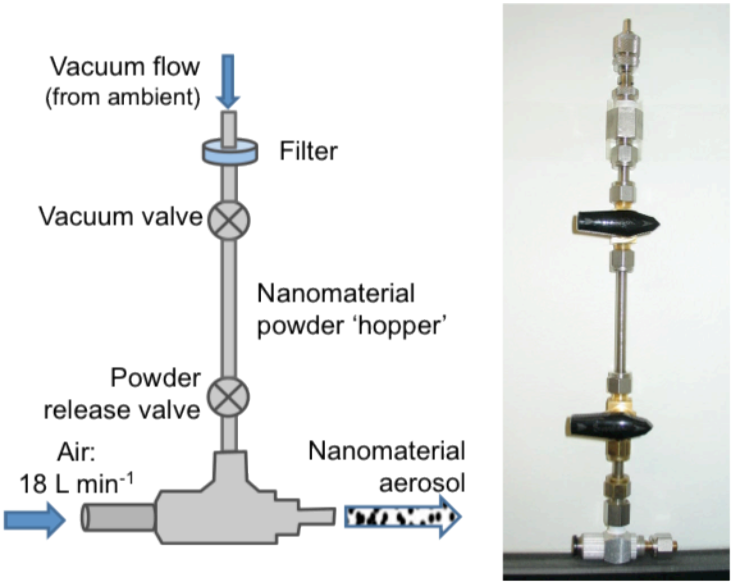

Figure 3-1: Schematic and photo of disperser setup.

The disperser setup developed in this work differs from that of Tang *et al.* in three ways: powder supply, aerosol destination, and pressure.[18] First, the ENP powder is enclosed in a hopper for safety reasons, in contrast to the funnel used in Tang's work, which was open to ambient air. Second, the Tang system dispersed the aerosol directly into an aerosol sizing instrument (Mastersizer S laser diffractometer, Malvern, Worcs, UK), not into an environment at ambient

pressure. Last, our system is operated at ~150 kPa gauge pressure, in contrast to the higher (up to 620 kPa) pressures used in Tang's work.

In order to allow for safe handling practices while allowing for the dry dispersion of ENPs into an enclosed chamber, a nanomaterial hopper is attached to the vacuum arm of the disperser. A 10-cm length of stainless steel tubing (6.4 mm o.d.) serves as the hopper, which is bookended by brass ball valves. The hopper may be detached from the disperser below the lower valve to allow the user to load the ENPs into the hopper in a safe handling environment, such as an air curtain hood or other enclosure.[23] Upon reassembly, the upper valve is opened to allow ambient air to flow into the disperser during operation. A filter may be attached to the upper valve as an additional safety measure. Compressed breathing air is then introduced to the disperser at a flow rate of ~18 L min^{-1}.

The powder release valve controls NP entry into the disperser. When the valve is opened, ENP powder falls into the air stream flowing through the disperser. Within the disperser, the powder undergoes rapid, forceful collisions,[18] breaking it apart. Because aerosol generation happens rapidly (within seconds), the airflow may be stopped shortly after the powder is introduced.

Manufactured Nanoparticles

The disperser's ability to generate nano-scale aerosol was demonstrated with both carbonaceous and metal oxide ENPs: C_{60} (MER Corp., Tucson, AZ, USA), TiO_2 (primary particle size 30 – 40 nm, NanoAmor, Houston, TX, USA), and CeO_2 (primary particle size 15 – 30 nm, NanoAmor, Houston, TX, USA). Attempts to generate aerosols from MWNT (NanoAmor) did not produce

repeatable results. These ENPs were chosen to facilitate comparison to other aerosolization techniques and because they are currently used in toxicity studies.

As received from the manufacturer, C_{60} was in a crystalline form (with crystals > 0.1 mm) and required milling in order to reduce the particle size prior to use. Milling was performed using a beadbeater with 2-mL polypropylene vials and 1-mm glass beads (mini-Beadbeater-1, vials and beads from BioSpec, Bartlesville, OK, USA). After milling, the beads, which had become coated with pulverized C_{60}, were decanted into a larger glass vial and shaken vigorously. The beads were decanted a second time, and C_{60} powder clinging to the walls of the glass vial was scraped off using a stainless steel spatula. TiO_2 and CeO_2 were used as received. Aliquots of all ENP's were weighed in a capped 2-mL plastic vial before being loaded into the hopper.

Analytical Techniques

The ENP aerosols were dispersed directly into a ~500-L flexible, polyethylene chamber (AtmosBag, Sigma Aldrich, St. Louis, MO, USA). Each ENP type was dispersed in 9-12 separate trials. Between trials, the bag was cleaned by evacuating it and refilling it with filtered breathing air; this cleaning process was repeated until the particle concentration in the bag was below 100 # cm^{-3}. The compressed breathing air used to disperse the ENPs was confirmed not to introduce particles into the chamber.

The aerosol size distribution was measured using a Scanning Mobility Particle Sizer (SMPS, TSI, Shoreview, MN) and an Aerodynamic Particle Sizer (APS, TSI). The size ranges measured by these instruments overlap slightly (SMPS: 14 – 750 nm; APS: 530 nm – 20 μm) and can be merged into a single size distribution using the software DataMerge (TSI). The SMPS was

equipped with the "long" differential mobility analyzer (DMA) and the 0.071 cm impactor, and it scanned the maximum size range (14-750 nm) over 5 min. Multiple charge correction was employed, and the CPC was set in low-flow mode. The size distribution measurement was initiated within 30 s of dispersion.

Density values entered into the SMPS and APS software were 0.6, 0.4, and 0.2 g cm^{-3} for C_{60}, TiO_2, CeO_2, respectively. The density of 0.6 g cm^{-3} for C_{60} was measured for C60 powder resulting from the milling procedure described above, while the values for TiO_2 and CeO_2 are relevant for the ENP powders, as reported by the manufacturer. While the true density of the generated aerosols may differ from these values, the size distributions as measured by the SMPS are independent of assumed particle density. The assumed densities influence the mass concentration estimates that are based on the size distributions. All particle size data shown in this work are from the merged distributions produced by DataMerge (TSI).

Particle morphology was examined using transmission electron microscopy (TEM, Philips EM420, 120kV, LaB_6 filament, spot size 2). Aerosol particles were deposited directly onto copper TEM grids using the third stage of an impactor with a cut size of 50 nm (MPS-3, California Measurements, Sierra Madre, CA, USA).

Results

Size distributions

Figure 3-2 shows typical size distributions of the three ENP aerosols. The smallest aerosols were obtained using CeO_2, which had the smallest primary particle size, while the largest were of C_{60}.

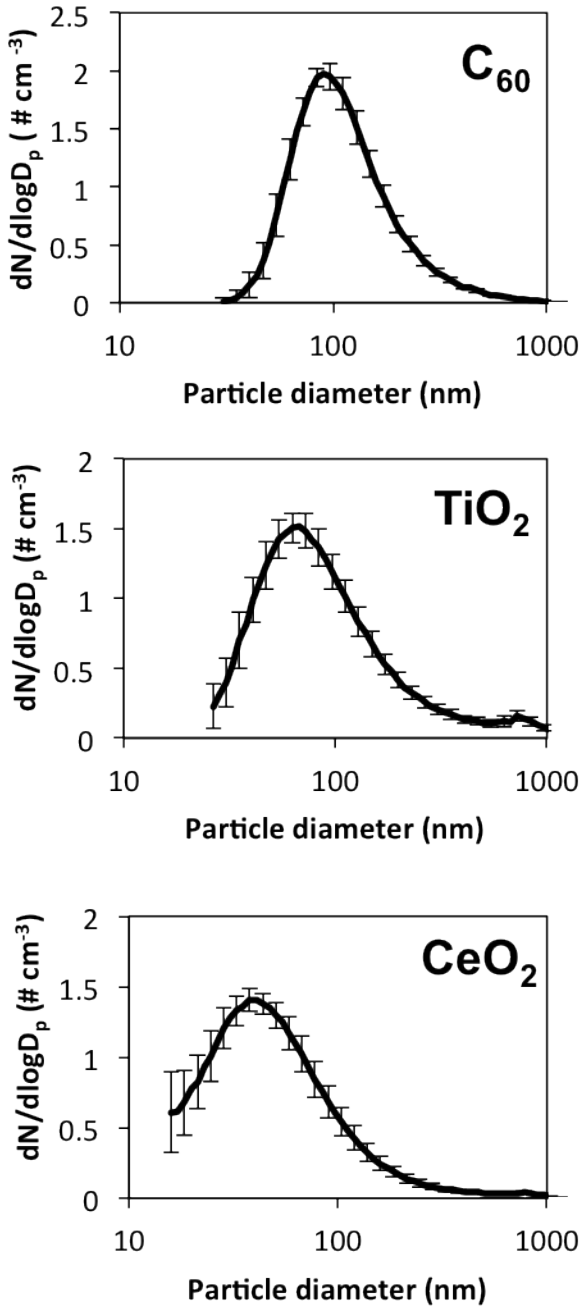

Figure 3-2: Mean size distributions (error bars show standard deviation) of nanoparticle aerosols. Mean size distributions are normalized to the particle count.

All distributions were unimodal, right-skewed, and approximately lognormal. Particle size statistics are summarized in Table 3-1. All data are number-weighted and refer to the agglomerate, not primary, particle size. The geometric mean diameters differed from the median diameters by 3%, 14%, and 16% for C_{60}, TiO_2, and CeO_2, respectively (in a perfectly lognormal distribution, these metrics would be identical). Mode diameters for aerosol particles of each ENP were approximately 90 nm, 65 nm, and 40 nm for C_{60}, TiO_2, and CeO_2, respectively.

Table 3-1: Particle statistics for produced ENP aerosols.

ENP	*n*	Mode	Median	GM[a]	GSD[b]
C_{60}	9	91 ± 4	107	110	1.7
TiO_2	12	65 ± 6	77	88	2.1
CeO_2	17	40 ± 6	43	50	2.1

[a] Geometric mean

[b] Geometric standard deviation

The mode diameter of the aerosols was not influenced by the mass of ENP powder loaded into the disperser. Figure 3-3 shows the mode diameter as a function of loaded ENP mass for each of the three substances. For all ENPs, the relationship between the two variables was not significant.

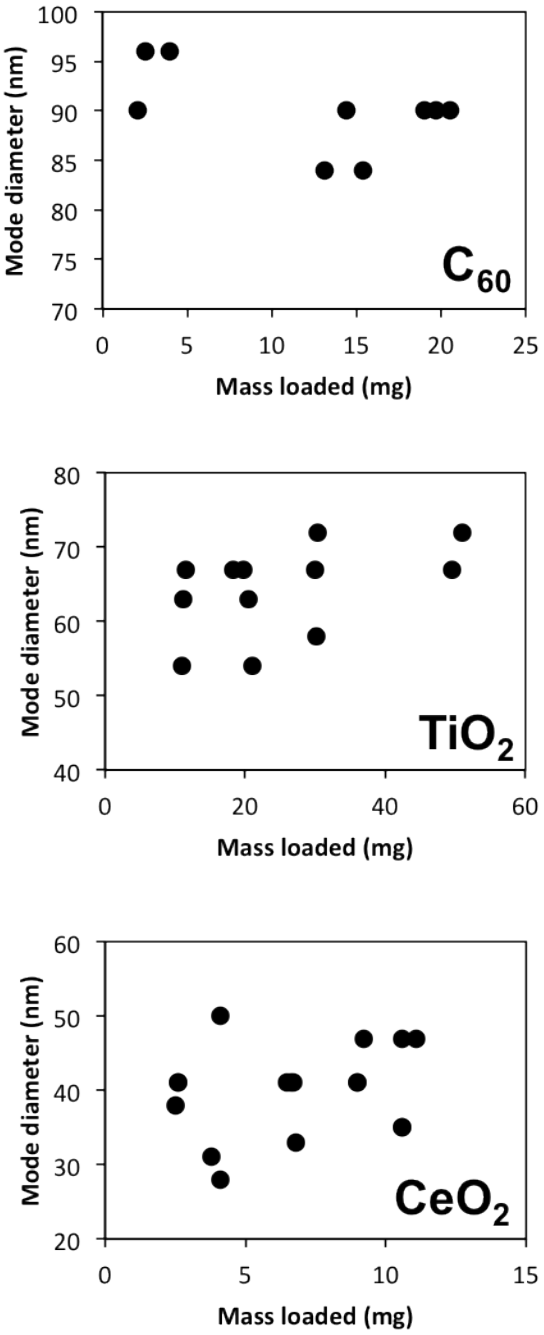

Figure 3-3: Aerosol mode diameter as a function of nanoparticle mass loaded into the disperser.

Aerosol mass concentration

Figure 3-4 shows the estimated aerosol mass concentration produced in the chamber as a function of ENP mass initially loaded into the disperser. For each type of ENP, increased loaded mass resulted in an increased aerosol mass concentration. The least-squares linear regression lines shown in Figure 3-4 are significant at the $p < 0.005$ level for all ENPs. For CeO_2, the regression omits the five outlying points. The tendency of CeO_2 to occasionally produce outlying aerosol mass concentrations in this system is discussed below.

Particle morphology

The morphology of the resulting aerosol was examined using TEM. Figure 3-5 shows TEM images for each type of ENP aerosol. In both TiO_2 and CeO_2 aerosols, the primary particles could be seen easily, and their sizes agreed with the primary particle size range advertised by the manufacturer. Both TiO_2 and CeO_2 aerosols appeared tightly packed and of irregular rounded shape. The aerosols were larger than the mode diameter indicated by DataMerge; a potential reason for this discrepancy is discussed below. The C_{60} particles showed lattice fringes in a portion of the particle, which overall exhibited an irregular shape.

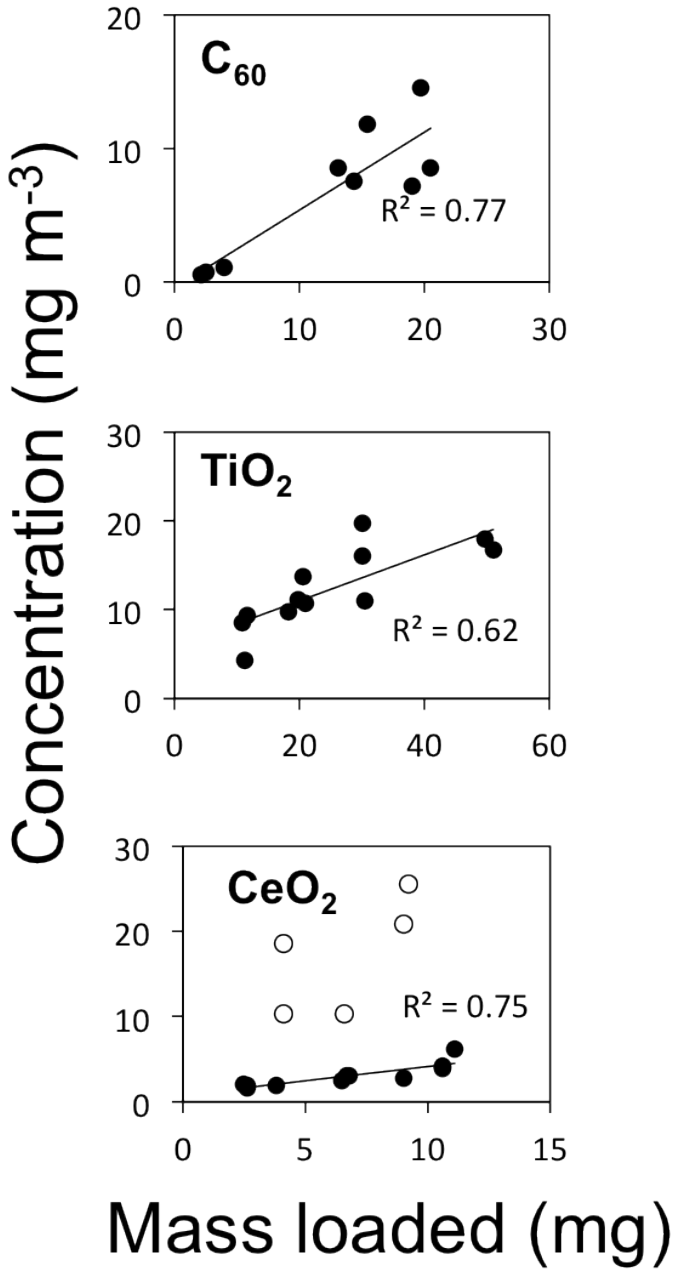

Figure 3-4: Aerosol mass concentration as a function of nanoparticle mass loaded into the disperser. The mass concentrations for C_{60} are upper-bound values, while the concentrations for the metal oxides are lower-bound values.

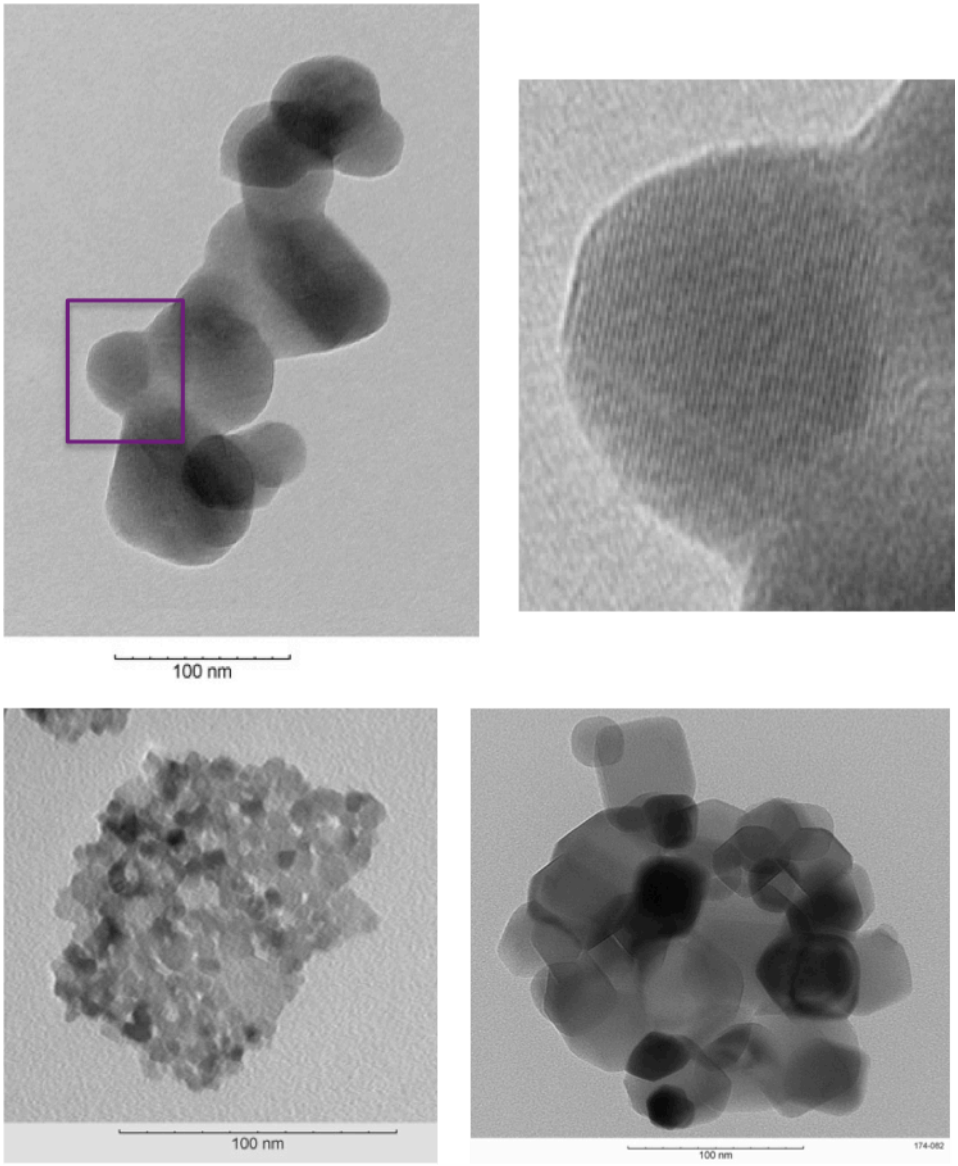

Figure 3-5: TEM images of nanoparticle aerosols produced using this dispersion system. Clockwise from top left: C_{60} aerosol; inset of C_{60} particle showing lattice fringes; TiO_2 aerosol showing primary particles; CeO_2 aerosol showing primary particles. All scale bars are 100 nm.

Discussion

Particle size and size distribution

This work has demonstrated a cost-effective method of producing nano-scale aerosols from powdered ENPs. Particle size distributions achieved by this system exhibit modes below 100 nm, smaller than produced by other dry dispersion systems described in the literature, both commercial and custom-made, with the exception of the REHPS system described by To *et al.*[22] Particle statistics for the system described here and others from the literature are summarized in Table 3-2.

While the MWNT aerosol produced by Ma-Hock *et al.*[20] appears to be sub-100 nm, as measured by the SMPS, those authors question the validity of both SMPS and optical methods to accurately size MWNT aerosols due to their potential to form complex, tangled structures. This uncertainty is illustrated by the order-of-magnitude difference in aerosol size according to the two instruments used in the study. Titania and alumina ENP aerosols produced by the REHPS system exhibit median diameters from 40 to 90 nm, as shown in Table 3-2.[22] However, the REHPS system utilizes both elevated temperature (45 °C CO_2) and pressure (1.7 – 7.9 MPa), whereas the disperser described here operates at ambient temperature and significantly lower pressure (~150 kPa). Additionally, the system described in this work has been demonstrated to produce nano-scale aerosols from ENPs of various compositions (carbonaceous, metal oxide), whereas the REHPS system has been demonstrated for metal oxide aerosols alone.

Table 3-2: Statistics of nanoparticle aerosols generated by various dry powder dispersion techniques. All values are number weighted unless otherwise specified.

Particle type	Primary particle diam. (nm)	Dispersion system	D_{25} (nm)	Mode (nm)	Median (D_{50}) (nm)	Geo. mean (nm); geo. st. dev	D_{75} (nm)	Aerosol number conc. (# cm^{-3})	Aerosol mass conc. (mg m^{-3})	Ref.
TiO_2	30 - 40	vacuum generator	51	65	77	88; 2.1	124	$2.2 \times 10^5 - 1.1 \times 10^6$	4.3 – 19.7	this work
	21	REHPS	*N/A*	*N/A*	37 - 79 [a]	*N/A*	*N/A*	*N/A*	*N/A*	22
		SSPD	*N/A*	*N/A*	260, 547 [b]	*N/A*; 2.25, 1.47 [b]	*N/A*	2.7×10^6 [b]	*N/A*	17
		SSPD	*N/A*	[c]	*N/A*	[c]	*N/A*	159	*N/A*	21
		ADAGE	*N/A*	[c]	*N/A*	[c]	*N/A*	172	*N/A*	
		FBG	*N/A*	269	*N/A*	171.5; 1.56	*N/A*	15,786	*N/A*	
	5	Palas RBG	108	*N/A*	185	*N/A*	284	161,898	1.96	7
		TSI FBG	81	*N/A*	194	*N/A*	470	19,573	7.15	
Al_2O_3	13	REHPS	*N/A*	*N/A*	35 - 91 [a]	*N/A*	*N/A*	*N/A*	*N/A*	22
ZnO	30-50	SSPD	*N/A*	*N/A*	276, 753 [b]	*N/A*; 1.76, 1.39 [b]	*N/A*	1.4×10^5 [b]	*N/A*	17
SiO_2	10 - 30	SSPD	*N/A*	*N/A*	125, 751 [b]	*N/A*; 1.9, 1.5 [b]	*N/A*	9.5×10^5 [b]	*N/A*	17
	20	SSPD	*N/A*	195	*N/A*	128.8; 2.06	*N/A*	4,344	*N/A*	21
		ADAGE	*N/A*	126 [d]	*N/A*	62.7; 2.66	*N/A*	3,290	*N/A*	
CeO_2	10 - 30	vacuum generator	29	40	43	50; 2.1	69	$3.0 \times 10^5 - 1.7 \times 10^6$	1.7 – 25.6	this work
C_{60}	molecular	vacuum generator	77	91	107	110; 1.7	151	$6.9 \times 10^4 - 1.3 \times 10^6$	0.2 – 5.1	this work
SWCNT	1 to 2	ADAGE	*N/A*	7 [e]	*N/A*	33.6; 3.61	*N/A*	7,586		21
	unknown	*N/A*	*N/A*	*N/A*	*N/A*	1.3 - 1.7 [f]	*N/A*	*N/A*	0.3 - 1	19
MWCNT	5-15	brush generator	*N/A*	*N/A*	58-64; 540 -580 [g]	0.7 - 2.0 [f]; 2.1 - 4.1	*N/A*	30-1,182; 365 - 31,695 [g]	0.1 - 2.5	20
	20 - 90	acoustic generator	*N/A*	350	*N/A*	*N/A*	*N/A*	4.2×10^4	*N/A*	24
	unknown	Wright Dust Feeder	*N/A*	*N/A*	*N/A*	900 - 940	*N/A*	8 - 364	0.1 - 5.98	25

[a] range is due to varying pressures used in REHPS system
[b] data separated by commas are from SMPS and APS respectively; number concentrations are normalized to total aerosol mass, in # cm^{-3} g^{-1}
[c] counts too low to determine this statistic
[d] distribution is bimodal with a minor peak at 24.1 nm
[e] distribution is bimodal with a minor peak at 146 nm
[f] mass mean aerodynamic diameter, µm
[g] first range is by SMPS, second range is by OPC

Aerosol size in this work is reported in terms of mobility diameter, d_m. The accuracy of d_m as a measure of an aerosol's true size has been questioned, especially for irregularly shaped aerosols, such as those composed of carbon nanotubes.[20, 26] While the aerosols in this work are not spherical, as is assumed when d_m is calculated, the particle morphology is noticeably more densely packed than are carbon nanotube aerosols. Work by Shin *et al.*[27] with silver nanoparticle aerosols demonstrates that the "projected area diameter," d_{pa}, determined from TEM images is equal to or less than d_m for aerosols in the size range of ~80 – 250 nm. While d_{pa} may exceed d_m slightly for particles with d_m <50 nm, overall d_m should be a fairly accurate proxy for d_{pa} for these aerosols, given their size and morphology. Aerosols smaller than 100 nm deposit with 20-70% efficiency in the alveolar region;[28, 29] consequently, the aerosols in this work are relevant to inhalation toxicology studies in terms of size.

In contrast to results from other dry dispersion techniques, the aerosol size distributions produced by this method are unimodal, approximately lognormal, and relatively narrow. Schmoll *et al.*'s ADAGE system[21] produces bimodal distributions for all ENPs tested. TSI's Small Scale Powder Disperser (SSPD) as tested by Tsai *et al.*[17] produces unimodal, but very broad, size distributions (with 'peaks' that plateau over several hundred nanometers) for all three ENPs tested. The size distributions produced by the Palas RBG (rotating brush generator) and fluidized bed generator (FBG) utilized by Noel *et al.*[7] are also relatively broad, with interquartile (D_{25} – D_{75}) ranges of 108 – 284 nm and 81 – 470 nm, respectively. In comparison, interquartile ranges for the aerosols produced in this work, shown in Table 3-2, suggest narrower size distributions and are as follows: C_{60}, 77 – 151 nm; TiO_2, 51 – 124 nm; CeO_2, 29 – 69 nm. The size distributions in this work also appear to be comparable in terms of relative width to those produced by the REHPS

system, although a quantitative comparison is not possible. The size of the nozzle through which the ENPs are dispersed in each system (254 μm in To *et al.*[22] v. 1 mm in this work) may affect the width of the size distribution. Tang *et al*.[18] found that narrower custom nozzles resulted in wider size distributions of BSA and mannitol aerosols, although the applicability of that relationship to ENPs has not been directly investigated.

Aerosol number and mass concentration

This disperser can produce aerosol number concentrations that match or surpass those generated by other systems, as shown in Table 3-2. When dispersed into a ~500 L chamber, the ENPs produced number concentrations of $6.82 \times 10^4 - 1.40 \times 10^6$, $1.12 \times 10^5 - 7.95 \times 10^5$, and $2.95 \times 10^5 - 7.25 \times 10^5$ # cm^{-3} for C_{60}, TiO_2, and CeO_2 respectively. Additionally, the number concentration can be controlled by changing the loaded ENP mass, chamber size, or both. In general, number concentrations higher than these are not desirable because coagulation would become important.

Using bulk powder density values for all materials (0.6 g cm^{-3} for C_{60}, 0.4 g cm^{-3} for TiO_2 and 0.2 g cm^{-3} for CeO_2), these number concentrations translate into mass concentrations (Figure 3-4) that are of similar order of magnitude to those used for inhalation nanotoxicology studies.[3, 7, 20, 24] The actual densities of aerosol particles, however, are likely to be higher than the bulk powder densities since the primary particles appear tightly packed within the aerosols, as discussed below. Since the density of the aerosol particles will likely lie between the density of the powder and the density of the nanoparticle material, the mass concentrations shown in Figure 3-4 are conservative.

Direct comparison of aerosol number concentrations obtained in this study and by Tsai *et al.*[17] with the SSPD is challenging, as the SSPD results are normalized to aerosol mass. This direct method of aerosol mass measurement removes uncertainty about the density of ENP aerosols but can prohibit simple comparison of number concentration. A rough comparison can be made, however, by using the SMPS mass concentration estimate of the TiO_2 aerosols and bounds on the density of TiO_2 powder. Using the powder and nanoparticle densities of TiO_2 ENP powder as provided by the manufacturer (0.4 vs. 3.94 g cm^{-3}), we estimate that the number concentrations, normalized to mass, of the TiO_2 aerosols produced via our method range from 1.0×10^7 to 1.0×10^8 # cm^{-3} g^{-1}. These concentrations exceed the normalized concentrations of TiO_2 aerosol produced by the SSPD in Tsai's work (2.6×10^6 # cm^{-3} g^{-1}). While a firm conclusion is precluded by the uncertainty in aerosol density and the indirect estimate of mass concentration provided by the SMPS, it is likely that the number concentrations of TiO_2 aerosol produced in this system match, and possibly surpass, those produced by the SSPD as measured by Tsai *et al.*

The relationships between aerosol mass concentration and ENP mass loaded are statistically significant for all three materials, allowing the user to control the aerosol mass concentration produced. One exception is the group of outlying data points produced using CeO_2. The texture of CeO_2 is notably different from that of the other two tested ENPs; CeO_2 appears fluffy and does not pour well during handling. This cohesive behavior may affect the way the powder flows into the gas stream in the disperser.[30] Cohesive powders pack into open structures (i.e., with more empty space between primary particles) that flow less well than their less cohesive, more densely packed counterparts.[30, 31] Comparing the bulk and true densities of the metal oxide ENPs

provided by the manufacturer (0.4 vs. 3.94 g cm^{-3} for TiO_2, < 0.2 vs. 7.132 g cm^{-3} for CeO_2), it appears that CeO_2 packs much less densely than does TiO_2, and thus would flow poorly by comparison. This cohesivity may allow for less reproducible behavior within the disperser and result in occasional outlying mass concentrations. Both the 20-fold difference between bulk and true densities of MWNT (~0.1 vs. 2.1 g cm^{-3}, #1228NMG, NanoAmor, Houston, TX), and the fibrous nature of MWNT that allows them to become irregularly intertwined with one another, suggest that cohesiveness of MWNT may also be a hurdle to their successful nano-scale dispersion.

Morphology, crystallinity

TEM examination of the resulting ENP aerosols shows particles of irregular shape, as one might expect following a chaotic dry dispersion process. The TEM images, especially for TiO_2 and CeO_2, show aerosols larger than the mode diameter indicated by the SMPS. This is likely due to the use of impaction, which favors larger aerosols, as the mechanism for collecting samples onto TEM grids. An alternative sampling mechanism, thermophoretic precipitation, may result in a more representative sample of nano-scale aerosols since aerosols of diameter ~100 nm and less deposit with equal efficiency under thermophoresis.[32]

While the metal oxide ENPs have primary particle sizes from 10 to 40 nm, single C_{60} molecules are less than 1 nm across; the high-purity C_{60} molecules used in this study are packed into a crystal structure. The C_{60} crystals are milled as described above to reduce their size, and agglomerates of the crystalline C_{60} are broken up during dispersion. Consequently, the C_{60} aerosols result from a top-down size reduction process. The visible lattice fringes in Figure 3-5

show that the crystallinity of C_{60} remains intact through both milling and dispersion processes. This fundamental difference between the C_{60} and the metal oxides (crystalline molecules vs. primary particles) aligns well with the observation that the C_{60} aerosols were the largest of the three. Breaking down crystalline C_{60} even further – so the aerosols exhibited the same mode diameters as did the metal oxide aerosols – would require even stronger forces during milling and dispersion. By comparison, the formation of the metal oxide aerosols likely consists of both top-down and, possibly to a lesser extent, bottom-up processes, where as-received ENP agglomerates in powder form are broken up into both smaller agglomerates and possibly also into primary particles; these primary particles could re-agglomerate.

Future Work

One common feature of commercial dry dispersion equipment is the ability to produce a constant flow of aerosols over several minutes or more. If a continuous aerosol source is required, as in many toxicity studies, this method could be used to disperse aerosols into an upstream mixing chamber, from which a continuous stream of aerosols could be drawn. The disperser system could be converted into a continuous output aerosol generator through the addition of a feed mechanism to control the introduction of ENP powder into the disperser. Further work is required in order to determine if this method can successfully be adapted into an aerosol generation system that is capable of generating aerosols (a) continuously, (b) at target concentrations, and (c) smaller than 100 nm in size, as verified by several analytical methods, including TEM.

Conclusions

This work describes the development of a dry dispersion technique capable of producing sub-100 nm aerosols from manufactured nanoparticles cost-effectively at ambient temperature and an operating pressure near 150 kPa. The mass concentration of aerosols produced varies linearly with the mass of manufactured nanoparticles loaded into the system, and for the three tested materials, the generated aerosols exhibit a unimodal distribution and irregular morphology. For these three materials (C_{60}, TiO_2, CeO_2), this system is capable of producing manufactured nanomaterial aerosols with smaller mode and geometric mean diameters than commercially available dry powder dispersion equipment.

References

1. Win-Shwe, T. T.; Fujimaki, H. Nanoparticles and neurotoxicity. *Int. J. Mol. Sci.* **2011,** *12*, (9), 6267-6280.

2. Sung, J. H.; Ji, J. H.; Park, J. D.; Song, M. Y.; Song, K. S.; Ryu, H. R.; Yoon, J. U.; Jeon, K. S.; Jeong, J.; Han, B. S.; Chung, Y. H.; Chang, H. K.; Lee, J. H.; Kim, D. W.; Kelman, B. J.; Yu, I. J. Subchronic inhalation toxicity of gold nanoparticles. *Part. Fibre Toxicol.* **2011,** *8*.

3. Kim, J. S.; Sung, J. H.; Song, K. S.; Lee, J. H.; Kim, S. M.; Lee, G. H.; Ahn, K. H.; Lee, J. S.; Shin, J. H.; Park, J. D.; Yu, I. J. Persistent DNA damage measured by Comet assay of Sprague Dawley rat lung cells after five days of inhalation exposure and 1 month post-exposure to dispersed multi-wall carbon nanotubes (MWCNTs) generated by new MWCNT aerosol generation system. *Toxicol. Sci.* **2012,** *128*, (2), 439-448.

4. Srinivas, A.; Rao, P. J.; Selvam, G.; Goparaju, A.; Murthy, P. B.; Reddy, P. N. Oxidative stress and inflammatory responses of rat following acute inhalation exposure to iron oxide nanoparticles. *Hum. Exp. Toxicol.* **2012,** *31*, (11), 1113-1131.

5. Sotiriou, G. A.; Diaz, E.; Long, M. S.; Godleski, J.; Brain, J.; Pratsinis, S. E.; Demokritou, P. A novel platform for pulmonary and cardiovascular toxicological characterization of inhaled engineered nanomaterials. *Nanotoxicology.* **2012,** *6*, (6), 680-690.

6. RNCOS, I. R. S. Nanotechnology Market Forecast to 2014. **2012**, 175.

7. Noel, A.; Maghni, K.; Cloutier, Y.; Dion, C.; Wilkinson, K. J.; Halle, S.; Tardif, R.; Truchon, G. Effects of inhaled nano-TiO2 aerosols showing two distinct agglomeration states on rat lungs. *Toxicol. Lett.* **2012,** *214*, (2), 109-119.

8. Biskos, G.; Vons, V.; Yurteri, C. U.; Schmidt-Ott, A. Generation and sizing of particles for aerosol-based nanotechnology. *KONA Powder Part. J.* **2008,** *26*, 13-35.

9. Vehring, R.; Foss, W. R.; Lechuga-Ballesteros, D. Particle formation in spray drying. *J. Aerosol Sci.* **2007,** *38*, (7), 728-746.

10. Nandiyanto, A. B. D.; Okuyama, K. Progress in developing spray-drying methods for the production of controlled morphology particles: From the nanometer to submicrometer size ranges. *Adv. Powder Technol.* **2011,** *22*, (1), 1-19.

11. Peltonen, L.; Valo, H.; Kolakovic, R.; Laaksonen, T.; Hirvonen, J. Electrospraying, spray drying and related techniques for production and formulation of drug nanoparticles. *Expert Opin. Drug Deliv.* **2010,** *7*, (6), 705-719.

12. Masuda, H. Dry dispersion of fine particles in gaseous phase. *Adv. Powder Technol.* **2009,** *20*, (2), 113-122.

13. Sullivan, R. C.; Moore, M. J. K.; Petters, M. D.; Kreidenweis, S. M.; Qafoku, O.; Laskin, A.; Roberts, G. C.; Prather, K. A. Impact of particle generation method on the apparent hygroscopicity of insoluble mineral particles. *Aerosol Sci. Technol.* **2010,** *44*, (10), 830-846.

14. Thorne, P. S. Experimental grain dust atmospheres generated by wet and dry aerosolization techniques *Am. J. Ind. Med.* **1994,** *25*, (1), 109-112.

15. Calvert, G.; Ghadiri, M.; Tweedie, R. Aerodynamic dispersion of cohesive powders: A review of understanding and technology. *Adv. Powder Technol.* **2009,** *20*, (1), 4-16.

16. Calvert, G.; Hassanpour, A.; Ghadiri, M. Analysis of aerodynamic dispersion of cohesive clusters. *Chem. Eng. Sci.* **2013,** *86*, 146-150.

17. Tsai, C. J.; Lin, G. Y.; Liu, C. N.; He, C. E.; Chen, C. W. Characteristic of nanoparticles generated from different nano-powders by using different dispersion methods. *J. Nanopart. Res.* **2012,** *14*, (4).

18. Tang, P.; Fletcher, D. F.; Chan, H. K.; Raper, J. A. Simple and cost-effective powder disperser for aerosol particle size measurement. *Powder Technol.* **2008,** *187*, (1), 27-36.

19. Madl, A. K.; Teague, S. V.; Qu, Y. Q.; Masiel, D.; Evans, J. E.; Guo, T.; Pinkerton, K. E. Aerosolization system for experimental inhalation studies of carbon-based nanomaterials. *Aerosol Sci. Technol.* **2012,** *46*, (1), 94-107.

20. Ma-Hock, L.; Treumann, S.; Strauss, V.; Brill, S.; Luizi, F.; Mertler, M.; Wiench, K.; Gamer, A. O.; van Ravenzwaay, B.; Landsiedel, R. Inhalation toxicity of multiwall carbon nanotubes in rats exposed for 3 months. *Toxicol. Sci.* **2009,** *112*, (2), 468-481.

21. Schmoll, L. H.; Elzey, S.; Grassian, V. H.; O'Shaughnessy, P. T. Nanoparticle aerosol generation methods from bulk powders for inhalation exposure studies. *Nanotoxicology.* **2009,** *3*, (4), 265-275.

22. To, D.; Dave, R.; Yin, X. L.; Sundaresan, S. Deagglomeration of nanoparticle aggregates via rapid expansion of supercritical or high-pressure suspensions. *AlChE J.* **2009,** *55*, (11), 2807-2826.

23. Kuempel, E. D.; Geraci, C. L.; Schulte, P. A. Risk assessment and risk management of nanomaterials in the workplace: translating research to practice. *Ann. Occup. Hyg.* **2012,** *56*, (5), 491-505.

24. Chen, B. T.; Schwegler-Berry, D.; McKinney, W.; Stone, S.; Cumpston, J. L.; Friend, S.; Porter, D. W.; Castranova, V.; Frazer, D. G. Multi-walled carbon nanotubes: sampling criteria and aerosol characterization. *Inhal. Toxicol.* **2012,** *24*, (12), 798-820.

25. Pauluhn, J. Subchronic 13-week inhalation exposure of rats to multiwalled carbon nanotubes: toxic effects are determined by density of agglomerate structures, not fibrillar structures. *Toxicol. Sci.* **2010,** *113*, (1), 226-242.

26. Ku, B. K.; Maynard, A. D.; Baron, P. A.; Deye, G. J. Observation and measurement of anomalous responses in a differential mobility analyzer caused by ultrafine fibrous carbon aerosols. *J. Electrost.* **2007,** *65*, (8), 542-548.

27. Shin, W. G.; Wang, J.; Mertler, M.; Sachweh, B.; Fissan, H.; Pui, D. Y. H. Structural properties of silver nanoparticle agglomerates based on transmission electron microscopy: relationship to particle mobility analysis. *J. Nanopart. Res.* **2009,** *11*, (1), 163-173.

28. Asgharian, B.; Price, O. T. Deposition of ultrafine (NANO) particles in the human lung. *Inhal. Toxicol.* **2007,** *19*, (13), 1045-1054.

29. Oberdorster, G.; Oberdorster, E.; Oberdorster, J. Nanotoxicology: An emerging discipline evolving from studies of ultrafine particles. *Environ. Health Perspect.* **2005,** *113*, (7), 823-839.

30. Castellanos, A. The relationship between attractive interparticle forces and bulk behaviour in dry and uncharged fine powders. *Adv. Phys.* **2005,** *54*, (4), 263-376.

31. Ghoroi, C.; Han, X.; To, D.; Jallo, L.; Gurumurthy, L.; Dave, R. N. Dispersion of fine and ultrafine powders through surface modification and rapid expansion. *Chem. Eng. Sci.* **2013,** *85*, 11-24.

32. Strom, H.; Sasic, S. The role of thermophoresis in trapping of diesel and gasoline particulate matter. *Catal. Today.* **2012,** *188*, (1), 14-23.

Chapter 4 – Oxidation of C_{60} aerosols by atmospherically relevant levels of O_3

Submitted: October 2013

To: Environmental Science and Technology

Status: Accepted February 2014. DOI: 10.1021/es4045693. Text available at the following link:

http://pubs.acs.org/articlesonrequest/AOR-gsVeZrSzPpNmF2ZCfGvz

The 'Discussion' section of this text has been modified from the version published in *ES&T*.

Abstract

Atmospheric processing of carbonaceous nanoparticles (CNPs) may play an important role in determining their fate and environmental impacts. This work investigates the reaction between aerosolized C_{60} and atmospherically relevant mixing ratios of O_3 at differing levels of humidity. Results indicate that C_{60} is oxidized by O_3 and forms a variety of oxygen-containing functional groups on the aerosol surface, including $C_{60}O$, $C_{60}O_2$ and $C_{60}O_3$. The pseudo-first order reaction rate between C_{60} and O_3 ranges from 9×10^{-6} to 2×10^{-5} s^{-1}. The reaction is likely to be limited to the aerosol surface. Exposure to O_3 increases the oxidative stress exerted by the C_{60} aerosols as measured by the dichlorofluorescein acellular assay, but not by the uric acid, ascorbic acid, glutathione, or dithiothreitol assays. The initial prevalence of $C_{60}O$ and $C_{60}O_2$ as intermediate products is enhanced at higher humidity, as is the surface oxygen content of the aerosols. These results show that C_{60} can be oxidized when exposed to O_3 under ambient conditions, such as those found in environmental, laboratory, and industrial settings.

Introduction

C_{60} fullerenes (C_{60}) are one type of carbonaceous nanoparticle (CNP) that exhibit a closed cage structure of five- and six-membered rings of carbon atoms. C_{60} fullerenes have been noted for their semiconductive,[1] photosensitizing,[2, 3] and free radical-absorbing[4] properties. While C_{60} naturally occurs in some meteorites and in certain high-energy geologic/environmental settings (extraterrestrial impacts, lightning strikes, and wildfires),[5, 6] the potential release of purposefully engineered C_{60} due to the growth of nanotechnology could lead to its presence in a wider variety of ecosystems, and at higher concentrations, than is currently the case.[7, 8] Release of manufactured C_{60} to the environment could occur during production, use, and disposal of C_{60} or C_{60}-containing products.[9, 10] In addition, C_{60} of presumably incidental origin has been detected in atmospheric aerosols over the Mediterranean Sea[11] and North America.[12, 13]

The environmental impact of C_{60} has been the subject of numerous investigations in a variety of environmental settings, including soil[14, 15] and water.[16, 17] Toxicology testing has shown that a variety of outcomes can result from C_{60} exposure. Such outcomes range from protection against free radicals *in vivo*[18] to numerous harmful toxicological endpoints, which can include elevated oxidative stress in embryonic zebrafish,[19] bioaccumulation in earthworms,[20] and lysosomal destabilization in oysters, the degree of which is suggestive of reproductive failure.[21] Some investigations, however, show only minimal toxicological effects resulting from C_{60} exposure.[22-24] Many toxicology studies have been conducted using freshly generated C_{60} molecules, featuring either no functionalization or very specific functionalizations, such as phenylalanine[25] or well-characterized hydroxylation.[26-28] However, C_{60} that is released into the environment will likely become functionalized through interactions with solar radiation,[29] water and natural materials therein,[30] air,[31] soil, and biota.

Transformation of C_{60} in the atmosphere may have important implications for its environmental transport, fate, and effects.[31] Atmospheric transformation describes several processes, including aggregation, coating, and reactions such as oxidation. Ozone (O_3) is a major oxidant that plays an important role in atmospheric processing of many gas- and particle-phase organic species.[32] Most of the studies on the oxidation of C_{60} by O_3 have taken place in solution by bubbling O_3 through toluene[33, 34] or other solvents[35-38] in which C_{60} has been dissolved. Reaction with O_3 has been shown to increase the stability of C_{60} colloids in water.[39, 40] Cataldo[41] has examined the reaction with dry, powdered C_{60} and documented the formation of various carboxyl groups on the C_{60} material as well as the production of CO_2. The relevance of the results for environmental scenarios is not known, however, as the O_3 mixing ratio employed in that work, 6.4% O_3/O_2, is six orders of magnitude higher than found in the troposphere. Davis *et al.*[42, 43] have investigated the reaction rate and mechanism between gas-phase O_3 and surface-bound C_{60} in a series of ultrahigh vacuum studies. Although their work provides direct insight into primary ozonide formation, the chemistry may be significantly different under ambient conditions in which water, oxygen, and other species are present.

The goal of this work is to investigate the reaction between C_{60} and O_3 at atmospherically relevant O_3 mixing ratios by measuring the reaction rate and identifying reaction products. We use an aerosolized form of C_{60} to mimic the potential release of C_{60} into the atmosphere. Our results may inform studies of other engineered carbonaceous nanoparticles, as well as address key questions about the atmospheric processing of graphitic soot, for which C_{60} may serve as a well-characterized model system.

Experimental

Chamber

Reactions were carried out in a 6 m^3 polytetrafluoroethylene (PTFE) chamber, which was operated as a batch reactor. The chamber was shielded from light and was mixed by a small fan located in the center of the chamber floor. After each experiment, the chamber was flushed overnight to clean it, using laboratory compressed air passed through particle and hydrocarbon traps. Prior to each experiment, the particle count in the chamber was verified to be below ~1 × 10^3 # cm^{-3}. Temperature and humidity inside the chamber were measured via a wireless sensor. A schematic of the experimental setup is shown in the Supporting Information (Figure A-1).

O_3 was introduced into the chamber by flowing O_2 through a corona discharge ozone generator at 0.1 L min^{-1}. The C_{60}-O_3 reaction was investigated at initial O_3 mixing ratios of < 5 ppb (referred to as ~0 ppb), 45 ppb, and 120 ppb. Water vapor was introduced into the chamber via a household humidifier filled with nanopure water. The influence of water vapor was investigated by conducting the reaction at two relative humidity (RH) levels: 10-15% and ~65%.

C_{60} aerosols were introduced into the chamber by means of a custom nanoparticle powder dry dispersion system.[44] The C_{60} was 99.9% pure (MER Corp., Tucson, AZ). Chromatography of it revealed no distinguishable peaks of C_{60} oxides. The C_{60} powder was milled in a plastic vial with glass beads using a cell disrupter (BeadBeater) prior to dispersion. Because the dispersion process created a burst of aerosols, the reaction clock started immediately after dispersion was complete. Each experiment was conducted for up to 90 min, during which aerosol samples were collected at 6, 18, 30, 42, 60, and 90 min.

Sample collection and analytical techniques

The aerosol size distribution was measured using a Scanning Mobility Particle Sizer which consisted of a long differential mobility analyzer and a butanol-based ultrafine condensation particle counter. Larger particles were measured using an Aerodynamic Particle Sizer. Size distributions from each instrument were merged using DataMerge software. Details of instrument models and suppliers are provided in the SI.

The O_3 mixing ratio in the chamber was measured by a UV absorption analyzer. O_3 loss during each experiment was corrected both for instrument drift (measured daily) and O_3 losses under the given humidity and O_3 mixing ratio. Pseudo-first order rate constants were calculated as the slope of the least-squares linear regression line of the natural log of O_3 mixing ratio versus time.

Aerosol samples were collected on PTFE filters at a flow rate of 9 L min^{-1} for 10 min for analysis by high performance liquid chromatography (HPLC), liquid chromatography/mass spectrometry (LC/MS), UV-Visible spectrophotometry (UV-Vis), and oxidative stress assays. The filters were extracted in toluene (HPLC, LC/MS) or *o*-dichlorobenzene (ODCB, UV-Vis) via sonication, and the solution was concentrated to 1.0 mL prior to analysis by evaporation under nitrogen. Toluene was selected due to C_{60}'s high solubility in it, and ODCB was chosen to extract potential C_{60} oxidation products that were too oxygenated to be appreciably soluble in toluene. Samples for analysis by x-ray photoelectron spectroscopy (XPS) were collected by depositing C_{60} aerosols onto double-sided copper tape using the final stage (D_{50} = 250 nm) of a Sioutas impactor. These samples were collected at a flow rate of 9 L min^{-1} for 12 min.

Products of the reaction between C_{60} aerosols and O_3 were identified using LC/MS with electrospray ionization. Analyses were conducted in negative single ion mode, and analytes were separated using a pyrenylpropyl-bonded silica column using toluene as a mobile phase at 0.5 mL

min^{-1}. The relative prevalence of selected products was monitored using HPLC. The oxygen content of the aerosol surface was measured using XPS and the MultiPak software package. Samples were analyzed in both survey and high-resolution modes, and the primary C1s peak was referenced to 285.1 eV.[45] Particle morphology was observed using transmission electron microscopy (TEM).

The potential of the C_{60} aerosols to exert oxidative stress was measured using a variety of cell-free assays.[46-49] Selected antioxidants were uric acid (UA), ascorbic acid (AA), dithiothreitol (DTT), and glutathione (GSH), while dichlorofluorescin (DCFH), along with its oxidation product dichlorofluorescein (DCF), was used as a fluorescent probe. All assay procedures have been described in detail elsewhere.[50] Briefly, each antioxidant was incubated for 1 h with 20 μL of a phosphate-buffered saline (PBS) extract of C_{60} aerosols. Antioxidant depletion was then determined either by quantifying the concentration of remaining antioxidant via UV-Vis spectroscopy (GSH and DTT) or HPLC (ascorbic and uric acids), or by monitoring the production of the oxidation product via fluorescence (DCFH/DCF).

Further experimental details may be found in the SI.

Results

Reactants

The particle number concentrations used in this work averaged $1.04 \pm 0.40 \times 10^5$ # cm^{-3}. Variability stemmed from the dry dispersion aerosolization method. Because of losses to the chamber walls, the number concentration decreased over the course of a 90-min experiment. First order loss coefficients ranged form 0.001 – 0.01 min^{-1}, typical for a chamber of this size.[51,

[52] Figure 4-1a shows the average initial size distribution, normalized to the total particle count for each run, of the C_{60} aerosols for 45 chamber experiments. The mode diameter is ~100 nm.

Figure 4-1b-c shows particle morphology. The aerosols exhibited an irregular shape, as expected from the chaotic dispersion process. Given a mode diameter of 100 nm and slightly irregular morphology, we estimate the fraction of C_{60} molecules at the aerosol surface to be ~1%.

Portions of the particles were crystalline, as shown in Figure 4-1c. The C_{60} provided by the manufacturer was crystalline in nature, and the diffraction pattern suggests that the crystals were not disrupted completely through the milling and dispersion processes, although they were reduced in size. This (poly)crystallinity permits comparison of the results described below to those obtained in studies using vapor-deposited C_{60} films.[42, 43]

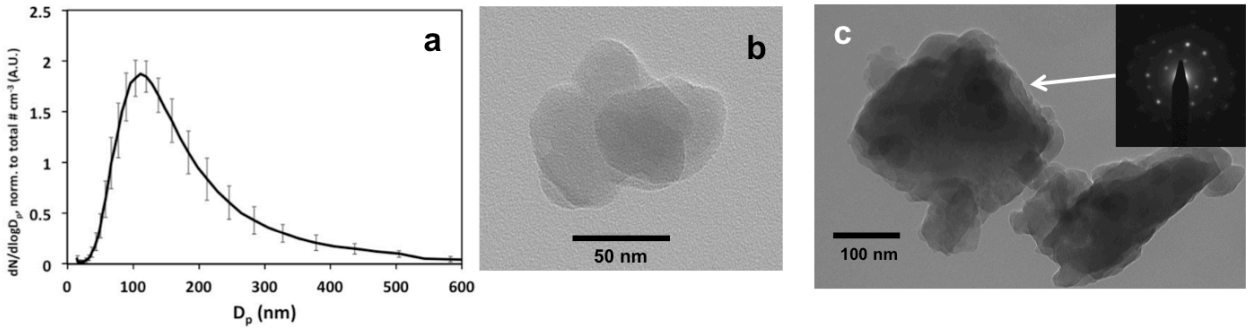

Figure 4-1: a) Normalized size distribution of the C_{60} aerosols immediately after particle dispersion (n = 45 runs). The average particle number concentration was 1.04 ± 0.4 × 10^5 # cm^{-3}. b-c) TEM images of C_{60} aerosols collected at t = 30 min during reaction with O_3 initially at a mixing ratio of 120 ppb. Particles exhibit irregular shapes and a layered, sheet-like structure. The diffraction pattern in (c) was taken from the particle on the left and indicates crystallinity.

O_3 loss over time, corrected for wall losses, is shown in Figure A-2. O_3 loss occurred continuously throughout the 90-min experiment, and greater O_3 loss occurred at higher initial

mixing ratios. The shape of the curves suggested that the reaction could be described by a pseudo-first order rate constant. Pseudo-first order rate constants ranged from $k = 9 \times 10^{-6}$ to 2×10^{-5} s^{-1} over the tested O_3 mixing ratios and humidity levels. O_3 losses were not significantly different at a RH of 10-15% v. ~65%.

Aerosol Chemistry

Figure 4-2a shows the oxygen content of the C_{60} aerosols after exposure to O_3. Higher initial O_3 mixing ratios corresponded to a higher degree of oxygenation of the aerosol surface. When plotted on log-linear axes, the relationship between surface oxygen and initial O_3 mixing ratio was linear, and the slope was statistically significant at the $p < 0.05$ level for both RH conditions. In this analysis, we assigned the initial O_3 mixing ratio of ~0 ppb a value of 5 ppb to enable inclusion of the data point on the log scale.

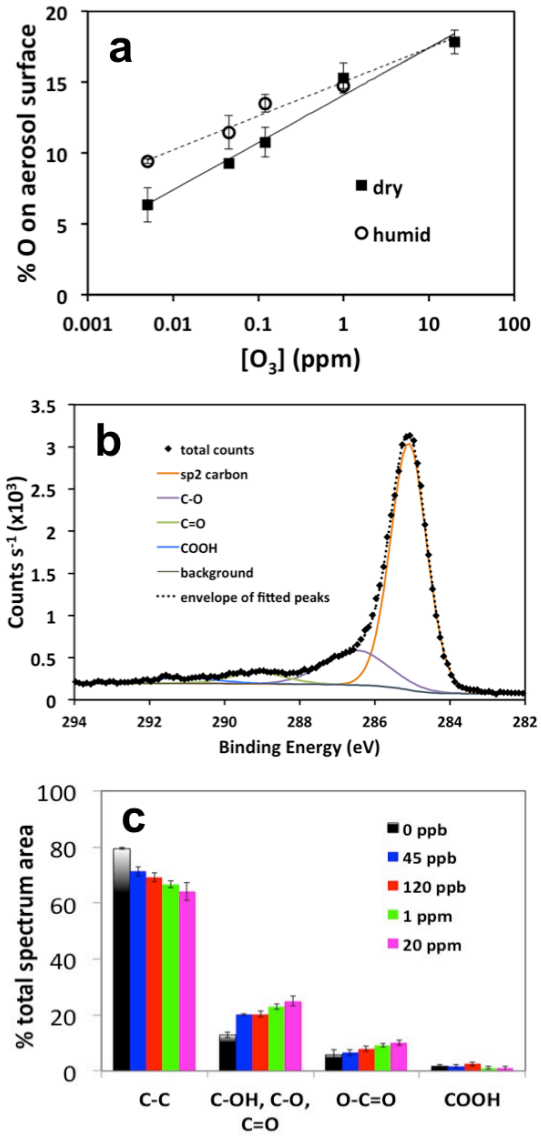

Figure 4-2: a) Percentage of oxygen on the aerosol surface as a function of initial O_3 mixing ratio. b) High-resolution scan of C1s peak, fitted with four peaks indicating the different oxidation states of C (RH 10-15% sample). c) Relative contributions to the C1s peak (RH 10-15% sample) for O_3 mixing ratio ranging from 0 – 20 ppm.

Additionally, surface oxygen content was higher under humid (~65% RH) relative to dry (10-15% RH) conditions for initial O_3 mixing ratios up to 120 ppb. The surface oxygen contents of the as-received C_{60} and milled C_{60} powder (i.e., prior to aerosolization) were < 2% and ~3%,

respectively (see Figure A-3). These values were significantly lower than that of the C_{60} that was aerosolized and exposed to ~0 ppb O_3. This pattern held for $C_{60}O$ content as well; as-received and milled C_{60} powders contained undetectable levels of $C_{60}O$, while this reaction product was detected in the aerosols exposed to ~0 ppb O_3. These differences suggest that the dispersion process exposed new C_{60} surfaces, which oxidized upon contact with air even at low O_3 mixing ratios.

A high-resolution scan of the C1s peak under RH 10-15% conditions is shown in Figure 4-2b. The presence of multiple peaks indicated that carbon was in several different bonding environments at the aerosol surface. We fit the XPS spectra using peak positions and assignments from the literature for chemically similar systems. The primary peak at 285.1 eV represents underivatized fullerenic carbon,[45] while the higher-energy peaks at 286.3, 289.1, and 291.1 eV correspond to C-O, C=O, and COOH moieties, respectively.[39, 53-56] The relative contribution of each of these peaks to the overall C1s spectrum is shown in Figure 4-2c. The prevalence of the C-C peak decreased with increasing initial O_3 mixing ratio, while the area of peaks attributed to oxygen bonding increased. High-resolution scans of samples collected at ~65% RH produced a more complex spectrum (Figure A-3) that was not fitted as well using the same peak positions. The fit showed the C-O peak to be much larger than the sp2 carbon peak; the reasons for this are unknown and should be the subject of further study. Additionally, the effect of RH on surface chemistry will require further study.

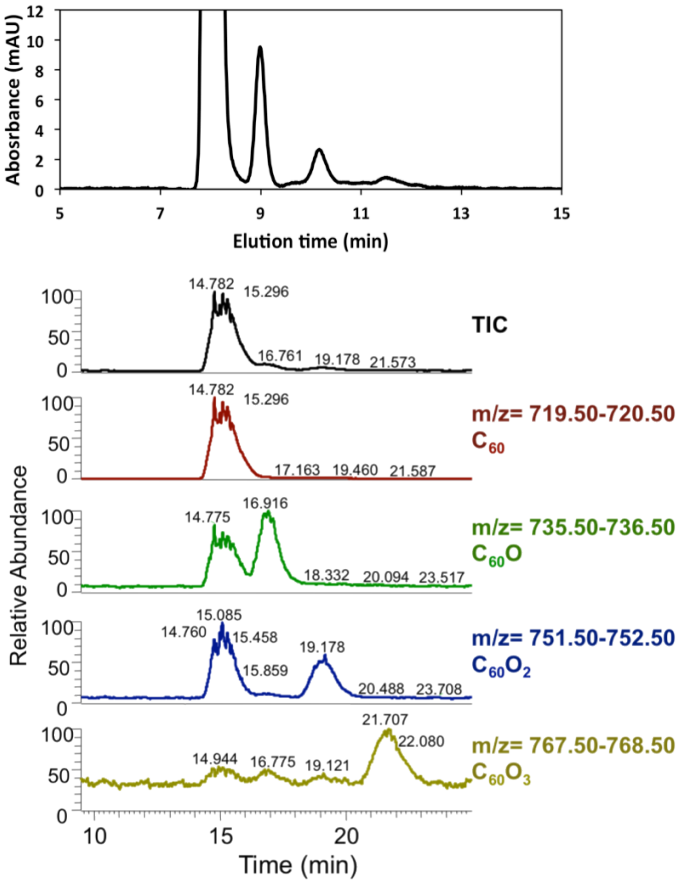

Figure 4-3: a) Chromatogram of O_3-exposed C_{60} aerosols, extracted in toluene. Several peaks follow the C_{60} peak (t = 8 min). b) Identification of the species represented by the smaller peaks by LC/MS. $C_{60}O$, $C_{60}O_2$, and $C_{60}O_3$ form in the O_3-C_{60} reaction.

As has previously been done with water-stable C_{60} colloids,[40, 57] several reaction products were separated and identified using HPLC and LC/MS. Figure 4-3 shows (a) a typical chromatogram of C_{60} exposed to O_3 and (b) chromatograms of selected ions at *m*/*z* ratios of 720, 735, 751, and 768, corresponding to C_{60}, $C_{60}O$, $C_{60}O_2$, and $C_{60}O_3$, respectively. While oxides with more than four oxygen atoms per C_{60} cage may have formed, we did not investigate higher *m*/*z* ratios, as chromatograms did not reliably show peaks eluting after $C_{60}O_3$.

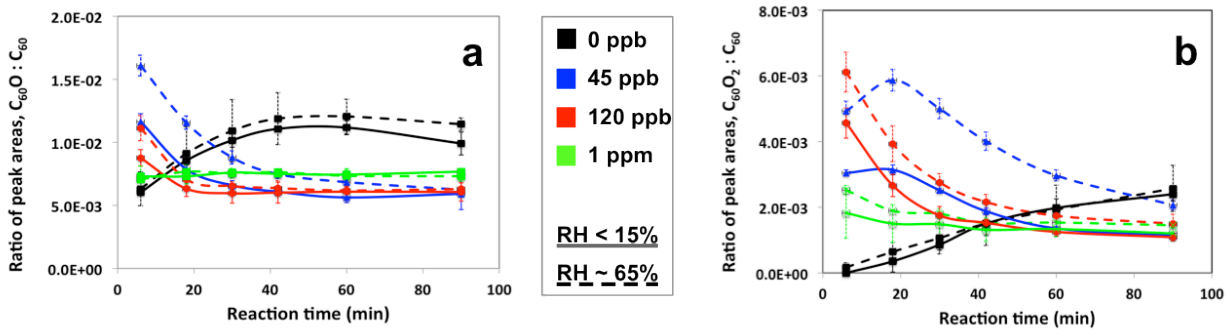

Figure 4-4: Relative abundance of a) $C_{60}O$ and b) $C_{60}O_2$ with time, as determined by HPLC. Both species are present at very low levels (relative abundance < 0.01 by t = 90 min). The initial O_3 mixing ratio does not influence final abundance of either species, except in the case of ~0 ppb. See text for explanation.

The evolution of $C_{60}O$ and $C_{60}O_2$ during the reaction was followed via HPLC. Figure 4-4 shows the relative prevalence of these two products over the course of the 90-min reaction, for both dry and humid (10-15% and ~65% RH) conditions, at all four tested O_3 mixing ratios. The vertical-axis values represent the ratio of the product peak area to the C_{60} peak area. We employed this metric because quantifying the concentrations of the C_{60} oxidation products would have required high-quality analytical standards of them, which were not available. Both $C_{60}O$ and $C_{60}O_2$ formed under all tested conditions. The relative abundance of $C_{60}O$ was maximal around t = 5 min and stabilized by t = 40 min. The timing of the peak in $C_{60}O_2$ differed by O_3 mixing ratio. The peak appeared earliest at high initial O_3 mixing ratios (1 ppm and 120 ppb) and shifted later in time at low mixing ratios (45 ppb and ~0 ppb). It is likely that the C_{60} aerosols exposed to 120 ppb and 1,000 ppb did experience a peak in their $C_{60}O_2$:C_{60} ratio, but that the peak occurred prior to the first sampling point at t = 6 min. These results suggest that $C_{60}O$ and $C_{60}O_2$ may be intermediates in a reaction mechanism that proceeds from C_{60} through one or both of these species to the formation of higher oxidation products. The increasing prevalence of both

$C_{60}O$ and $C_{60}O_2$ with time at ~0 ppb O_3 suggests that these species may have formed comparatively slowly due to the lower O_3 mixing ratio (1-5 ppb). The time series at ~0 ppb may represent a "slow-motion" version of the reaction at higher O_3 mixing ratios; over a longer timescale, these two species may have reached similar final abundances as at the other mixing ratios.

The presence of water vapor enhanced the formation of both $C_{60}O$ and $C_{60}O_2$; this effect was greatest at 45 and 120 ppb. Lastly, the relative concentrations of both species stabilized at a peak area ratio of < 0.01 under all O_3 and RH conditions.

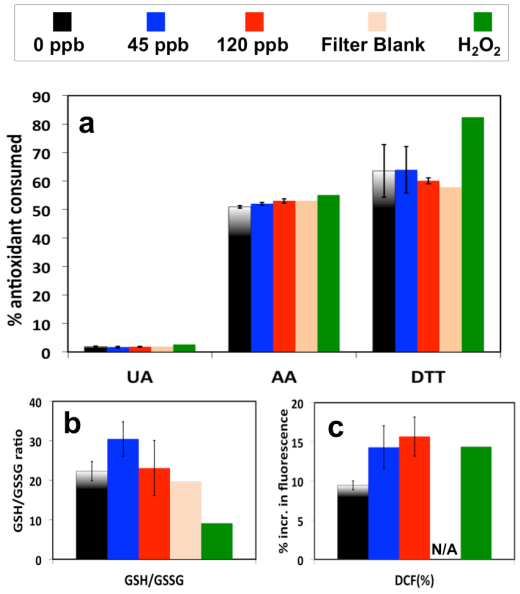

Figure 4-5: Consumption of five different antioxidants by C_{60} aerosols extracted in phosphate-buffered saline (PBS). a-b) Uric acid, ascorbic acid, dithiothreitol, and glutathione were depleted similarly by all C_{60} samples, filter blank, and/or H_2O_2 control. c) C_{60} exposed to O_3 oxidized dichlorofluorescin (DCFH) more readily than did unexposed C_{60}. All samples collected at 10-15% RH.

Oxidative stress potential

The ability of O_3-exposed C_{60} aerosols to deplete a variety of antioxidants is shown in Figure 4-5. Results for hydrogen peroxide (H_2O_2) are shown as a positive control. No significant difference in antioxidant depletion, either between different mixing ratios of O_3, or between any C_{60} aerosols and the filter blank, was observed for the uric acid and DTT assays. C_{60} aerosols exposed to 120 ppb of O_3 consumed slightly more ascorbic acid than did those exposed at mixing ratios of 0 or 45 ppb. In the case of glutathione (for which the ratio between GSH and its oxidized form, GSSG, is considered an indicator of oxidative stress[58]), there was no trend between O_3 exposure and glutathione loss. Results of the DCF assay are shown as a percentage increase over the blank, and C_{60} exposed to O_3 oxidized dichlorofluorescin (DCFH) more readily than did unexposed C_{60}.

Discussion

Reaction rate

The reaction between C_{60} and O_3 is of interest with respect both to the environmental fate and impacts of manufactured CNPs and to the atmospheric processing and aging of carbonaceous aerosols. The pseudo-first order reaction rates derived in this work ($k = 9 \times 10^{-6} – 2 \times 10^{-5}$ s^{-1}) are more than one order of magnitude lower than two previously published C_{60}-O_3 reaction rates, each of which were obtained under much richer O_3 conditions.[41, 42] The reaction rates calculated here are also several orders of magnitude lower than those for several polycyclic aromatic hydrocarbons (PAHs) on various aerosol cores or substrates, as shown in Figure 4-6.[41, 42, 59-65] Since the aerosols in this study are entirely composed of C_{60}, we may consider C_{60} to be both the core and the surface of the aerosols. Multiple researchers, including those whose results

are depicted in Figure 4-6, have suggested that a Langmuir-Hinshelwood mechanism may apply to reactions between O_3 and vinyl-terminated organic surfaces,[66] PAH,[60-63] and soot.[64, 65]

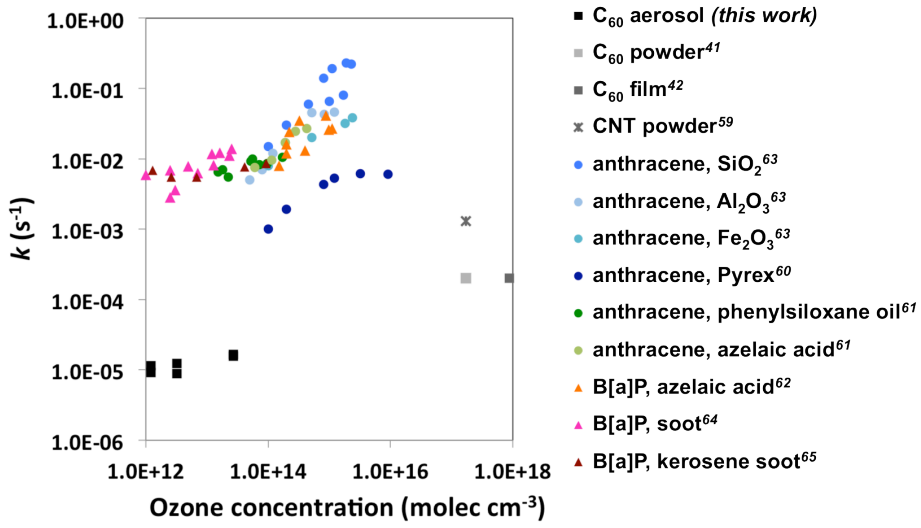

Figure 4-6: Pseudo-first order rate constants for reactions between various cyclic carbonaceous compounds and O_3, as a function of O_3 mixing ratio. Data from this work are plotted as black squares. Rate constants measured under humid and dry conditions were plotted together for all works. The legend indicates coating compound, followed by the composition of the aerosol core (or substrate, in the case of Pyrex).

The reaction between C_{60} and O_3 first begins with a collision between the gas-phase O_3 and the solid-phase C_{60} particle. The collision rate between a particle and a gas-phase species can be calculated using the following equation:[32]

$$\frac{\#\text{ of collisions}}{\text{unit area} \times \text{s}} = N_g \sqrt{\frac{RT}{2\pi M}}$$

where N_g = trace gas concentration (molec cm^{-3}); R = ideal gas constant (J mol^{-1} K^{-1}); T = temperature (K); and M = molar weight of the gas (kg mol^{-1}).[32] For the conditions in the study described in Chapter 4, the collision rate is approximately 1.1×10^{16} collisions cm^{-2} s^{-1}.

The net uptake of a trace gas to a particle surface can be defined as "the ratio of the number of trace gas molecules removed from the gas phase (net loss) divided by the total number of trace gas collisions with the surface."[67] That is,

$$\text{gas uptake} = \gamma_0 = \frac{\text{\# gas molecules removed from gas phase}}{\text{\# gas collisions with surface}}$$

Kolb *et al.* note that the uptake coefficient can be time-dependent; examination of the O_3 loss data in the Chapter 4 experiments suggests this is likely the case here. The uptake coefficient for these experiments will be calculated for the integrated 90 min experiment on a unit volume basis.

Removal from gas phase (numerator): In experiments using an initial O_3 mixing ratio of 45 ppb, the final O_3 mixing ratio was reduced by approximately 2 ppb, which translates to 5.4×10^{10} molecules of O_3 lost cm^{-3}.

Collisions with surface (denominator): The above collision rate must be normalized to an aerosol surface area concentration of 1×10^{10} nm^2 cm^{-3} and extended it over the duration of the 90 min experiments. This results in approximately 6.0×10^{15} collisions cm^{-3}.

The final uptake coefficient is then on the order of 1×10^{-5}. This value is well within the range of uptake coefficient values measured in a variety of O_3-soot experiments.[67-69]

Reaction products

The reaction between C_{60} and O_3 begins with the formation of a primary ozonide, when the ozone molecule attaches preferably across a 6,6 bond in the C_{60} structure.[70] This unstable intermediate quickly decays to a Criegee biradical.[43] As detailed by Shang *et al*.,[71] the Criegee intermediate may decay into an epoxide structure, $C_{60}O$, or into a diketone, $C_{60}O_2$. Including reactions in which the primary ozonide may form over the 5,6 bond, two isomers of $C_{60}O$ may form, and eight isomers of $C_{60}O_2$ are available.[72] Of these, one (6,6 bond) is preferable for $C_{60}O$, and three are preferable for $C_{60}O_2$. The final product described in this study, $C_{60}O_3$, may form as a sequential combination of two (one epoxide and one diketone) or three (three epoxide) ozonolysis reactions. Chapleski *et al*.[73] have recently described the energetic favorability of the formation of various C_{60} ozonide isomers. Such work may be extended to explore the various potential isomers of $C_{60}O_3$. Such theoretical work may be informative regarding the potential isomers of $C_{60}O_3$ that may form under environmentally relevant conditions, whether containing only epoxide, or both epoxide and diketone, functionalities.

The formation of $C_{60}O$ as a result of C_{60} exposure to O_3 has been previously shown in aqueous, solvent-based, and 'dry' experimental systems.[33, 34, 39, 40, 74, 75] To our knowledge, this work marks the first time that $C_{60}O_2$ and $C_{60}O_3$ have been identified as reaction products under atmospherically relevant O_3 mixing ratios. These oxygen atoms may be located in epoxide, ketone, or other functional groups. Carbon nanotubes[76-79] and graphene[80] also form epoxide groups following exposure to O_3. Similar epoxide products have not been observed in studies of particle-phase PAH oxidation by O_3; quinones and other carbonyl moieties are instead often observed.[60, 63, 81] This difference between particle-phase PAHs and CNPs may be due to the attraction of the PAH molecules to the substrate to which they are sorbed and their consequent

thermodynamic tendency to oxidize into planar products.[82] The influence of parent compound aromaticity on reaction product identity must also be considered.

As shown in Figure 4-2a, exposure to O_3 results in elevated oxygen content of the C_{60} aerosol surface. XPS analyzes only the top few nanometers (< 5 nm) of the sample surface, so C_{60} molecules in the unreacted 'core' of the aerosol do not contribute to the measurements. The combination of O_3 and water vapor, both at atmospherically relevant levels, alters the surface chemistry of the C_{60} aerosols. After calibrating the unreacted fullerenic carbon peak to 285.1 eV,[45] subsequent peaks at 286.3, 289.1, and 291.1 eV are assigned to C-O,[54, 83, 84] C=O,[39] and COOH groups,[53, 85] respectively. The oxygen content and oxygen-containing functional groups in these C_{60} aerosols are similar to results shown for the ozonation of water-stable C_{60} clusters,[39] carbon nanotubes (CNTs),[76, 86, 87] and soot.[88] Similar oxygen-containing functional groups, and only slightly higher surface oxygen contents, have been detected on CNTs following acid treatment (used to enhance the hydrophilicity of the nanotubes)[89] and following O_3 exposure that greatly increased CNT stability in water.[87] Increased stability in water may also be acquired via photolysis,[55, 90] which was not addressed in this work.

Along with epoxides,[40] the oxygen-containing functional groups observed to result from atmospherically relevant O_3 exposure may have an important impact on the aqueous stability of C_{60} fullerenes, and other similar CNPs, exposed to the atmosphere. Aqueous stability of C_{60} aerosols in this work was investigated via UV-Vis and total organic carbon analysis (TOC) of aerosols extracted in water, but there were no significant differences with level of O_3 exposure. In the case of TOC analysis, this may be due to the very low sample mass obtainable from these small aerosols. Negative results for both analyses may also indicate that 90 min of exposure to atmospheric levels of O_3 may not result in enough surface oxygenation to stabilize the aerosols

in water. While Murdianti *et al*.[40] suggest that C_{60} aggregates may be stable in water if ~1.7% of C_{60} molecules are functionalized with a single oxygen molecule, the hydrodynamic sizes of the particles used in their study ranged from 70-139 nm, and oxidation occurred in the presence of liquid water.[40] The differences between this work and Murdianti *et al*.[40] in terms of particle size distribution, presence of liquid water, and potential variability of oxidation products make it difficult to translate the water-based results to an air-based system. In addition to aqueous solvents, we also attempted extraction in acetone followed by UV-Vis analysis, but results were inconclusive.

Although the final abundances of epoxide reaction products were low and independent of O_3 mixing ratio (Figure 4-4), surface oxygen levels were relatively high (Figure 4-2b), and O_3 loss was continual throughout the exposure period (Figure A-2). Especially considering the diversity of O-containing functional groups present on the aerosol surface (Figure 4-2c), it seems plausible that unidentified O-containing reaction products may have formed. Chibante *et al.*[75] note that toluene-insoluble products of the C_{60}-O_3 reaction form as the reaction proceeds, and that these products are rich in oxygen. In our experiments, a brown residue often remained on the air-dried Teflon filter following sonication in toluene, especially at higher O_3 exposure as measured in ppb·min. The presence of this toluene-insoluble material may indicate the formation of a C_{60}-based substance that exhibits reduced hydrophobicity.

While the addition of more than ~15 O_3 molecules to the C_{60} cage is energetically unfavorable,[73] the presence of a crystal structure limits even further the number of oxygen atoms that may be added. Higher oxidation products such as $C_{60}O_4$, $C_{60}O_5$, etc. are possible, but it is unlikely that such an oxygen-rich C_{60} species could form without the molecule becoming cross-linked to

neighboring C_{60} molecules in the crystal structure. Due to the potential for neighboring cages to become cross-linked, this C_{60}-based substance is likely to be chemically complex and diverse. The possibility of cross-linking (dimerization) is discussed further in Appendix A.

While no detectable portion of the O_3-exposed C_{60} samples in this work were stably suspendable in water, it is possible that more extensive atmospheric processing than occurred in this experiment (longer duration of O_3 exposure, photolysis, etc.) may result in a water-stable fullerene-based material.[91] Just as the oxidation of soot aerosols renders those particles hydrophilic enough to serve as cloud condensation nuclei,[92] the atmospheric processing of C_{60} may alter its hydrophobicity significantly. The formation of these diverse oxidation products under atmospherically relevant O_3 conditions during a 90-min exposure suggests that atmospheric processing of CNPs may be an important determinant in the fate, transport, and environmental impact of these materials.

Oxidative stress potential

Oxidative stress is an important mechanism by which inhaled particles cause negative health effects.[93, 94] As expected, the response of the selected antioxidants to the C_{60} aerosols varied widely by antioxidant compound. The observation that ascorbic acid and glutathione were depleted while uric acid was not matches Zielinski *et al.*'s[46] results for carbon black particles. Holder *et al.*[47] found oxidized soot to deplete DTT more extensively than does unozonated soot, but our results with C_{60} do not show this trend. The extent of oxidation differs substantially between the two studies, however, (~35 times higher O_3 exposure in terms of ppb · min in Holder *et al.*) so it is likely that their soot was more extensively functionalized. Additionally, the

existence of a well-defined molecular formula for C_{60}, and the absence of one for soot, must be taken into account when comparing these results.

C_{60} exposed to O_3 enhanced the fluorescence of DCFH more extensively than did unexposed C_{60}. This influence of functionalization on DCFH depletion corroborates the results of Pichardo *et al.*,[95] who noted enhanced lipid peroxidation and reactive oxygen species (ROS) generation (as measured by DCFH depletion) when exposing human intestinal cells to carboxylated nanotubes. Yuan *et al.*[96] exposed human hepatoma cells to carbon nanotubes and graphene sheets that exhibited a variety of carbon-oxygen moieties (C-O, C=O, COOH) and found that while the effects of graphene were less intense, nanotube exposure was associated with elevated levels of ROS and apoptotic cells, as well as interrupted protein synthesis. These carbon-oxygen moieties are also found on the oxidized C_{60} in our work. Despite the fact that neither grapheme nor CNT exhibit the defined molecular formula that characterizes C_{60} fullerenes, the commonality in functional groups between the materials in the Yuan *et al*.[96] and this work justify concern over the impact of atmospheric processing on the toxicity of C_{60} and other CNPs. As the current work focuses on the integrated effect of the O_3-exposed C_{60} aerosols, future research could investigate the relationship between the oxidative stress potential of the aerosol and the speciation of its oxidation products.

While the current work does not investigate the influence of photolysis on the oxidative stress potential of oxidized C_{60}, research with carboxylated nanotubes demonstrates that ROS [singlet oxygen ($^1O_2$), superoxide anions ($O_2^{\cdot -}$), and hydroxyl radicals ($\cdot OH$)] are generated when exposing water-stable carboxylated nanotubes to sunlight.[97] Given the similarities in functional groups and surface oxygen content between O_3-exposed nanotubes and the O_3-exposed C_{60}

discussed above, it is possible that photolysis of CNPs during atmospheric processing could contribute to their potential to generate ROS.

The limitations of this work include the exclusion of light from the reaction chamber and the use of pure C_{60} aerosols. As discussed above, photolysis may influence the C_{60}-O_3 reaction in terms of rate, distribution of products, and/or ROS generation potential. The variety of matrices or substrates to which manufactured or incidental C_{60} may be bound may alter its reaction with O_3 and subsequent behavior in the environment. The results shown here suggest that atmospheric transformation of C_{60} fullerenes would alter them substantially and may result in the introduction of highly oxygenated and cross-linked fullerenes into the environment. Atmospheric transformation, including but not limited to oxidation, must be considered in order to more accurately understand the environmental impacts of nanotechnology.

Associated Content

Appendix A. Schematic of experimental setup. O_3 loss during the C_{60}-O_3 reaction. XPS C1s, O1s spectra of RH ~65% C_{60} aerosol sample; oxygen content of as-received and milled C_{60} powders. SEM images of XPS sample. O_3 loss data with least-square regression lines. Raw and normalized UV-Vis spectra showing evidence suggestive of C_{60} dimerization. Table providing commercial information and operating conditions for analytical instruments. Specifics regarding experimental design. Discussion of potential dimerization/oligomerization of C_{60}.

Acknowledgements

This work was supported by the National Science Foundation (NSF) and the Environmental Protection Agency (EPA) under NSF Cooperative Agreement EF-0830093, Center for the Environmental Implications of Nanotechnology (CEINT), by NSF CBET-0537117, and by the Environmental Protection Agency via an EPA STAR fellowship for A. Tiwari (#FP91730801). This work has not been formally reviewed by EPA, and no official endorsement should be inferred. JRM acknowledges funding from NSF (CHE-0948293). The Institute for Critical Technology and Applied Science (ICTAS) at Virginia Tech also provided support for this work. Assistance was provided by Jody Smiley, Mehdi Ashraf, Andrew Giordani, Jerry Hunter, Steve McCartney, and Julie Petruska.

References

1. Saito, S.; Oshiyama, A. Cohesive mechanism and energy bands of solid C60 *Phys. Rev. Lett.* **1991,** *66*, (20), 2637-2640.

2. Arbogast, J. W.; Darmanyan, A. P.; Foote, C. S.; Rubin, Y.; Diederich, F. N.; Alvarez, M. M.; Anz, S. J.; Whetten, R. L. Photophysical properties of C60 *J. Phys. Chem.* **1991,** *95*, (1), 11-12.

3. Guldi, D. M.; Prato, M. Excited-state properties of C-60 fullerene derivatives. *Acc. Chem. Res.* **2000,** *33*, (10), 695-703.

4. Krusic, P. J.; Wasserman, E.; Keizer, P. N.; Morton, J. R.; Preston, K. F. Radical reactions of C60. *Science.* **1991,** *254*, (5035), 1183-1185.

5. Buseck, P. R.; Tsipursky, S. J.; Hettich, R. Fullerenes from the geological environment. *Science.* **1992,** *257*, (5067), 215-217.

6. Buseck, P. R. Geological fullerenes: review and analysis. *Earth. Planet. Sci. Lett.* **2002,** *203*, (3-4), 781-792.

7. Nowack, B.; Bucheli, T. D. Occurrence, behavior and effects of nanoparticles in the environment. *Environ. Pollut.* **2007,** *150*, (1), 5-22.

8. Wiesner, M. R.; Lowry, G. V.; Alvarez, P.; Dionysiou, D.; Biswas, P. Assessing the risks of manufactured nanomaterials. *Environ. Sci. Technol.* **2006,** *40*, (14), 4336-4345.

9. Yeganeh, B.; Kull, C. M.; Hull, M. S.; Marr, L. C. Characterization of airborne particles during production of carbonaceous manomaterials. *Environ. Sci. Technol.* **2008,** *42*, (12), 4600-4606.

10. Duncan, L. K.; Jinschek, J. R.; Vikesland, P. J. C-60 colloid formation in aqueous systems: Effects of preparation method on size, structure, and surface, charge. *Environ. Sci. Technol.* **2008,** *42*, (1), 173-178.

11. Sanchis, J.; Berrojalbiz, N.; Caballero, G.; Dachs, J.; Farre, M.; Barcelo, D. Occurrence of Aerosol-Bound Fullerenes in the Mediterranean Sea Atmosphere. *Environmental Science & Technology.* **2012,** *46*, (3), 1335-1343.

12. Utsunomiya, S.; Jensen, K. A.; Keeler, G. J.; Ewing, R. C. Uraninite and fullerene in atmospheric particulates. *Environ. Sci. Technol.* **2002,** *36*, (23), 4943-4947.

13. Benn, T.; Herckes, P.; Westerhoff, P. Fullerenes in Environmental Samples: C-60 in Atmospheric Particulate Matter. In *Analysis and Risk of Nanomaterials in Environmental and Food Samples*, Elsevier Science Bv: Amsterdam, 2012; Vol. 59, pp 291-303.

14. Johansen, A.; Pedersen, A. L.; Jensen, K. A.; Karlson, U.; Hansen, B. M.; Scott-Fordsmand, J. J.; Winding, A. Effects of C-60 fullerene nanoparticles on soil bacteria and protozoans. *Environ. Toxicol. Chem.* **2008,** *27*, (9), 1895-1903.

15. Li, D.; Lyon, D. Y.; Li, Q.; Alvarez, P. J. J. Effect of soil sorption and aquatic natural organic matter on the antibacterial activity of a fullerene water suspension. *Environ. Toxicol. Chem.* **2008,** *27*, (9), 1888-1894.

16. Baun, A.; Hartmann, N. B.; Grieger, K.; Kusk, K. O. Ecotoxicity of engineered nanoparticles to aquatic invertebrates: a brief review and recommendations for future toxicity testing. *Ecotoxicol.* **2008,** *17*, (5), 387-395.

17. Oberdorster, E.; Zhu, S. Q.; Blickley, T. M.; McClellan-Green, P.; Haasch, M. L. Ecotoxicology of carbon-based engineered nanoparticles: Effects of fullerene (C-60) on aquatic organisms. *Carbon.* **2006,** *44*, (6), 1112-1120.

18. Gharbi, N.; Pressac, M.; Hadchouel, M.; Szwarc, H.; Wilson, S. R.; Moussa, F. [60]Fullerene is a powerful antioxidant in vivo with no acute or subacute toxicity. *Nano Lett.* **2005,** *5*, (12), 2578-2585.

19. Usenko, C. Y.; Harper, S. L.; Tanguay, R. L. Fullerene C-60 exposure elicits an oxidative stress response in embryonic zebrafish. *Toxicol. Appl. Pharmacol.* **2008,** *229*, (1), 44-55.

20. Li, D.; Fortner, J. D.; Johnson, D. R.; Chen, C.; Li, Q. L.; Alvarez, P. J. J. Bioaccumulation of C-14(60) by the earthworm Eisenia fetida. *Environmental Science & Technology.* **2010,** *44*, (23), 9170-9175.

21. Ringwood, A. H.; Levi-Polyachenko, N.; Carroll, D. L. Fullerene exposures with oysters: embryonic, adult, and cellular responses. *Environmental Science & Technology.* **2009,** *43*, (18), 7136-7141.

22. Ema, M.; Matsuda, A.; Kobayashi, N.; Naya, M.; Nakanishi, J. Dermal and ocular irritation and skin sensitization studies of fullerene C-60 nanoparticles. *Cutan. Ocul. Toxicol.* **2013,** *32*, (2), 128-134.

23. Blickley, T. M.; McClellan-Green, P. Toxicity of aqueous fullerene in adult and larval Fundulus heteroclitus. *Environ. Toxicol. Chem.* **2008,** *27*, (9), 1964-1971.

24. Baker, G. L.; Gupta, A.; Clark, M. L.; Valenzuela, B. R.; Staska, L. M.; Harbo, S. J.; Pierce, J. T.; Dill, J. A. Inhalation toxicity and lung toxicokinetics of C-60 fullerene nanoparticles and microparticles. *Toxicol. Sci.* **2008,** *101*, (1), 122-131.

25. Rouse, J. G.; Yang, J. Z.; Barron, A. R.; Monteiro-Riviere, N. A. Fullerene-based amino acid nanoparticle interactions with human epidermal keratinocytes. *Toxicol. Vitro.* **2006,** *20*, (8), 1313-1320.

26. Isakovic, A.; Markovic, Z.; Todorovic-Markovic, B.; Nikolic, N.; Vranjes-Djuric, S.; Mirkovic, M.; Dramicanin, M.; Harhaji, L.; Raicevic, N.; Nikolic, Z.; Trajkovic, V. Distinct cytotoxic mechanisms of pristine versus hydroxylated fullerene. *Toxicol. Sci.* **2006,** *91*, (1), 173-183.

27. Gelderman, M. P.; Simakova, O.; Clogston, J. D.; Patri, A. K.; Siddiqui, S. F.; Vostal, A. C.; Simak, J. Adverse effects of fullerenes on endothelial cells: Fullerenol C-60(OH)(24) induced tissue factor and ICAM-1 membrane expression and apoptosis in vitro. *Int. J. Nanomedicine.* **2008,** *3*, (1), 59-68.

28. Saitoh, Y.; Miyanishi, A.; Mizuno, H.; Kato, S.; Aoshima, H.; Kokubo, K.; Miwa, N. Super-highly hydroxylated fullerene derivative protects human keratinocytes from UV-induced cell injuries together with the decreases in intracellular ROS generation and DNA damages. *J. Photochem. Photobiol. B-Biol.* **2011,** *102*, (1), 69-76.

29. Hou, W. C.; Jafvert, C. T. Photochemical transformation of aqueous C-60 clusters in sunlight. *Environ. Sci. Technol.* **2009,** *43*, (2), 362-367.

30. Chang, X. J.; Vikesland, P. J. Effects of carboxylic acids on nC(60) aggregate formation. *Environ. Pollut.* **2009,** *157*, (4), 1072-1080.

31. Tiwari, A. J.; Marr, L. C. The Role of Atmospheric Transformations in Determining Environmental Impacts of Carbonaceous Nanoparticles. *Journal of Environmental Quality.* **2010,** *39*, (6), 1883-1895.

32. Finlayson-Pitts, B.; Pitts, J., *Chemistry of the Upper and Lower Atmosphere*. Academic Press: 2000.

33. Davydov, V. Y.; Filatova, G. N.; Knipovich, O. M. Oxidation of C-60 and C-70 fullerenes by ozone. *Molecular Crystals and Liquid Crystals Science and Technology Section C-Molecular Materials.* **1998,** *10*, (1-4), 221-224.

34. Deng, J. P.; Mou, C. Y.; Han, C. C. Electrospray and laser-desorption ionization studies of C60O and isomers of C60O2 *J. Phys. Chem.* **1995,** *99*, (41), 14907-14910.

35. Razumovskii, S. D.; Bulgakov, R. G.; Nevyadovskii, E. Y. Kinetics and stoichiometry of the reaction of ozone with fullerene C-60 in a CCl4 solution. *Kinet. Catal.* **2003,** *44*, (2), 229-232.

36. Heymann, D.; Bachilo, S. M.; Weisman, R. B.; Cataldo, F.; Fokkens, R. H.; Nibbering, N. M. M.; Vis, R. D.; Chibante, L. P. F. C60O3, a fullerene ozonide: Synthesis and dissociation to C60O and O-2. *J. Am. Chem. Soc.* **2000,** *122*, (46), 11473-11479.

37. Bulgakov, R. G.; Nevyadovskii, E. Y.; Belyaeva, A. S.; Golikova, M. T.; Ushakova, Z. I.; Ponomareva, Y. G.; Dzhemilev, U. M.; Razumovskii, S. D.; Valyamova, F. G. Water-soluble polyketones and esters as the main stable products of ozonolysis of fullerene C-60 solutions. *Russ. Chem. Bull.* **2004,** *53*, (1), 148-159.

38. Heymann, D.; Bachilo, S. M.; Aronson, S. Thermolysis and photolysis of C-60 diozonides. *Fuller. Nanotub. Carbon Nanostruct.* **2005,** *13*, (1), 73-88.

39. Fortner, J. D.; Kim, D. I.; Boyd, A. M.; Falkner, J. C.; Moran, S.; Colvin, V. L.; Hughes, J. B.; Kim, J. H. Reaction of water-stable C-60 aggregates with ozone. *Environ. Sci. Technol.* **2007,** *41*, (21), 7497-7502.

40. Murdianti, B. S.; Damron, J. T.; Hilburn, M. E.; Maples, R. D.; Koralege, R. S. H.; Kuriyavar, S. I.; Ausman, K. D. C-60 oxide as a key component of aqueous C-60 colloidal suspensions. *Environ. Sci. Technol.* **2012,** *46*, (14), 7446-7453.

41. Cataldo, F. Ozone reaction with carbon nanostructures 1: Reaction between solid C-60 and C-70 fullerenes and ozone. *J. Nanosci. Nanotechnol.* **2007,** *7*, (4-5), 1439-1445.

42. Davis, E. D. Ultrahigh vacuum studies of the kinetics and reaction mechanisms of ozone with surface-bound fullerenes. Virginia Polytechnic Institute and State University, Blacksburg, Virginia, 2011.

43. Davis, E. D.; Wagner, A.; McEntee, M.; Kaur, M.; Troya, D.; Morris, J. R. Reaction Probability and Infrared Detection of the Primary Ozonide in Collisions of O-3 with Surface-Bound C-60. *J. Phys. Chem. Lett.* **2012,** *3*, (21), 3193-3198.

44. Tiwari, A. J.; Fields, C. G.; Marr, L. C. A Cost-Effective Method of Aerosolizing Dry Powdered Nanoparticles. *Aerosol Sci. Technol.* **2013,** *47*, (11), 1267-1275.

45. NIST; Naumkin, A. V., Kraut-Vass, A., Gaarenstroom, S. W., Powell, C. J. NIST X-ray Photoelectron Spectroscopy Database. http://srdata.nist.gov/xps/query_chem_name_detail.aspx?ID_NO=26005&CName=Buckminsterfullerene (12 July 2013).

46. Zielinski, H.; Mudway, I. S.; Berube, K. A.; Murphy, S.; Richards, R.; Kelly, F. J. Modeling the interactions of particulates with epithelial lining fluid antioxidants. *Am. J. Physiol.-Lung Cell. Mol. Physiol.* **1999,** *277*, (4), L719-L726.

47. Holder, A. L.; Carter, B. J.; Goth-Goldstein, R.; Lucas, D.; Koshland, C. P. Increased cytotoxicity of oxidized flame soot. *Atmos. Pollut. Res.* **2012,** *3*, (1), 25-31.

48. Ames, B. N.; Cathcart, R.; Schwiers, E.; Hochstein, P. Uric acid provides an antioxidant defense in humans against oxidant- and radical-caused aging and cancer: A hypothesis *Proceedings of the National Academy of Sciences of the United States of America-Biological Sciences.* **1981,** *78*, (11), 6858-6862.

49. Ates, B.; Ercal, B. C.; Manda, K.; Abraham, L.; Ercal, N. Determination of glutathione disulfide levels in biological samples using thiol-disulfide exchanging agent, dithiothreitol. *Biomed. Chromatogr.* **2009,** *23*, (2), 119-123.

50. Vejerano, E., Holder, A.L., Ma, Y., Pruden-Bagchi, A., Marr, L.C. Oxidative stress potential and cytotoxicity of particulate matter from nanowaste incineration. *Particle & Fibre Toxicology.* **2014,** *in preparation*.

51. Cocker, D. R.; Flagan, R. C.; Seinfeld, J. H. State-of-the-art chamber facility for studying atmospheric aerosol chemistry. *Environmental Science & Technology.* **2001,** *35*, (12), 2594-2601.

52. Pathak, R. K.; Stanier, C. O.; Donahue, N. M.; Pandis, S. N. Ozonolysis of alpha-pinene at atmospherically relevant concentrations: Temperature dependence of aerosol mass fractions (yields). *J. Geophys. Res.-Atmos.* **2007,** *112*, (D3), 8.

53. Arayachukeat, S.; Palaga, T.; Wanichwecharungruang, S. P. Clusters of carbon nanospheres derived from graphene oxide. *ACS Appl. Mater. Interfaces.* **2012,** *4*, (12), 6807-6814.

54. Casero, E.; Alonso, C.; Vazquez, L.; Petit-Dominguez, M. D.; Parra-Alfambra, A. M.; de la Fuente, M.; Merino, P.; Alvarez-Garcia, S.; de Andres, A.; Pariente, F.; Lorenzo, E.

Comparative response of biosensing platforms based on synthesized graphene oxide and electrochemically reduced graphene. *Electroanalysis.* **2013,** *25*, (1), 154-165.

55. Hwang, Y. S.; Li, Q. L. Characterizing photochemical transformation of aqueous nC(60) under environmentally relevant conditions. *Environmental Science & Technology.* **2010,** *44*, (8), 3008-3013.

56. Parekh, B.; Debies, T.; Knight, P.; Santhanam, K. S. V.; Takacs, G. A. Surface functionalization of multiwalled carbon nanotubes with UV and vacuum UV photo-oxidation. *J. Adhes. Sci. Technol.* **2006,** *20*, (16), 1833-1846.

57. Hilburn, M. E.; Murdianti, B. S.; Maples, R. D.; Williams, J. S.; Damron, J. T.; Kuriyavar, S. I.; Ausman, K. D. Synthesizing aqueous fullerene colloidal suspensions by new solvent-exchange methods. *Colloid Surf. A-Physicochem. Eng. Asp.* **2012,** *401*, 48-53.

58. Nemeth, I., Boda, D. The ratio of oxidized/reduced glutathione as an index of oxidative stress in various experimental models of shock syndrome. *Biomedica Biochemica Acta.* **1989**, (48), S53-57.

59. Cataldo, F. A study on the action of ozone on multiwall carbon nanotubes. *Fuller. Nanotub. Carbon Nanostruct.* **2008,** *16*, (1), 1-17.

60. Kwamena, N. O. A.; Earp, M. E.; Young, C. J.; Abbatt, J. P. D. Kinetic and product yield study of the heterogeneous gas-surface reaction of anthracene and ozone. *J. Phys. Chem. A.* **2006,** *110*, (10), 3638-3646.

61. Kwamena, N. O. A.; Staikova, M. G.; Donaldson, D. J.; George, I. J.; Abbatt, J. P. D. Role of the aerosol substrate in the heterogeneous ozonation reactions of surface-bound PAHs. *J. Phys. Chem. A.* **2007,** *111*, (43), 11050-11058.

62. Kwamena, N. O. A.; Thornton, J. A.; Abbatt, J. P. D. Kinetics of surface-bound benzo a pyrene and ozone on solid organic and salt aerosols. *J. Phys. Chem. A.* **2004,** *108*, (52), 11626-11634.

63. Ma, J. Z.; Liu, Y. C.; He, H. Degradation kinetics of anthracene by ozone on mineral oxides. *Atmos. Environ.* **2010,** *44*, (35), 4446-4453.

64. Poschl, U.; Letzel, T.; Schauer, C.; Niessner, R. Interaction of ozone and water vapor with spark discharge soot aerosol particles coated with benzo a pyrene: O-3 and H2O adsorption,

benzo a pyrene degradation, and atmospheric implications. *J. Phys. Chem. A.* **2001,** *105*, (16), 4029-4041.

65. Bedjanian, Y.; Nguyen, M. L. Kinetics of the reactions of soot surface-bound polycyclic aromatic hydrocarbons with O(3). *Chemosphere.* **2010,** *79*, (4), 387-393.

66. Lu, J. W.; Fiegland, L. R.; Davis, E. D.; Alexander, W. A.; Wagner, A.; Gandour, R. D.; Morris, J. R. Initial reaction probability and dynamics of ozone collisions with a vinyl-terminated self-assembled monolayer. *J. Phys. Chem. C.* **2011,** *115*, (51), 25343-25350.

67. Kolb, C. E.; Cox, R. A.; Abbatt, J. P. D.; Ammann, M.; Davis, E. J.; Donaldson, D. J.; Garrett, B. C.; George, C.; Griffiths, P. T.; Hanson, D. R.; Kulmala, M.; McFiggans, G.; Poschl, U.; Riipinen, I.; Rossi, M. J.; Rudich, Y.; Wagner, P. E.; Winkler, P. M.; Worsnop, D. R.; O' Dowd, C. D. An overview of current issues in the uptake of atmospheric trace gases by aerosols and clouds. *Atmos. Chem. Phys.* **2010,** *10*, (21), 10561-10605.

68. Han, C.; Liu, Y. C.; Ma, J. Z.; He, H. Effect of soot microstructure on its ozonization reactivity. *J. Chem. Phys.* **2012,** *137*, (8).

69. Lelievre, S.; Bedjanian, Y.; Pouvesle, N.; Delfau, J. L.; Vovelle, C.; Le Bras, G. Heterogeneous reaction of ozone with hydrocarbon flame soot. *PCCP.* **2004,** *6*, (6), 1181-1191.

70. Sabirov, D. S.; Khursan, S. L.; Bulgakov, R. G. Ozone addition to C-60 and C-70 fullerenes: A DFT study. *J. Mol. Graph.* **2008,** *27*, (2), 124-130.

71. Shang, Z. F.; Pan, Y. M.; Cai, Z. S.; Zhao, X. Z.; Tang, A. C. An AM1 study of the reaction of ozone with C-60. *J. Phys. Chem. A.* **2000,** *104*, (9), 1915-1919.

72. Wang, B. C.; Chen, L.; Lee, K. J.; Cheng, C. Y. Semiempirical molecular dynamics studies of C-60/C-70 fullerene oxides: C60O, C60O2 and C70O. *Theochem.* **1999,** *469*, 127-134.

73. Chapleski, R. C. J., Morris, J.R., Troya, D. A theoretical study of the ozonolysis of C60: primary ozonide formation, dissociation, and multiple ozone additions. *PCCP.* **2014**, (16), 5977.

74. Deng, J. P.; Mou, C. Y.; Han, C. C. Oxidation of fullerenes by ozone. *Fullerene Sci. Technol.* **1997,** *5*, (5), 1033-1044.

75. Chibante, L. P. F.; Heymann, D. On the geochemistry of fullerenes - stability of C60 in ambient air and the role of ozone *Geochim. Cosmochim. Acta.* **1993,** *57*, (8), 1879-1881.

76. Simmons, J. M.; Nichols, B. M.; Baker, S. E.; Marcus, M. S.; Castellini, O. M.; Lee, C. S.; Hamers, R. J.; Eriksson, M. A. Effect of ozone oxidation on single-walled carbon nanotubes. *J. Phys. Chem. B.* **2006,** *110*, (14), 7113-7118.

77. Cai, L. T.; Bahr, J. L.; Yao, Y. X.; Tour, J. M. Ozonation of single-walled carbon nanotubes and their assemblies on rigid self-assembled monolayers. *Chem. Mater.* **2002,** *14*, (10), 4235-4241.

78. Peng, K.; Liu, L. Q.; Li, H. C.; Meyer, H.; Zhang, Z. Room temperature functionalization of carbon nanotubes using an ozone/water vapor mixture. *Carbon.* **2011,** *49*, (1), 70-76.

79. Kim, S.; Lee, Y. I.; Kim, D. H.; Lee, K. J.; Kim, B. S.; Hussain, M.; Choa, Y. H. Estimation of dispersion stability of UV/ozone treated multi-walled carbon nanotubes and their electrical properties. *Carbon.* **2013,** *51*, 346-354.

80. Huh, S.; Park, J.; Kim, Y. S.; Kim, K. S.; Hong, B. H.; Nam, J. M. UV/ozone-oxidized large-scale graphene platform with large chemical enhancement in surface-enhanced Raman scattering. *ACS Nano.* **2011,** *5*, (12), 9799-9806.

81. Ringuet, J.; Albinet, A.; Leoz-Garziandia, E.; Budzinski, H.; Villenave, E. Reactivity of polycyclic aromatic compounds (PAHs, NPAHs and OPAHs) adsorbed on natural aerosol particles exposed to atmospheric oxidants. *Atmos. Environ.* **2012,** *61*, 15-22.

82. Chu, S. N.; Sands, S.; Tomasik, M. R.; Lee, P. S.; McNeill, V. F. Ozone oxidation of surface-adsorbed polycyclic aromatic hydrocarbons: role of PAH-surface interaction. *J. Am. Chem. Soc.* **2010,** *132*, (45), 15968-15975.

83. Wang, C.; Shang, C.; Ni, M. L.; Dai, J.; Jiang, F. (Photo)chlorination-induced physicochemical transformation of aqueous fullerene nC(60). *Environmental Science & Technology.* **2012,** *46*, (17), 9398-9405.

84. Xing, G. M.; Zhang, J.; Zhao, Y. L.; Tang, J.; Zhang, B.; Gao, X. F.; Yuan, H.; Qu, L.; Cao, W. B.; Chai, Z. F.; Ibrahim, K.; Su, R. Influences of structural properties on stability of fullerenols. *J. Phys. Chem. B.* **2004,** *108*, (31), 11473-11479.

85. Wal, R. L. V.; Bryg, V. M.; Hays, M. D. XPS analysis of combustion aerosols for chemical composition, surface chemistry, and carbon chemical state. *Anal. Chem.* **2011,** *83*, (6), 1924-1930.

86. Liu, Z. Q.; Ma, J.; Cui, Y. H.; Zhang, B. P. Effect of ozonation pretreatment on the surface properties and catalytic activity of multi-walled carbon nanotube. *Applied Catalysis B-Environmental.* **2009,** *92*, (3-4), 301-306.

87. Li, M. H.; Boggs, M.; Beebe, T. P.; Huang, C. P. Oxidation of single-walled carbon nanotubes in dilute aqueous solutions by ozone as affected by ultrasound. *Carbon.* **2008,** *46*, (3), 466-475.

88. Orrling, D.; Fitzgerald, E.; Ivanov, A.; Molina, M. Enhanced sulfate formation on ozone-exposed soot. *J. Aerosol Sci.* **2011,** *42*, (9), 615-620.

89. Klink, S.; Ventosa, E.; Xia, W.; La Mantia, F.; Muhler, M.; Schuhmann, W. Tailoring of CNT surface oxygen groups by gas-phase oxidation and its implications for lithium ion batteries. *Electrochem. Commun.* **2012,** *15*, (1), 10-13.

90. Lee, J.; Cho, M.; Fortner, J. D.; Hughes, J. B.; Kim, J. H. Transformation of aggregate C-60 in the aqueous phase by UV irradiation. *Environmental Science & Technology.* **2009,** *43*, (13), 4878-4883.

91. Cataldo, F. Polymeric fullerene oxide (fullerene ozopolymers) produced by prolonged ozonation of C-60 and C-70 fullerenes. *Carbon.* **2002,** *40*, (9), 1457-1467.

92. Decesari, S.; Facchini, M. C.; Matta, E.; Mircea, M.; Fuzzi, S.; Chughtai, A. R.; Smith, D. M. Water soluble organic compounds formed by oxidation of soot. *Atmos. Environ.* **2002,** *36*, (11), 1827-1832.

93. Setyan, A.; Sauvain, J. J.; Guillemin, M.; Riediker, M.; Demirdjian, B.; Rossi, M. J. Probing functional groups at the gas-aerosol interface using heterogeneous titration reactions: a tool for predicting aerosol health effects? *ChemPhysChem.* **2010,** *11*, (18), 3823-3835.

94. Brauner, E. V.; Forchhammer, L.; Moller, P.; Simonsen, J.; Glasius, M.; Wahlin, P.; Raaschou-Nielsen, O.; Loft, S. Exposure to ultrafine particles from ambient air and oxidative stress-induced DNA damage. *Environ. Health Perspect.* **2007,** *115*, (8), 1177-1182.

95. Pichardo, S.; Gutierrez-Praena, D.; Puerto, M.; Sanchez, E.; Grilo, A.; Carnean, A. M.; Jos, A. Oxidative stress responses to carboxylic acid functionalized single wall carbon nanotubes on the human intestinal cell line Caco-2. *Toxicol. Vitro.* **2012,** *26*, (5), 672-677.

96. Yuan, J. F.; Gao, H. C.; Sui, J. J.; Duan, H. W.; Chen, W. N.; Ching, C. B. Cytotoxicity evaluation of oxidized single-walled carbon nanotubes and graphene oxide on human hepatoma HepG2 cells: an iTRAQ-coupled 2D LC-MS/MS proteome analysis. *Toxicol. Sci.* **2012,** *126*, (1), 149-161.

97. Chen, C. Y.; Jafvert, C. T. Photoreactivity of carboxylated single-walled carbon nanotubes in sunlight: reactive oxygen species production in water. *Environ. Sci. Technol.* **2010,** *44*, (17), 6674-6679.

Chapter 5 – Conclusions

Within the field of environmental nanotechnology, a knowledge gap exists regarding the role of the atmosphere in determining the transport, fate, and ecological consequences of ENPs. Oftentimes, it has been considered an inert compartment through which ENPs transit while on their way to and from the aqueous and terrestrial environments.[1]

Outcomes of Research Objective #1

Review the potential for transformation of carbon-based nanoparticles in the atmosphere.

This work reviews how atmospheric processing may transform the chemical and physical attributes of carbonaceous nanoparticles (CNPs) and how those transformations may alter the CNPs' environmental impacts. The conclusions of this work can help researchers design more environmentally relevant experiments when examining the environmental impacts of nanotechnology. This work may also help inform policymakers engaged in formulating nanotechnology-specific regulations about the role of the atmosphere in determining the environmental impacts of nanotechnology.

Outcomes of Research Objective #2

Develop a method to generate nano-scale aerosols from dry powdered C_{60} nanoparticles.

This work describes a method to produce sub-100 nm aerosol particles from manufactured nanomaterial powders without the use of solvents. The aerosolization technique can create nano-scale aerosols from both carbonaceous and metal oxide nanoparticles; this combination of size

and particle diversity has not been demonstrated by any custom or commercially available device to date. With the occasional exception of cerium dioxide, the technique produces aerosol mass concentrations that are related linearly to the mass of nanoparticle powder utilized, providing researchers with a reliable aerosol source. This technique will be useful for studies focusing on nanoparticle processes and may also be useful in toxicology experiments.

Outcomes of Research Objective #3

Identify and quantify the reaction rate, reaction products, and oxidative stress potential of aerosol-phase C_{60} nanoparticles due to exposure to atmospherically relevant levels of O_3.

This work describes the rate and products of the reaction between aerosolized C_{60} and atmospherically relevant levels of O_3. We demonstrate that C_{60} reacts quickly, that $C_{60}O$, $C_{60}O_2$, and $C_{60}O_3$ are produced in the reaction, and that the initial – but not final – abundance of $C_{60}O$ and $C_{60}O_2$ is enhanced by water vapor. We examine the oxidative stress potential of O_3-exposed C_{60} aerosols and find it to be elevated according to one assay. We compare the pseudo-first order reaction rate in this reaction to those of other carbonaceous nanoparticles and PAHs and confirm that the rate is lower than for PAHs tested at a comparable O_3 mixing ratio. As oxidation proceeds, C_{60} molecules may possibly become cross-linked with one another, forming dimers and perhaps more extensive oligomers.

These results verify that atmospheric transformations are of significance with respect to the fate of CNPs in the environment. This work provides evidence to researchers and policymakers that the atmosphere must be considered as more than just a transport pathway with respect to CNPs.

This work will assist the scientific and regulatory communities in formulating more realistic investigations and nanotechnology-related policy, respectively.

Implications

The contribution of this work to the scientific literature is twofold: to facilitate research into the inhalation toxicity and atmospheric transformation of ENPs by demonstrating a way to create nano-scale aerosols from ENP powders, and to show that the environmental behavior of CNPs (specifically C_{60} fullerenes) can be substantially altered by atmospheric processing. Taken together, these contributions have made important progress towards determining the environmental impacts of nanotechnology.

The development of an aerosolization technique that produces nano-scale aerosols from ENP powders will grant researchers more control over the surface chemistry and size of the aerosols they generate. This advance will enable researchers to expand into studies that may be more representative of realistic scenarios in the fields of aerosol chemistry, inhalation toxicology, and environmental nanotechnology.

Demonstration that C_{60} fullerenes react with atmospherically relevant levels of O_3 on a rapid time scale verifies that the atmosphere plays an important role in determining the environmental impacts of C_{60}. This knowledge will enable environmental nanotechnology researchers to improve the accuracy and environmental relevance of their work. Improvement in the scientific understanding of the environmental behavior of ENPs will further assist in the development of scientifically sound environmental policy pertaining to nanotechnology.

Recommendations for Future Work

We recommend that future research pertaining to the environmental impacts of nanotechnology incorporate nanoparticles that bear chemical resemblance to those having been atmospherically processed. As noted previously, much of the research done in this field has used pristine, unfunctionalized nanoparticles for ecotoxicity and human health research; this level of purity may not often be realistic. Nanoparticles that have undergone functionalization and/or internal mixing with other atmospheric constituents should be tested for their ecological and human health impacts alongside their unfunctionalized predecessors.

In order to potentially diversify the research applications of the aerosolization technique described in Chapter 3, we recommend development of a 'feeder' mechanism to enable continuous delivery of nanoparticle powder to the disperser. This would permit aerosol generation over a longer period of time (minutes, perhaps hours). Such a development could make the aerosolization technique much better suited for use in inhalation toxicology studies. In addition to enhancing the technique in this manner, we recommend confirming the size of the resulting ENP aerosols through TEM analysis of particles deposited via thermophoretic precipitation; this particle collection technique is far less biased to larger particle sizes than is impaction,[2] and could provide a more accurate understanding of the size distribution of the ENP aerosol.

In the interest of further exploring the importance of other atmospheric constituents to the atmospheric processing of C_{60}, we recommend consideration of photons and hydroxyl radicals.

Hydroxyl radicals are highly reactive and are produced through photolysis of ozone followed by reaction of the $O(^1D)$ product with water vapor. Recently, their formation has also been predicted from the interaction of water vapor and the Criegee intermediate of limonene ozonolysis.[3] Hydroxyl radicals readily react with alkenes,[4] and as fullerenes undergo many reactions similar to alkenes,[5] their reaction with OH in the atmosphere can be presumed to be significant. Beyond their role in producing hydroxyl radicals, photons may also promote further reactions on alkene surfaces that have undergone ozonolysis.[6] We can anticipate, then, that photons and hydroxyl radicals may play significant and interlinking roles in the atmospheric processing of C_{60}; these reactions should be investigated experimentally.

While we selected C_{60} fullerenes for this work due to the relative ease of aerosolizing them, CNT hold a larger share of the ENP marketplace than do fullerenes.[7] As such, atmospheric processing of CNT must be explored, including oxidation, coating, and internal mixing. Unintentional aerosolization of CNTs has already been demonstrated,[8] and multiple inhalation toxicity studies have demonstrated their deleterious effects on exposed organisms.[9, 10] Beyond inhalation studies, ecotoxicological research on CNTs has shown that surface functionalization is an important variable;[11] the impact of atmospheric processing aqueous-phase CNT ecotoxicology should not be overlooked. Pursuing these lines of research is an important next step to making research on the environmental impacts of nanotechnology more accurate.

Lastly, we recommend that future work should investigate the issue of potential dimerization (and subsequent oligomerization) of C_{60} upon oxidation with O_3. Results obtained during the work described in Chapter 4 suggest that oligomerization occurs, but more work is required to

substantiate this claim. If C_{60} molecules oligomerize with neighboring C_{60} molecules upon oxidation, the resulting oligomer could have different toxicological and environmental impacts than simpler reaction products. Future work should ideally go beyond C_{60} to investigate the possibility of cross-linking during CNT oxidation, and between a CNP and a neighboring carbonaceous substance that is not an ENP. If CNPs become chemically bonded to non-ENP substances (for example, humic or humic-like substances[12]) through environmental processing, this could significantly alter the way in which we think about the transport, fate, and impacts of CNPs in the environment.

References

1. Tiwari, A. J.; Marr, L. C. The Role of Atmospheric Transformations in Determining Environmental Impacts of Carbonaceous Nanoparticles. *Journal of Environmental Quality.* **2010,** *39*, (6), 1883-1895.

2. Strom, H.; Sasic, S. The role of thermophoresis in trapping of diesel and gasoline particulate matter. *Catal. Today.* **2012,** *188*, (1), 14-23.

3. Jiang, L.; Lan, R.; Xu, Y. S.; Zhang, W. J.; Yang, W. Reaction of Stabilized Criegee Intermediates from Ozonolysis of Limonene with Water: Ab Initio and DFT Study. *Int. J. Mol. Sci.* **2013,** *14*, (3), 5784-5805.

4. Finlayson-Pitts, B.; Pitts, J., *Chemistry of the Upper and Lower Atmosphere*. Academic Press: 2000.

5. Taylor, R.; Walton, D. R. M. The chemistry of fullerenes. *Nature.* **1993,** *363*, (6431), 685-693.

6. Park, J.; Gomez, A. L.; Walser, M. L.; Lin, A.; Nizkorodov, S. A. Ozonolysis and photolysis of alkene-terminated self-assembled monolayers on quartz nanoparticles: implications for photochemical aging of organic aerosol particles. *PCCP.* **2006,** *8*, (21), 2506-2512.

7. Project on Emerging Nanotechnologies Analysis, Consumer Products, Nanotechnology Project. http://www.nanotechproject.org/inventories/consumer/analysis_draft/ (14 February 2014).

8. Maynard, A. D.; Baron, P. A.; Foley, M.; Shvedova, A. A.; Kisin, E. R.; Castranova, V. Exposure to carbon nanotube material: Aerosol release during the handling of unrefined single-walled carbon nanotube material. *J. Toxicol. Env. Health Pt A.* **2004,** *67*, (1), 87-107.

9. Donaldson, K.; Aitken, R.; Tran, L.; Stone, V.; Duffin, R.; Forrest, G.; Alexander, A. Carbon nanotubes: A review of their properties in relation to pulmonary toxicology and workplace safety. *Toxicol. Sci.* **2006,** *92*, (1), 5-22.

10. Lam, C. W.; James, J. T.; McCluskey, R.; Arepalli, S.; Hunter, R. L. A review of carbon nanotube toxicity and assessment of potential occupational and environmental health risks. *Crit. Rev. Toxicol.* **2006,** *36*, (3), 189-217.

11. Petersen, E. J.; Zhang, L. W.; Mattison, N. T.; O'Carroll, D. M.; Whelton, A. J.; Uddin, N.; Nguyen, T.; Huang, Q. G.; Henry, T. B.; Holbrook, R. D.; Chen, K. L. Potential Release Pathways, Environmental Fate, And Ecological Risks of Carbon Nanotubes. *Environmental Science & Technology.* **2011,** *45*, (23), 9837-9856.

12. Graber, E. R.; Rudich, Y. Atmospheric HULIS: How humic-like are they? A comprehensive and critical review. *Atmos. Chem. Phys.* **2006,** *6*, 729-753.

Appendix A: Supplementary Information to Chapter 4

This appendix contains the following information:

- Schematic of experimental setup
- Ozone loss data
- High resolution XPS spectra
- SEM images of impacted aerosol sample
- Ozone reaction rate as a function of mixing ratio
- Raw and normalized UV-Vis spectra
- Commercial information and operating conditions for analytical instruments, samplers, and sampling substrates
- Further experimental details
- Discussion pertaining to potential C_{60} dimerization

Schematic of Experimental Setup

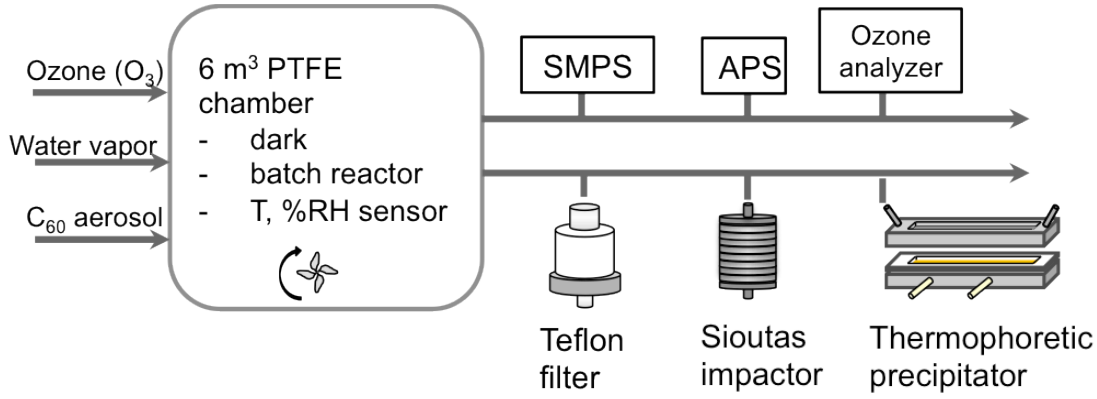

Figure A-1: Schematic of chamber, online and offline sampling.

Ozone Loss Data

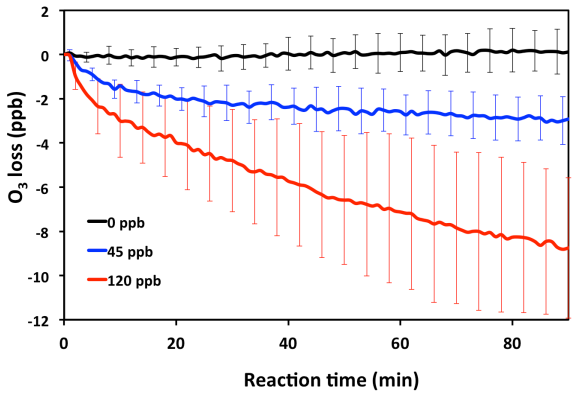

Figure A-2: O_3 loss during the 90-min reaction with C_{60} at 10-15% RH. (*n* = 10, 6, and 6 for 0, 45, and 120 ppb, respectively), shown with error bars of ± 1 standard deviation. Losses at ~65% RH were not significantly different. O_3 loss at an intial mixing ratio of 1 ppm totaled 84 ± 4 ppb (not shown for scale).

High-resolution XPS Spectra

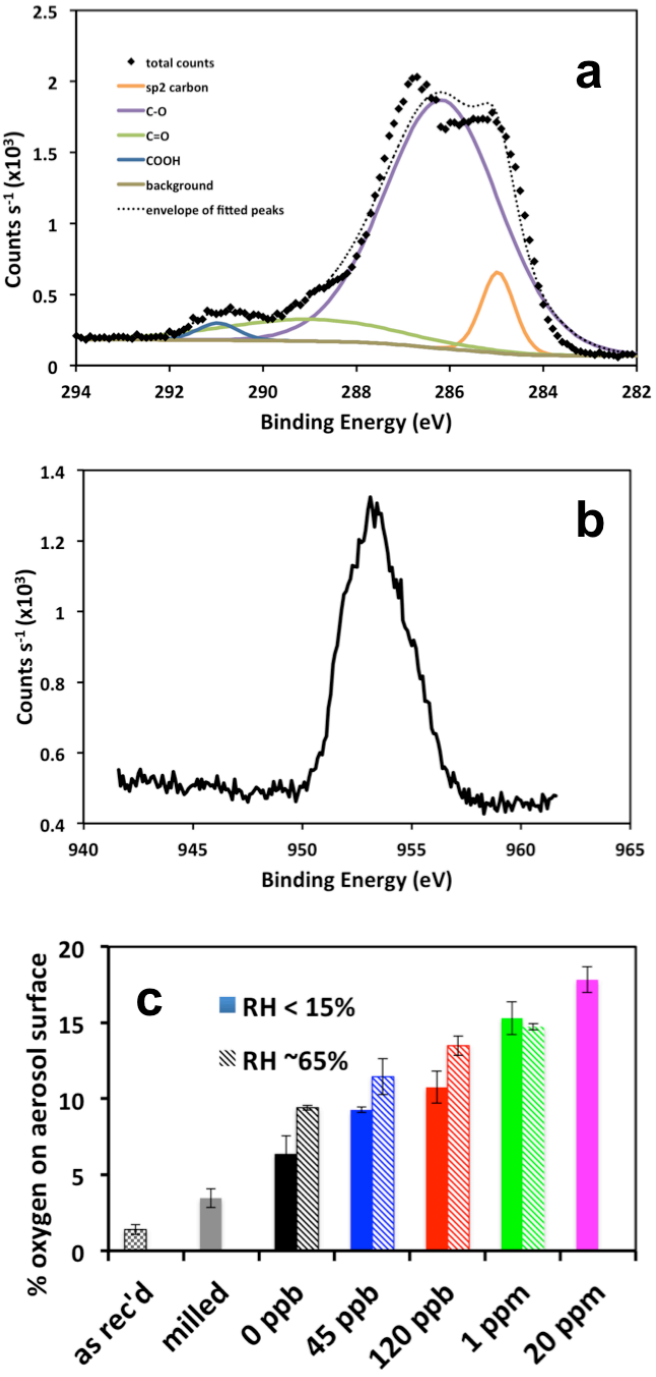

Figure A-3: a) XPS C1s spectrum of ~65% RH sample, along with peak fitting scheme used for 10-15% RH samples. b) O1s spectrum of RH < 15% sample. c) Surface oxygen content of C_{60} as received (as rec'd), post-milling (milled), and exposed to O_3. The aerosol data are identical to those shown in Figure 4-2a.

SEM images of impacted aerosol sample

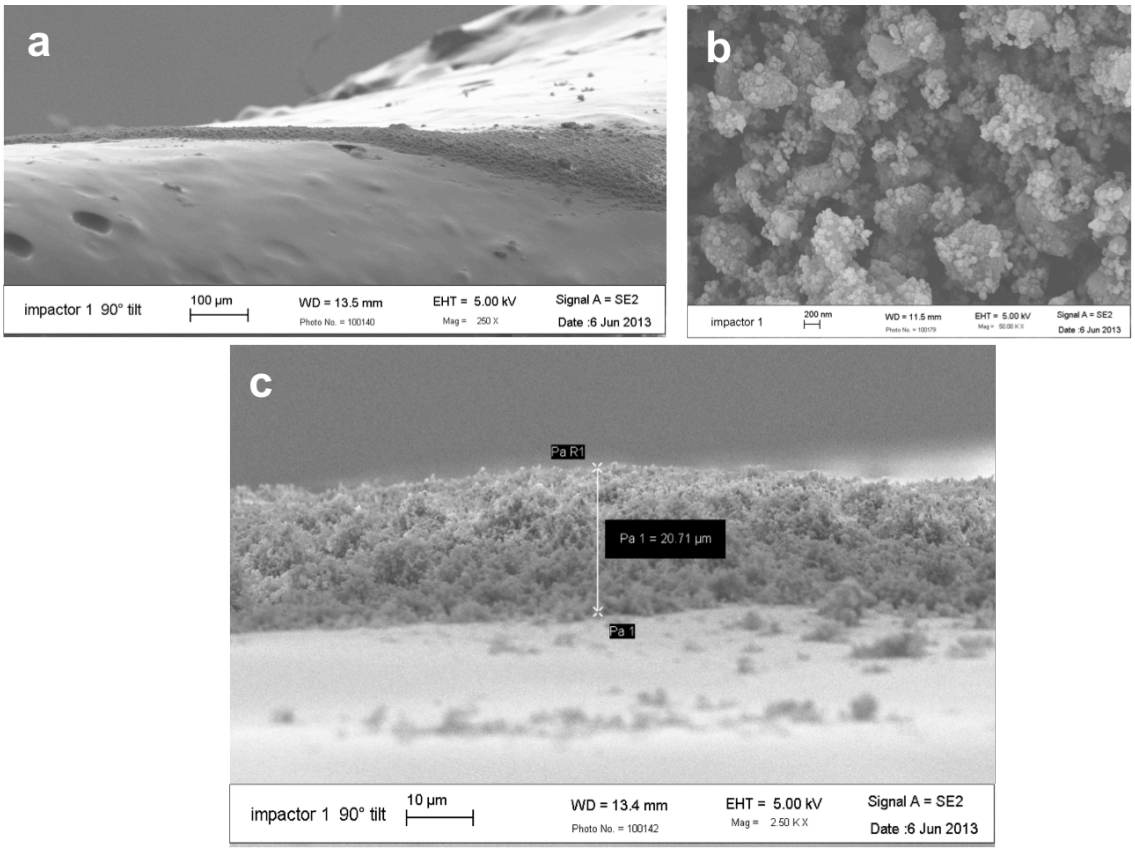

Figure A-4: SEM images of a C_{60} aerosol sample collected via impactor for XPS analysis. All XPS samples covered the substrate completely; consequently, we presume that the XPS spectra represent the chemistry of the aerosols alone and would not be influenced by the copper tape or its adhesive. a) The strip of deposited fullerenes is visible on the copper tape (scale bar 100 µm). b) The texture of the deposited C_{60} aerosol sample from above (scale bar 200 nm). c) Side view of the C_{60} aerosol strip with a measured height of 20 µm (scale bar 10 µm).

Ozone reaction rate as a function of mixing ratio

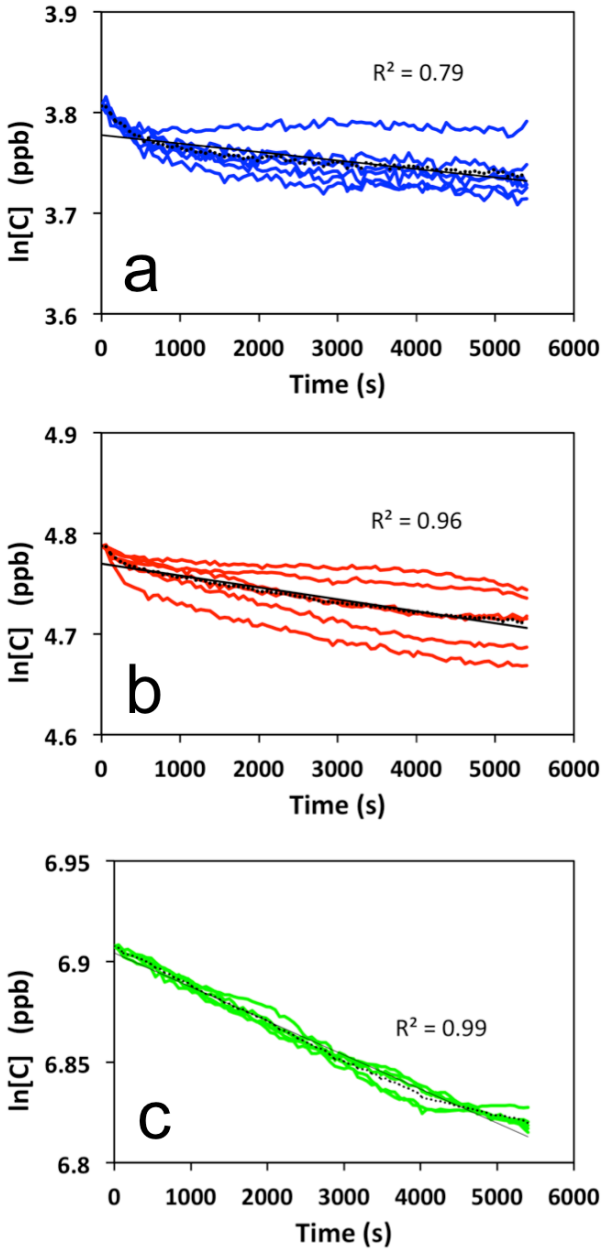

Figure A-5: O_3 loss after injection of C_{60} aerosols at initial O_3 mixing ratios of a) 45 ppb, b) 120 ppb, and c) 1 ppm. In each panel the dashed black line is the average of all the colored lines, and the solid black line is the linear least-squares regression line for the average.

Raw and normalized UV-Vis spectra

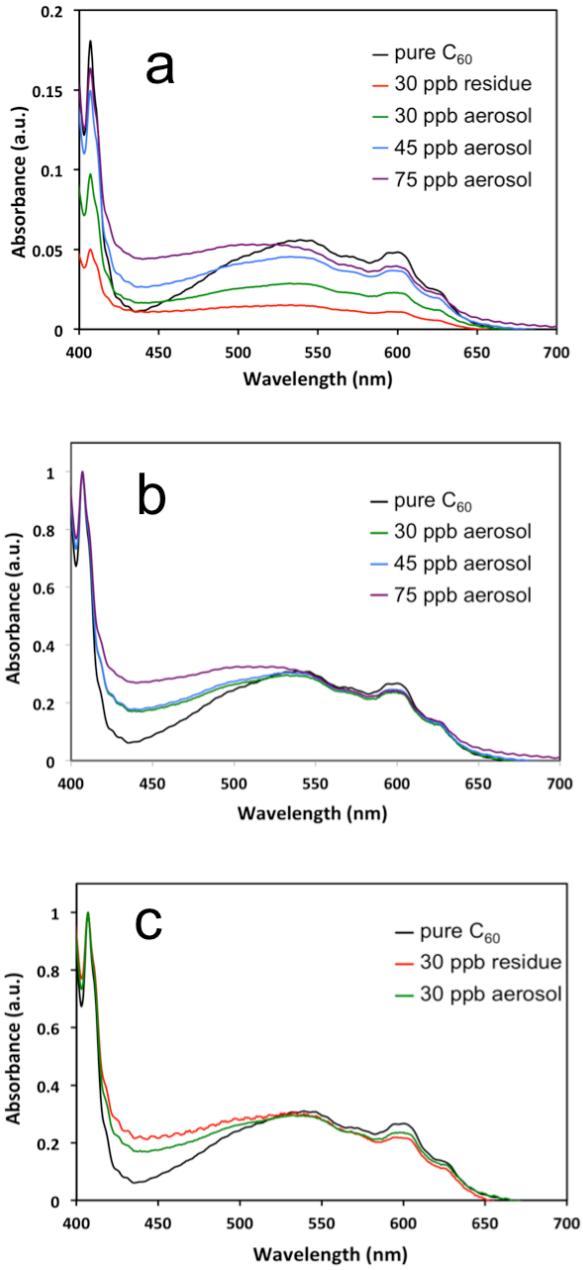

Figure A-6: UV-Vis spectra of pure C_{60} and O_3-exposed C_{60} in ODCB (10-15% RH). a) The 'residue' sample was extracted in toluene and dried prior to extraction in ODCB in order to remove toluene-soluble species (such as unreacted C_{60}) from it. b) Spectra are normalized to the peak at λ = 407 nm. O_3-exposed aerosols at t = 65 min of exposure to initial O_3 mixing ratios of 30, 45, and 75 ppb, with pure C_{60} in ODCB for comparison. C) Spectra are normalized to the peak at λ = 407 nm. C_{60} aerosols exposed to an initial O_3

mixing ratio of 30 ppb for *t* = 53 min, pre-extracted in toluene to remove toluene-soluble species ("residue"), and C_{60} aerosols exposed to 30 ppb O_3 for t = 65 min which was not pre-extracted in toluene (as shown in (a)), with pure C_{60} in ODCB for comparison.

Commercial information and operating conditions for analytical instruments, samplers, and sampling substrates

Table A-1: Commercial information and operating conditions regarding analytical techniques, samplers, and sampling substrates.

Analytical technique, sampler, or substrate	**Specifics**
Ozone generator	HG500, Ozone Solutions, Hull, IA
Ozone analyzer	49C, Thermo Scientific, Franklin, MA
BeadBeater	BioSpec, Bartlesville, OK
Scanning Mobility Particle Sizer (SMPS)	3936NL, TSI, Shoreview, MN
Ultrafine Condensation Particle Counter	3025A, TSI, Shoreview, MN
Aerodynamic Particle Sizer (APS)	3321, TSI, Shoreview, MN
PTFE filter, 47 mm, 1 μm pore size	JAWP04700, Millipore, Billerica, MA
Triple quadrupole mass	Thermo Instrument TSQ, Thermo Finnegan, San Jose,

spectrometry with electrospray ionization (ESI-MS)	CA
BuckyPrep column (HPLC, LC/MS)	091-3113, 4.6 × 250 mm, SES Research, Houston, TX
High-performance liquid chromatography (HPLC)	HP 1090, 1 mL min^{-1} toluene mobile phase, BuckyPrep column, 335 nm diode array detection
X-ray photoelectron spectroscopy (XPS)	Quantera XSM, Phi, Chanhassen, MN. Step size 1 eV and 0.1 eV respectively, spot size 200 μm, Al mono source
Transmission electron microscopy (TEM)	120 kV, FEI Philips EM420
Sioutas impactor	225-370, SKC Inc., Eighty Four, PA
HPLC-grade toluene	99.7%, JT Baker, VWR
ODCB	99%, Sigma-Aldrich

Further experimental details

At an O_2 flow rate of 0.1 L min^{-1}, 1.7 mL of O_2/O_3 flow resulted in an approximately 10 ppb rise in the O_3 mixing ratio of the chamber; thus, introduction of O_3 at the mixing ratios utilized did not result in a significant increase in the O_2 content of the chamber air. Therefore, the experimental results cannot be attributed to elevated exposure to O_2.

Samples were collected for HPLC analysis at t = 6, 18, 30, 42, 60, and 90 min into the reaction (sampling midpoints of a 12-min period). Samples for UV-Vis were collected at t = 65 min and were extracted in *o*-dichlorobenzene (ODCB). A 'residue' sample was created for UV-Vis analysis by collecting aerosols from the first 53 min of exposure to an initial O_3 mixing ratio of 30 ppb, extracting them in toluene to remove toluene-soluble molecules, and drying them in a vacuum desiccator. These filters contained a toluene-insoluble, brown residue, which was extracted in ODCB for analysis.

For XPS analysis, three samples were collected consecutively from one chamber run to represent each concentration, beginning at t = 90 min. The XPS spectral peaks are created from the energy of photoelectrons emitted from the top few nanometers into the sample, so the gathered data is representative of the surface of the collected aerosols only. To enable observation of particle morphology, aerosols were deposited onto copper TEM grids (FCF200-Cu-50, Electron Microscopy Sciences, Hatfield, PA) by placing the grids in a custom thermophoretic precipitator (TP). The top of the aluminum precipitator was heated to 90 °C using a resistive heater and the bottom was cooled with flowing ice-cooled water. Chamber air was drawn through the TP at 1.5 L min^{-1}.

Discussion pertaining to potential C_{60} dimerization

The potential for C_{60} dimers to form during O_3 exposure was investigated using UV-Vis spectroscopy. Figure A-6 shows raw UV-Vis spectra for O_3-exposed C_{60} aerosols at three different initial O_3 mixing ratios (30, 45, and 75 ppb), as well as a 'residue' sample from an experiment at 30 ppb, from which toluene-soluble species (i.e., unreacted C_{60} as well as oxidized C_{60} still soluble in toluene) had been removed, as described above. Pure C_{60} is shown for comparison, and all samples were in ODCB. For pure C_{60}, there was a significant decrease in absorbance between 430 and 500 nm relative to the region between 500 and 650 nm; the O_3-exposed samples did not show such a decrease. Additionally, the absorbance of all O_3-exposed C_{60} in the 580 – 630 nm region was diminished relative to that of the pure C^{60}, which showed notable absorbance features.

While aqueous extractions of the residue did not produce meaningful results via either total organic carbon analysis or UV-Vis spectroscopy, the spectral features of the O_3-exposed samples when extracted in ODCB (Figure A-6) suggest the presence of C_{60} dimers.[1] The muted absorbance of the residue sample at 590 nm relative to the aerosol samples may be attributed to the removal of toluene-soluble C_{60} and reaction products from that sample prior to extraction in ODCB. Normalizing the spectra to the peak at 407 nm (Figure A-6a) shows more clearly that elevated initial O_3 mixing ratio is associated with higher absorbance between 430 and 500 nm, and decreased absorbance near 590 nm. Additionally, the removal of toluene-soluble species prior to extraction in ODCB further enhances the absorbance between 430 and 500 nm. These trends suggest that higher O_3 mixing ratios lead to more extensive dimerization, and that the toluene-insoluble substance that forms during the C_{60}-O_3 reaction consists of cross-linked C_{60} molecules.

Dimers may form during C_{60} reaction with O_3 when a primary ozonide – the first step in

C_{60}[2] and alkene[3] oxidation by O_3 – forms over two carbon atoms on neighboring C_{60} cages, as opposed to two carbons on the same cage (which decays into an epoxide). While the spectra shown in Figure A-6 suggest the presence of dimers, it is also possible that further cross-linking may occur, resulting in oligomers. Potential cross-linking of alkene-terminated self-assembled monolayers after exposure to gas-phase O_3 has been mentioned previously;[4] cross-linking more extensive than that needed for dimerization may have occurred in these samples. Oligomerization has previously been observed during the reaction of gas-phase compounds with ozone[5] and during oxidation of aerosol surface species.[6] It is possible that $C_{60}O$ and $C_{60}O_2$ may be intermediates as the reaction proceeds to the cross-linking of neighboring C_{60} cages, resulting in dimers and possibly larger polymers.[7, 8]

References

1. Resmi, M. R.; Ma, S. G.; Caprioli, R.; Pradeep, T. C120On from C60Br24. *Chem. Phys. Lett.* **2001,** *333*, (6), 515-521.

2. Davis, E. D.; Wagner, A.; McEntee, M.; Kaur, M.; Troya, D.; Morris, J. R. Reaction Probability and Infrared Detection of the Primary Ozonide in Collisions of O-3 with Surface-Bound C-60. *J. Phys. Chem. Lett.* **2012,** *3*, (21), 3193-3198.

3. Finlayson-Pitts, B.; Pitts, J., *Chemistry of the Upper and Lower Atmosphere*. Academic Press: 2000.

4. Fiegland, L. R.; Saint Fleur, M. M.; Morris, J. R. Reactions of C=C-terminated self-assembled monolayers with gas-phase ozone. *Langmuir.* **2005,** *21*, (7), 2660-2661.

5. Sadezky, A. W., R.; Kanawati, B.; Rompp, A.; Spengler, B.; Melloudi, A.; Le Bras, G.; Chaimbault, P.; Moortagt, G.K. Oligomer formation during gas-phase ozonolysis of small alkenes and enol ethiers: new evidence for the central role of the Criegee Intermediate as oligomer chain unit. *Atmos. Chem. Phys.* **2008,** *8*, (10), 2667-2699.

6. Hallquist, M. W., J.C.; Baltensperger, U.; Rudich, Y.; Simpson, D.; Claeys, M.; Dommen, J.; Donahue, N.M.; George, C.; Goldstein, A.H.; Hamilton, J.F.; Herrmann, H.; Hoffmann, T.; Iinuma, Y.; Jang, M.; Jenkin, M.E.; Jimenez, J.L.; KiendlerpScharr, A.; Maenhaut, W.; McFiggans, G.; Mentel, T.F.; Monod, A.; Prevot, A.S.H.; Seinfeld, J.H.; Surratt, J.D.; Szmigielski, R.; Wildt, J. The formation, properties, and impact of secondary organic aerosol: current and emerging issues. *Atmos. Chem. Phys.* **2009,** *9*, (14), 5155-5236.

7. Cataldo, F. Polymeric fullerene oxide (fullerene ozopolymers) produced by prolonged ozonation of C-60 and C-70 fullerenes. *Carbon.* **2002,** *40*, (9), 1457-1467.

8. Razanau, L.; Mieno, T.; Kazachenko, V. Thin polymerized C-60 coatings deposited in electrostatic field via electron-beam dispersion of fullerite. *Thin Solid Films.* **2010,** *519*, (4), 1285-1292.